

1-1-1991

## IFF Tactical Electronic Simulation And Test System: Technical Issue Research Status Report

W. B. Mikhael

Find similar works at: <https://stars.library.ucf.edu/istlibrary>  
University of Central Florida Libraries <http://library.ucf.edu>

This Research Report is brought to you for free and open access by the Digital Collections at STARS. It has been accepted for inclusion in Institute for Simulation and Training by an authorized administrator of STARS. For more information, please contact [STARS@ucf.edu](mailto:STARS@ucf.edu).

---

### Recommended Citation

Mikhael, W. B., "IFF Tactical Electronic Simulation And Test System: Technical Issue Research Status Report" (1991). *Institute for Simulation and Training*. 111.  
<https://stars.library.ucf.edu/istlibrary/111>

INSTITUTE FOR SIMULATION AND TRAINING

PREPARED UNDER CONTRACT NUMBER N61339-91-C-0100  
for  
NAVAL TRAINING SYSTEMS CENTER  
and  
NAVAL AIR TEST CENTER

# TACTICAL ELECTRONICS SIMULATION TEST SYSTEM

Technical Issue Research Status Report  
CDRL A003

December 23, 1991

Institute for Simulation and Training  
12424 Research Parkway, Suite 300  
Orlando, FL 32826

and

Department of Electrical Engineering  
University of Central Florida  
Orlando, FL 32816

University of Central Florida  
Division of Sponsored Research

**IST**

N 09

IST-CR-91-15

**IFF TACTICAL ELECTRONIC SIMULATION and TEST SYSTEM:  
TECHNICAL ISSUE RESEARCH STATUS REPORT**

**Contract No:** N61339-91-C-0100  
**CDRL** A003

**Reporting Period:** June 24, 1991 to December 24, 1991

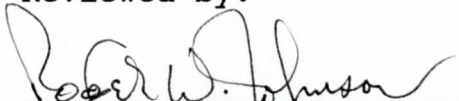
**From:** Dr. W. B. Mikhael P.I., E.E. Department Coordinator

Dr. C. Christodoulou P.I., E&M  
Mr. H. Pham, Research Assistant, E&M

Dr. D. Malocha P.I., Signal Generation  
Ms. N. Eisenhauer, Research Assistant, Signal Generation

Dr. M. Belkerdid P.I., Communication Systems Simulation  
Mr. G. Koller, Research Assistant, Communication Systems Simulation

Reviewed by:

  
\_\_\_\_\_  
Roger Johnson

Edited by:

  
\_\_\_\_\_  
Danette Carr

## TABLE OF CONTENTS

<b>SUMMARY</b>	-----	iii
<b>1. <u>EM &amp; RADAR</u></b>	-----	0
<b>1.1 INTRODUCTION</b>	-----	1
<b>1.2 RESULTS-Multipath Effects</b>	-----	1
1.2.1 Examples	-----	1
1.2.1.1 Example 1	-----	2
1.2.1.2 Example 2	-----	37
<b>1.3 RESULTS-Antenna Platform Effects</b>	-----	47
1.3.1 Examples	-----	48
1.3.1.1 Example 1	-----	48
1.3.1.2 Example 2	-----	52
1.3.1.3 Example 3 - A rocket model	-----	56
1.3.1.4 Example 4 - A Torrus model	-----	57
1.3.1.5 Example 5 - Airplane Geometry	-----	58
<b>1.4 CONCLUSIONS</b>	-----	62
<b>2. <u>SIGNAL GENERATION</u></b>	-----	63
2.1 Introduction	-----	64
2.2 Delay	-----	65
2.3 Amplitude Control	-----	68
2.4 Amplitude Dispersion	-----	69
2.5 Conclusion	-----	71
<b>Appendix 2.A Navy Tests Briefing</b>	-----	74
<b>Appendix 2.B Component Specifications</b>	-----	89
<b>3. <u>COMMUNICATIONS SYSTEMS MODELING</u></b>	-----	107
3.1 Introduction	-----	108
3.2 CDMA Environment	-----	109
3.3 CDMA: Equal Power Levels	-----	112
3.4 Multiple Spread Spectrum Synthesis	-----	114
3.5 Conclusions	-----	117
<b>Appendix 3.A Phase Multiplexed Correlation In Multiple Access   Spread Spectrum Systems</b>	-----	121

## SUMMARY

This report documents the work performed by the three technical teams: the Electro Magnetic & Radar team, the Signal Generation team, and the Communications Systems Modeling team.

The EM team acquired ECAC and GEMACS software packages. Terrain data has been requested from DMA. Some modeling and simulation work of different modes of EM propagation over several terrains and antenna platform effects have been performed. Also, the EM & Radar group performed simulations using GAUGE and GEMACS software packages for several geometries. Both GTD and the method of moments were used.

The Signal Generation and Conditioning team studied the quantitative bounds on path loss as a function of distance, and frequency and delay as a function of distance. Also, they accumulated information from various vendors of hardware in light of the signal generation/detection and conditioning requirements. In addition, the effects of doppler on the frequency and phase shift of a signal and two feasible approaches for signal conditioning hardware are given.

The Communications Systems Modeling team spent a considerable effort studying code acquisition in Direct Sequence Spread Spectrum Systems, data rate = 1, adjacent PN sequence generator's chip rate = 100 chips/sec., sample rate = 200 Hz. Additive (uncorrelated) Gaussian white noise was added to the channel. BOSS software was used for the simulation work. The communications group simulated a direct sequence spread spectrum receiver operating in a CDMA environment to investigate the system capacity in a manner that can model multipath.

# **IFF Tactical Electronic Simulation and Test System**

## **1. EM & Radar**

Dr. C. G. Christodoulou

# **IFF Tactical Electronic Simulation and Test System**

## **1. EM & Radar**

Dr. C. G. Christodoulou

**1.1 INTRODUCTION** This report presents the analysis and evaluation of two models for the simulation of multipath propagation effects. Also, this report presents the evaluation of GEMACS and its capabilities to simulate platform effects and 3-D radiation patterns.

Multipath effects are caused by the interference of reflected electromagnetic waveform with the primary, direct path waveform at the receiver. This interference may be either constructive or destructive, and it depends on the gain, phase, frequency and polarization of the transmitted wave. Furthermore, parameters such as the geometry of the transmitting and receiving platforms, and the electromagnetic properties of the reflecting surface play a big role in the final result of multipath effects.

In this report, the software package "ECAC" from the Electromagnetic Analysis Compatibility Center in Annapolis, Maryland, was used to determine the degree of attenuation in the signal in a communication link. Several scenarios with complex terrain and sea landscapes were tested and all results are presented herein.

Next, the problem of near field effects were studied using GEMACS. Although we have concentrated our efforts on the Platform effects and modeling of antennas, the problem of coupling between the various antennas and 3-dimensional patterns can be analyzed using GEMACS.

## **1.2 RESULTS-Multipath Effects**

Both the the Integrated Rough Earth Model (TIREM) and (MIXPATH) models of the ECAC software package were studied. Some of the parameters that we varied were :

- Distance and elevation profiles. These were inputted manually since we have not received yet any actual terrain data.
- Geographic coordinates (Latitude and Longitude) of the transmitter and receiver.
- Environmental parameters of the terrain (permittivity, conductivity, etc.) .
- Antenna heights, their frequency, and polarization
- Antenna gains and transmitter power.
- Topographic profiles between the transmitter and the receiver.

### **1.2.1 Examples**

Two examples are enclosed, one for TIREM and one for MIXPATH.



### 1.2.1.1 Example 1

In the first example of TIREM, the Propagation loss between the receiver and transmitter is evaluated. A hypothetical terrain shown in Figure 1.1 was used for this example. The model predicts the best mode of propagation, i.e. line-of-sight, diffraction, or atmospheric scatter modes. The modes are selected from the irregular profile shown in Figure 1.1. Figure 1.2 shows the results within the frequency range of 1 to 12 GHz, and Figure 1.3 depicts the changes in the propagation loss as you vary the humidity term.

The input parameters used with this example are :

#### **Transmitter:**

Height = 100 ft  
Polarization = Vertical  
Power = 100 W  
Antenna Gain= 30 dBi

#### **Receiver :**

Height= 100 ft  
Antenna Gain= 30 dBi

Medium dry ground was used for the given terrain and a Continental climatic zone.

Pages 6 to 36 show the input and output data formats. The input data are supplied to the computer in the format that appears in screens 1.1 to 24.1. The results are given in the format shown in screen 25.1 for various frequencies

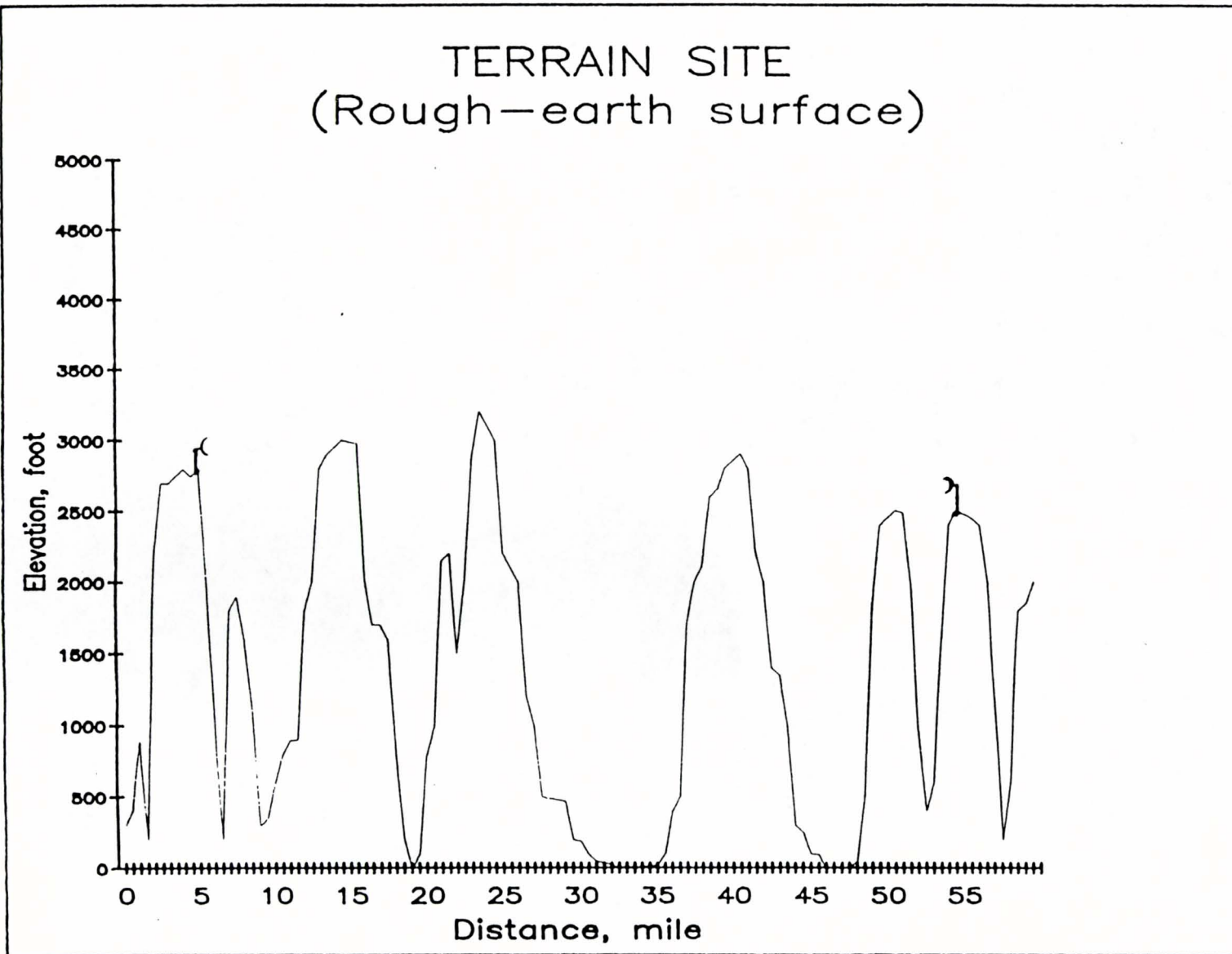


Fig.1.1 A hypothetical complex terrain

# Propagation loss versus frequency Diffraction mode

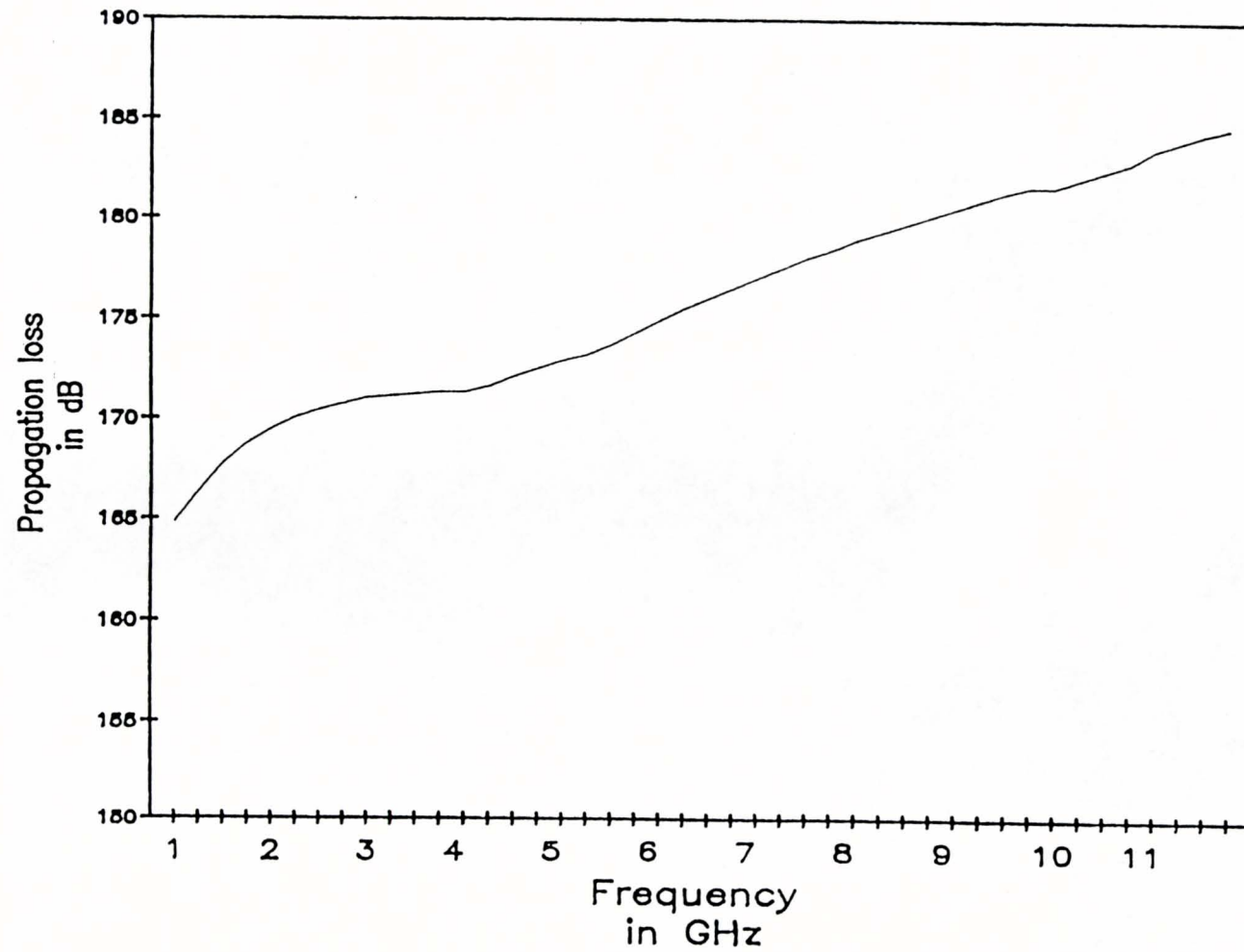


Fig. 1,2 Losses versus frequency (Diffraction mode)

# Propagation Loss versus Frequency Complex Terrain – Very Dry Ground

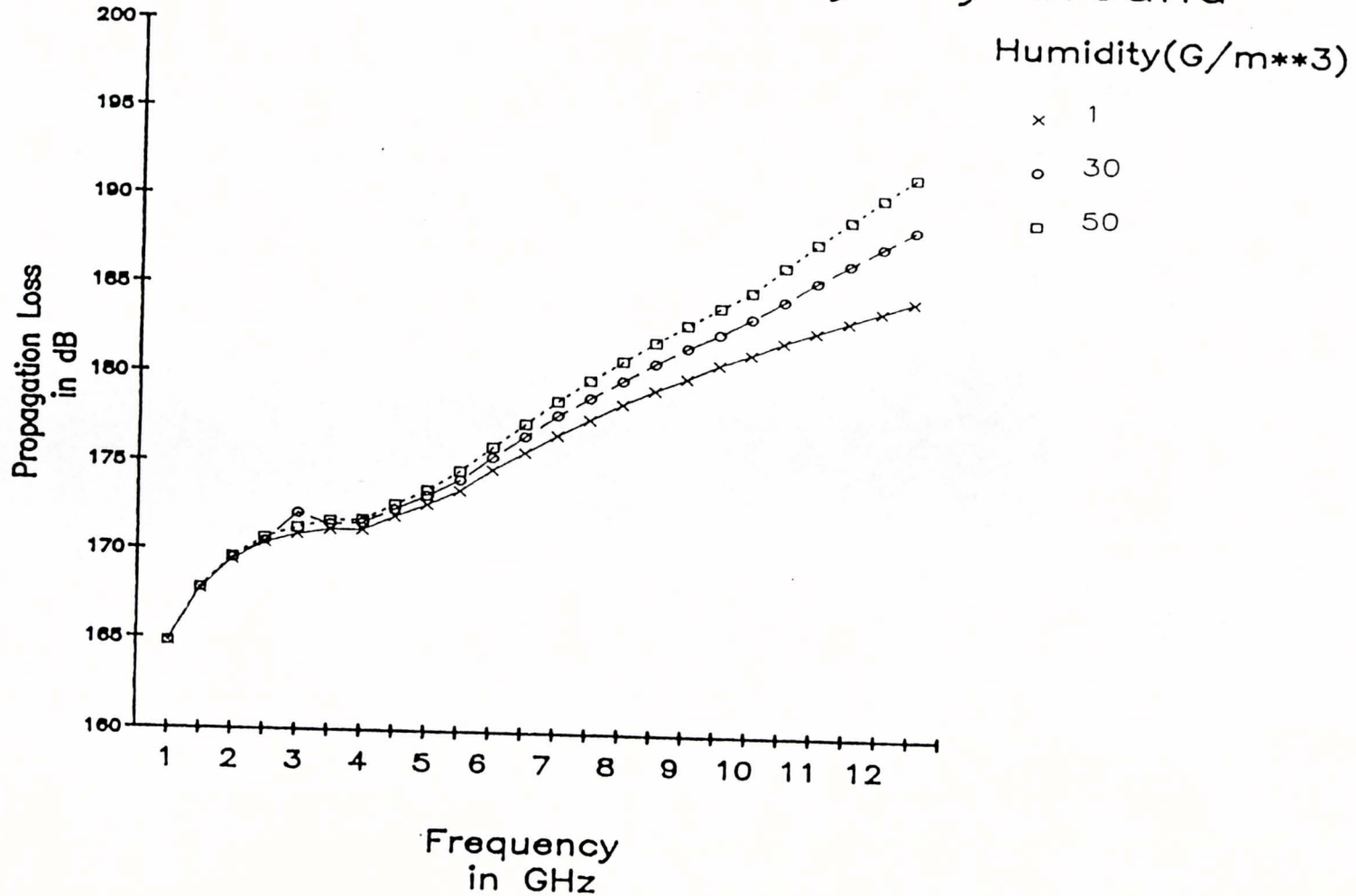


Fig. 1.3 Propagation losses over a complex terrain with various humidity values

===== SCREEN NUMBER 1.1 =====\*\* UNCLASSIFIED \*\*\*

```

*****
*
* TERRAIN INTEGRATED ROUGH-EARTH MODEL *
*
* (TIREM) *
*
*****

```

THE TERRAIN INTEGRATED ROUGH-EARTH MODEL (TIREM) EXAMINES THE TERRAIN PROFILE BETWEEN TRANSMITTER AND RECEIVER AND CALCULATES THE PROPAGATION LOSS BY CHOOSING THE PREDICTION ALGORITHM THAT BEST REPRESENTS THE ACTUAL PROPAGATION MODE. LINE-OF-SIGHT, DIFFRACTION, AND TROPOSPHERIC SCATTER MODES ARE SELECTED FOR EITHER SMOOTH OR IRREGULAR PROFILES, AS APPROPRIATE. TIREM IS APPLICABLE FROM 20 MHz TO 20 GHz.

TRANSMIT TO CONTINUE

===== SCREEN NUMBER 2.1 =====\*\* UNCLASSIFIED \*\*\*

-----  
 TRANSMITTER INPUTS  
 -----

TRANSMITTER ID: [ TRANSMIT ]

TRANSMITTER ANTENNA STRUCTURAL HEIGHT: [ 100 ] ( FT )

TRANSMITTER ANTENNA POLARIZATION: [ V ] V - VERTICAL  
 H - HORIZONTAL

TRANSMITTER FREQUENCY: [ 1000 ] ( MHZ )

TRANSMITTER POWER: [ 100 ] ( W )

TRANSMITTER ANTENNA GAIN: [ 30 ] ( dBi )

TRANSMITTER ANTENNA MAXIMUM DIMENSION: [ 10 ] ( FT )

===== SCREEN NUMBER 3.1 =====\*\*\* UNCLASSIFIED \*\*\*

-----  
RECEIVER INPUTS  
-----

RECEIVER ID: [ RECEIVER ]  
RECEIVER ANTENNA STRUCTURAL HEIGHT: [ 100 ] ( FT )  
RECEIVER ANTENNA GAIN: [ 30 ] ( dBi )  
RECEIVER ANTENNA MAXIMUM DIMENSION: [ 10 ] ( FT )

===== SCREEN NUMBER 4.1 =====\*\*\* UNCLASSIFIED \*\*\*

-----  
TROPOSCATTER ANALYSIS  
-----

ARE YOU EVALUATING A TROPOSCATTER LINK ? [ N ] Y - YES  
N - NO

IF YES,

ENTER THE TRANSMITTER ANTENNA 3 dB BEAMWIDTH: [ ] ( DEG )

ENTER THE RECEIVER ANTENNA 3 dB BEAMWIDTH: [ ] ( DEG )

===== SCREEN NUMBER 5.1 =====\*\*\* UNCLASSIFIED \*\*\*

-----  
GROUND CONSTANTS INPUTS  
-----

ENTER EITHER THE CCIR GROUND TYPE OR THE GROUND CONSTANTS:

- A - SEA WATER (20 DEGREES C)
- B - WET GROUND
- C - FRESH WATER (20 DEGREES C)
- D - MEDIUM DRY GROUND
- E - VERY DRY GROUND
- F - PURE WATER (NOT USED)
- G - ICE (FRESH WATER, -1 DEGREE C)
- H - ICE (FRESH WATER, -10 DEGREES C)

CCIR GROUND TYPE: [ D ]

- OR -

RELATIVE PERMITTIVITY: [       ]  
ELECTRICAL CONDUCTIVITY: [       ] (SIEMENS/M)

===== SCREEN NUMBER 6.1 =====\*\*\* UNCLASSIFIED \*\*\*

-----  
ATMOSPHERIC PARAMETER INPUTS  
-----

ENTER THE SEA-LEVEL ATMOSPHERIC REFRACTIVITY: [ 350.] (N-UNITS)

FOR FREQUENCY GREATER THAN 1 GHZ  
ENTER THE LOCAL SURFACE HUMIDITY: [ 10 ] (GRAMS/CUBIC METER)

===== SCREEN NUMBER 7.1 =====\*\*\* UNCLASSIFIED \*\*\*

-----  
PROFILE TYPE / TOPOGRAPHIC FILE INPUTS  
-----

ENTER THE TYPE OF PROFILE TO BE USED:

- [ 2] 1 - TOPOGRAPHIC FILE PROFILE  
2 - USER-ENTERED PROFILE

-----  
FOR TOPOGRAPHIC FILE PROFILE:  
-----

ENTER THE TOPOGRAPHIC DEFAULT ELEVATION (OPTIONAL): [ ] ( FT)

===== SCREEN NUMBER 12.1 =====\*\*\* UNCLASSIFIED \*\*\*

-----  
USER-ENTERED PROFILE TYPE INPUTS  
-----

ENTER THE TYPE OF USER-ENTERED PROFILE: [ 2]

## 1 - EQUALLY-SPACED PROFILE

ENTER THE DISTANCE BETWEEN PROFILE  
POINTS FOR EQUALLY-SPACED PROFILE: [ ] ( SM)

ENTER THE UNITS FOR ELEVATIONS: [ FT]

## 2 - UNEQUALLY-SPACED PROFILE

ENTER TRANSMITTER SITE ELEVATION FOR  
UNEQUALLY-SPACED PROFILE (POINT 1): [ 3000 ] ( FT)

ENTER THE UNITS FOR DISTANCES: [ SM]



===== SCREEN NUMBER 14.1 =====\*\*\* UNCLASSIFIED \*\*\*

-----  
 USER-ENTERED, UNEQUALLY-SPACED PROFILE INPUTS  
 -----

ENTER DISTANCE BETWEEN POINTS AND PROFILE ELEVATIONS FOR POINTS 2 - 9 :

DISTANCE UNITS: SM

ELEVATION UNITS: FT

-----  
 DIST: 3                    ELEV: 2000    |    DIST: 8                    ELEV: 3000    |  
 -----

DIST: 6                    ELEV: 2200    |    DIST: 2                    ELEV: 3200    |  
 -----

DIST: 17                   ELEV: 2900    |    DIST: 10                   ELEV: 2500    |  
 -----

DIST: 4                    ELEV: 3000    |    DIST:                      ELEV:           |  
 -----

\*\*\* THE LAST ELEVATION ENTERED MUST BE THE RX SITE ELEVATION \*\*\*

===== SCREEN NUMBER 15.1 =====\*\*\* UNCLASSIFIED \*\*\*

-----  
 VARIABILITY OPTIONS  
 -----

ENTER THE VARIABILITY OPTION:

- [ 1 ] 1 - LONG-TERM POWER-FADING STATISTICS
- 2 - MODELING VARIABILITY
- 3 - NO VARIABILITY CONSIDERED

ENTER THE PERCENTAGE OF A YEAR FOR WHICH THE LOSS IS NOT EXCEEDED: [ 99. ]

===== SCREEN NUMBER: 16.1 =====\*\*\* UNCLASSIFIED \*\*\*

-----  
CLIMATIC ZONE INPUTS  
-----

- 1 - CONTINENTAL TEMPERATE
- 2 - MARITIME TEMPERATE OVER LAND
- 3 - MARITIME TEMPERATE OVER WATER
- 4 - MARITIME SUBTROPICAL OVER LAND
- 5 - MEDITERRANEAN (NOT USED; USE 3 OR 4)
- 6 - DESERT
- 7 - EQUATORIAL
- 8 - CONTINENTAL SUBTROPICAL

ENTER THE CLIMATIC ZONE: [ 1 ]

===== SCREEN NUMBER: 17.1 =====\*\*\* UNCLASSIFIED \*\*\*

-----  
PARAMETER INCREMENT / DECREMENT OPTIONS  
-----

ENTER THE PARAMETER TO BE INCREMENTED/DECREMENTED:

- [ 2 ] 0 - NO PARAMETER INCREMENTING/DECREMENTING
- 1 - PROFILE ENDPOINTS (DECREMENTING)
- 2 - FREQUENCY
- 3 - TRANSMITTER ANTENNA STRUCTURAL HEIGHT
- 4 - RECEIVER ANTENNA STRUCTURAL HEIGHT
- 5 - VARIABILITY PERCENTAGE

===== SCREEN NUMBER 19.1 =====\*\*\* UNCLASSIFIED \*\*\*

-----  
FREQUENCY INCREMENT / DECREMENT INPUTS  
-----

=====  
: CURRENT FREQUENCY: 1000. (MHZ) :  
: ALLOWABLE RANGE: 20.00 - 20000. (MHZ) :  
=====

ENTER THE FINAL FREQUENCY VALUE: [ 8000 ] (MHZ)

ENTER THE INCREMENT/DECREMENT VALUE: [ 250 ] (MHZ)

CHOOSE THE TYPE OF INCREMENT/DECREMENT: [ +] + --> ADDITION  
- --> SUBTRACTION  
\* --> MULTIPLICATION  
/ --> DIVISION

===== SCREEN NUMBER 23.1 =====\*\*\* UNCLASSIFIED \*\*\*

-----  
OUTPUT OPTIONS  
-----

OUTPUT FROM TIREM CAN BE SENT TO THE SCREEN (IN FULL-SCREEN FORMAT), TO AN ASCII FILE, TO A PLOT FILE, OR ANY COMBINATION OF THE ABOVE. WHEN INCREMENTING / DECREMENTING A PARAMETER, A RESULTS SCREEN FOR EACH VALID VALUE OF THE PARAMETER IS GENERATED. IN FULL-SCREEN OUTPUT FORMAT, THE USER HITS TRANSMIT TO SEE EACH OF THESE RESULTS SCREENS IN SUCCESSION.

ENTER AN X IN THE DESIRED BOXES:

- [ X] OUTPUT RESULTS TO SCREEN IN FULL-SCREEN FORMAT
- [ X] OUTPUT RESULTS TO AN ASCII OUTPUT FILE  
ENTER ASCII FILE NAME: [ Wahid3.OUT ]
- [ ] OUTPUT PROFILE TO PLOT FILE  
ENTER PLOT FILE NAME: [ Wahid3.PLT ]

===== SCREEN NUMBER 24.1 =====\*\* UNCLASSIFIED \*\*\*

\*\*\*\*\* TTP TIREM INPUT PARAMETERS \*\*\*\*\*  
[ VERSION: 1.0 ]-----  
GENERAL PARAMETERS:

TOPOGRAPHIC DATA FILE: USER-ENTERED	PERMITTIVITY: 14.79108
DATUM CODE: 0	CONDUCTIVITY: .03311 (SIEMENS/M)
CLIMATIC ZONE: 1	REFRACTIVITY: 350. (N-UNITS)
VARIABILITY PERCENT: 99. (%)	HUMIDITY: 10. (GM/M**3)

-----  
TRANSMITTER PARAMETERS:

## RECEIVER PARAMETERS:

IDENTIFIER: [ TRANSMIT ]	IDENTIFIER: [ RECEIVER ]
ANTENNA HEIGHT: 100. (FT)	ANTENNA HEIGHT: 100. (FT)
SITE ELEVATION: 3000. (FT)	SITE ELEVATION: 3000. (FT)
LOCATION: - - - - -	LOCATION: - - - - -
MAXIMUM ANT DIM: 10. (FT)	MAXIMUM ANT DIM: 10. (FT)
ANTENNA GAIN: 30. (dBi)	ANTENNA GAIN: 30. (dBi)
FREQUENCY: 1000. (MHZ)	
POWER: 100. ( W )	
POLARIZATION: [V]	** TRANSMIT TO CONTINUE **

===== SCREEN NUMBER 25.1 =====\*\* UNCLASSIFIED \*\*\*

## \*\*\*\*\* TTP TIREM RESULTS [VERSION: 1.0] \*\*\*\*\*

STEPPING PARAMETER: FREQUENCY	CURRENT VALUE: 1000. (MHZ)
INCRMT/DECRMT VALUE: 250. (MHZ)	INCRMT/DECRMT TYPE: [+]

-----  
OUTPUT PARAMETERS:

## POWER FADING STATISTICS:

PROPAGATION MODE: DIFFRACTION			
TX TAKE-OFF ANGLE: .0 (DEG)	(%)	:	BASIC LOSS
RX TAKE-OFF ANGLE: -.1 (DEG)			
NEAR FLD BOUNDARY-TX: 203.65 (FT)	0.01	:	148.0
NEAR FLD BOUNDARY-RX: 203.65 (FT)	0.10	:	151.1
PATH LENGTH: 50. (SM)	1.00	:	154.7
PROPAGATION LOSS: 164.8 (dB)	10.00	:	159.8
FREE-SPACE LOSS: 130.6 (dB)	50.00	:	164.8
ABSORPTION LOSS: .4 (dB)	90.00	:	167.8
BEARING (TX-RX): .00 (DEG)	99.00	:	170.3
SCATTERING ANGLE: .355193 (DEG)	99.90	:	172.1
FIELD STRENGTH: .00032 (V/M)	99.99	:	173.6
POWER DENSITY: -69. (dBm/M**2)	99.00	:	170.3

-----  
\*\* TRANSMIT TO CONTINUE \*\*

===== SCREEN NUMBER 25.2 =====\*\* UNCLASSIFIED \*\*\*

\*\*\*\*\* TTP TIREM RESULTS [VERSION: 1.0] \*\*\*\*\*

STEPPING PARAMETER: FREQUENCY CURRENT VALUE: ~~1250.~~ (MHZ)
INCRMT/DECRMT VALUE: 250. (MHZ) INCRMT/DECRMT TYPE: [+]

Table with 2 main columns: OUTPUT PARAMETERS and POWER FADING STATISTICS. Includes rows for PROPAGATION MODE, TX TAKE-OFF ANGLE, RX TAKE-OFF ANGLE, NEAR FLD BOUNDARY-TX, NEAR FLD BOUNDARY-RX, PATH LENGTH, PROPAGATION LOSS, FREE-SPACE LOSS, ABSORPTION LOSS, BEARING (TX-RX), SCATTERING ANGLE, FIELD STRENGTH, and POWER DENSITY.

\*\* TRANSMIT TO CONTINUE \*\*

===== SCREEN NUMBER 25.3 =====\*\* UNCLASSIFIED \*\*\*

\*\*\*\*\* TTP TIREM RESULTS [VERSION: 1.0] \*\*\*\*\*

STEPPING PARAMETER: FREQUENCY CURRENT VALUE: 1500. (MHZ)
INCRMT/DECRMT VALUE: 250. (MHZ) INCRMT/DECRMT TYPE: [+]

Table with 2 main columns: OUTPUT PARAMETERS and POWER FADING STATISTICS. Includes rows for PROPAGATION MODE, TX TAKE-OFF ANGLE, RX TAKE-OFF ANGLE, NEAR FLD BOUNDARY-TX, NEAR FLD BOUNDARY-RX, PATH LENGTH, PROPAGATION LOSS, FREE-SPACE LOSS, ABSORPTION LOSS, BEARING (TX-RX), SCATTERING ANGLE, FIELD STRENGTH, and POWER DENSITY.

\*\* TRANSMIT TO CONTINUE \*\*

===== SCREEN NUMBER 25.4 =====\*\* UNCLASSIFIED \*\*\*

\*\*\*\*\* TTP TIREM RESULTS [VERSION: 1.0] \*\*\*\*\*

STEPPING PARAMETER: FREQUENCY CURRENT VALUE: 1750.1 (MHZ)
INCRMT/DECRMT VALUE: 250. (MHZ) INCRMT/DECRMT TYPE: [+]

Table with 4 columns: Parameter, Value, Percentage, Basic Loss. Rows include Propagation Mode (DIFFRACTION), TX/RX Take-off Angles, Near FLD Boundary (TX/RX), Path Length, Propagation Loss, Free-space Loss, Absorption Loss, Bearing, Scattering Angle, Field Strength, and Power Density.

\*\* TRANSMIT TO CONTINUE \*\*

===== SCREEN NUMBER 25.5 =====\*\* UNCLASSIFIED \*\*\*

\*\*\*\*\* TTP TIREM RESULTS [VERSION: 1.0] \*\*\*\*\*

STEPPING PARAMETER: FREQUENCY CURRENT VALUE: 2000. (MHZ)
INCRMT/DECRMT VALUE: 250. (MHZ) INCRMT/DECRMT TYPE: [+]

Table with 4 columns: Parameter, Value, Percentage, Basic Loss. Rows include Propagation Mode (DIFFRACTION), TX/RX Take-off Angles, Near FLD Boundary (TX/RX), Path Length, Propagation Loss, Free-space Loss, Absorption Loss, Bearing, Scattering Angle, Field Strength, and Power Density.

\*\* TRANSMIT TO CONTINUE \*\*

\*\*\*\*\* TTP TIREM RESULTS [VERSION: 1.0 ] \*\*\*\*\*

STEPPING PARAMETER: FREQUENCY CURRENT VALUE: ~~2250.00~~ 250.00 (MHZ)  
 INCRMT/DECRMT VALUE: 250.00 (MHZ) INCRMT/DECRMT TYPE: [+]

OUTPUT PARAMETERS:		POWER FADING STATISTICS:		
PROPAGATION MODE:	DIFFRACTION			
TX TAKE-OFF ANGLE:	.0 (DEG)	(%)	:	BASIC LOSS
RX TAKE-OFF ANGLE:	-.1 (DEG)			
NEAR FLD BOUNDARY-TX:	458.211 (FT)	0.01	:	155.5
NEAR FLD BOUNDARY-RX:	458.211 (FT)	0.10	:	158.1
PATH LENGTH:	50.0000 (SM)	1.00	:	161.3
PROPAGATION LOSS:	<del>170.0</del> 137.6 (dB)	10.00	:	165.6
FREE-SPACE LOSS:	137.6 (dB)	50.00	:	170.0
ABSORPTION LOSS:	.6 (dB)	90.00	:	172.7
BEARING (TX-RX):	.000000 (DEG)	99.00	:	175.0
SCATTERING ANGLE:	.355193 (DEG)	99.90	:	176.6
FIELD STRENGTH:	.00041 (V/M)	99.99	:	178.0
POWER DENSITY:	-67.00 (dBm/M**2)	99.00	:	175.0

\*\*\*\*\* TTP TIREM RESULTS [VERSION: 1.0 ] \*\*\*\*\*

STEPPING PARAMETER: FREQUENCY CURRENT VALUE: ~~2500.00~~ 250.00 (MHZ)  
 INCRMT/DECRMT VALUE: 250.00 (MHZ) INCRMT/DECRMT TYPE: [+]

OUTPUT PARAMETERS:		POWER FADING STATISTICS:		
PROPAGATION MODE:	DIFFRACTION			
TX TAKE-OFF ANGLE:	.0 (DEG)	(%)	:	BASIC LOSS
RX TAKE-OFF ANGLE:	-.1 (DEG)			
NEAR FLD BOUNDARY-TX:	509.123 (FT)	0.01	:	155.8
NEAR FLD BOUNDARY-RX:	509.123 (FT)	0.10	:	158.4
PATH LENGTH:	50.0000 (SM)	1.00	:	161.6
PROPAGATION LOSS:	<del>170.4</del> 138.5 (dB)	10.00	:	166.0
FREE-SPACE LOSS:	138.5 (dB)	50.00	:	170.4
ABSORPTION LOSS:	.7 (dB)	90.00	:	173.2
BEARING (TX-RX):	.000000 (DEG)	99.00	:	175.5
SCATTERING ANGLE:	.355193 (DEG)	99.90	:	177.1
FIELD STRENGTH:	.00043 (V/M)	99.99	:	178.5
POWER DENSITY:	-67.00 (dBm/M**2)	99.00	:	175.5

\*\*\*\*\* TTF TIREM RESULTS [VERSION: 1.0 ] \*\*\*\*\*

STEPPING PARAMETER: FREQUENCY CURRENT VALUE: ~~2750.00~~ (MHZ)  
 INCRMT/DECRMT VALUE: 250.00 (MHZ) INCRMT/DECRMT TYPE: [+]

OUTPUT PARAMETERS:		POWER FADING STATISTICS:	
PROPAGATION MODE:	DIFFRACTION		
TX TAKE-OFF ANGLE:	.0 (DEG)	(%)	BASIC LOSS
RX TAKE-OFF ANGLE:	-.1 (DEG)		
NEAR FLD BOUNDARY-TX:	560.036 (FT)	0.01	156.0
NEAR FLD BOUNDARY-RX:	560.036 (FT)	0.10	158.7
PATH LENGTH:	50.0000 (SM)	1.00	161.9
PROPAGATION LOSS:	<del>170.7</del> (dB)	10.00	166.3
FREE-SPACE LOSS:	139.3 (dB)	50.00	170.7
ABSORPTION LOSS:	.7 (dB)	90.00	173.5
BEARING (TX-RX):	.000000 (DEG)	99.00	175.8
SCATTERING ANGLE:	.355193 (DEG)	99.90	177.5
FIELD STRENGTH:	.00046 (V/M)	99.99	178.9
POWER DENSITY:	-66.00 (dBm/M**2)	99.00	175.8

\*\*\*\*\* TTF TIREM RESULTS [VERSION: 1.0 ] \*\*\*\*\*

STEPPING PARAMETER: FREQUENCY CURRENT VALUE: ~~3000.00~~ (MHZ)  
 INCRMT/DECRMT VALUE: 250.00 (MHZ) INCRMT/DECRMT TYPE: [+]

OUTPUT PARAMETERS:		POWER FADING STATISTICS:	
PROPAGATION MODE:	DIFFRACTION		
TX TAKE-OFF ANGLE:	.0 (DEG)	(%)	BASIC LOSS
RX TAKE-OFF ANGLE:	-.1 (DEG)		
NEAR FLD BOUNDARY-TX:	610.948 (FT)	0.01	156.2
NEAR FLD BOUNDARY-RX:	610.948 (FT)	0.10	158.8
PATH LENGTH:	50.0000 (SM)	1.00	162.1
PROPAGATION LOSS:	<del>171.0</del> (dB)	10.00	166.5
FREE-SPACE LOSS:	140.1 (dB)	50.00	170.9
ABSORPTION LOSS:	.8 (dB)	90.00	173.8
BEARING (TX-RX):	.000000 (DEG)	99.00	176.1
SCATTERING ANGLE:	.355193 (DEG)	99.90	177.8
FIELD STRENGTH:	.00048 (V/M)	99.99	179.2
POWER DENSITY:	-66.00 (dBm/M**2)	99.00	176.1



\*\*\*\*\* TTP TIREM RESULTS [VERSION: 1.0 ] \*\*\*\*\*

STEPPING PARAMETER: FREQUENCY CURRENT VALUE: ~~5250.00~~ 3500.00 (MHZ)  
 INCRMT/DECRMT VALUE: 250.00 (MHZ) INCRMT/DECRMT TYPE: [+]

OUTPUT PARAMETERS:		POWER FADING STATISTICS:		
PROPAGATION MODE:	DIFFRACTION			
TX TAKE-OFF ANGLE:	.0 (DEG)	(%)	:	BASIC LOSS
RX TAKE-OFF ANGLE:	-.1 (DEG)			
NEAR FLD BOUNDARY-TX:	661.860 (FT)	0.01	:	156.3
NEAR FLD BOUNDARY-RX:	661.860 (FT)	0.10	:	158.9
PATH LENGTH:	50.0000 (SM)	1.00	:	162.2
PROPAGATION LOSS:	<del>117.1</del> 140.8 (dB)	10.00	:	166.6
FREE-SPACE LOSS:	140.8 (dB)	50.00	:	171.1
ABSORPTION LOSS:	.8 (dB)	90.00	:	174.0
BEARING (TX-RX):	.000000 (DEG)	99.00	:	176.3
SCATTERING ANGLE:	.355193 (DEG)	99.90	:	178.0
FIELD STRENGTH:	.00051 (V/M)	99.99	:	179.4
POWER DENSITY:	-65.00 (dBm/M**2)	99.00	:	176.3

\*\*\*\*\* TTP TIREM RESULTS [VERSION: 1.0 ] \*\*\*\*\*

STEPPING PARAMETER: FREQUENCY CURRENT VALUE: ~~3500.00~~ 3500.00 (MHZ)  
 INCRMT/DECRMT VALUE: 250.00 (MHZ) INCRMT/DECRMT TYPE: [+]

OUTPUT PARAMETERS:		POWER FADING STATISTICS:		
PROPAGATION MODE:	DIFFRACTION			
TX TAKE-OFF ANGLE:	.0 (DEG)	(%)	:	BASIC LOSS
RX TAKE-OFF ANGLE:	-.1 (DEG)			
NEAR FLD BOUNDARY-TX:	712.773 (FT)	0.01	:	156.3
NEAR FLD BOUNDARY-RX:	712.773 (FT)	0.10	:	159.0
PATH LENGTH:	50.0000 (SM)	1.00	:	162.2
PROPAGATION LOSS:	171.2 (dB)	10.00	:	166.7
FREE-SPACE LOSS:	141.4 (dB)	50.00	:	171.2
ABSORPTION LOSS:	.8 (dB)	90.00	:	174.1
BEARING (TX-RX):	.000000 (DEG)	99.00	:	176.4
SCATTERING ANGLE:	.355193 (DEG)	99.90	:	178.1
FIELD STRENGTH:	.00054 (V/M)	99.99	:	179.5
POWER DENSITY:	-65.00 (dBm/M**2)	99.00	:	176.4

\*\*\*\*\* TTP TIREM RESULTS [VERSION: 1.0 ] \*\*\*\*\*

STEPPING PARAMETER: FREQUENCY CURRENT VALUE: ~~8750.00~~ (MHZ)  
 INCRMT/DECRMT VALUE: 250.00 (MHZ) INCRMT/DECRMT TYPE: [+]

OUTPUT PARAMETERS:		POWER FADING STATISTICS:	
PROPAGATION MODE:	DIFFRACTION		
TX TAKE-OFF ANGLE:	.0 (DEG)	(%)	BASIC LOSS
RX TAKE-OFF ANGLE:	-.1 (DEG)		
NEAR FLD BOUNDARY-TX:	763.685 (FT)	0.01	156.3
NEAR FLD BOUNDARY-RX:	763.685 (FT)	0.10	159.0
PATH LENGTH:	50.0000 (SM)	1.00	162.3
PROPAGATION LOSS:	171.3 (dB)	10.00	166.8
FREE-SPACE LOSS:	142.0 (dB)	50.00	171.3
ABSORPTION LOSS:	.9 (dB)	90.00	174.2
BEARING (TX-RX):	.000000 (DEG)	99.00	176.5
SCATTERING ANGLE:	.355193 (DEG)	99.90	178.2
FIELD STRENGTH:	.00058 (V/M)	99.99	179.6
POWER DENSITY:	-64.00 (dBm/M**2)	99.00	176.5

\*\*\*\*\* TTP TIREM RESULTS [VERSION: 1.0 ] \*\*\*\*\*

STEPPING PARAMETER: FREQUENCY CURRENT VALUE: ~~4000.00~~ (MHZ)  
 INCRMT/DECRMT VALUE: 250.00 (MHZ) INCRMT/DECRMT TYPE: [+]

OUTPUT PARAMETERS:		POWER FADING STATISTICS:	
PROPAGATION MODE:	DIFFRACTION		
TX TAKE-OFF ANGLE:	.0 (DEG)	(%)	BASIC LOSS
RX TAKE-OFF ANGLE:	-.1 (DEG)		
NEAR FLD BOUNDARY-TX:	814.598 (FT)	0.01	156.2
NEAR FLD BOUNDARY-RX:	814.598 (FT)	0.10	159.0
PATH LENGTH:	50.0000 (SM)	1.00	162.3
PROPAGATION LOSS:	171.3 (dB)	10.00	166.8
FREE-SPACE LOSS:	142.6 (dB)	50.00	171.3
ABSORPTION LOSS:	.9 (dB)	90.00	174.2
BEARING (TX-RX):	.000000 (DEG)	99.00	176.6
SCATTERING ANGLE:	.355193 (DEG)	99.90	178.3
FIELD STRENGTH:	.00061 (V/M)	99.99	179.7
POWER DENSITY:	-64.00 (dBm/M**2)	99.00	176.6

\*\*\*\*\* TTP TIREM RESULTS [VERSION: 1.0 ] \*\*\*\*\*

STEPPING PARAMETER: FREQUENCY CURRENT VALUE: 250.00 (MHZ)  
 INCRMT/DECRMT VALUE: 250.00 (MHZ) INCRMT/DECRMT TYPE: [+]

OUTPUT PARAMETERS:		POWER FADING STATISTICS:		
PROPAGATION MODE: DIFFRACTION			(%)	BASIC LOSS
TX TAKE-OFF ANGLE:	.0 (DEG)			
RX TAKE-OFF ANGLE:	-.1 (DEG)			
NEAR FLD BOUNDARY-TX:	865.510 (FT)	0.01	:	156.5
NEAR FLD BOUNDARY-RX:	865.510 (FT)	0.10	:	159.2
PATH LENGTH:	50.0000 (SM)	1.00	:	162.5
PROPAGATION LOSS:	171.86 (dB)	10.00	:	167.1
FREE-SPACE LOSS:	143.1 (dB)	50.00	:	171.6
ABSORPTION LOSS:	1.0 (dB)	90.00	:	174.5
BEARING (TX-RX):	.000000 (DEG)	99.00	:	176.9
SCATTERING ANGLE:	.355193 (DEG)	99.90	:	178.6
FIELD STRENGTH:	.00063 (V/M)	99.99	:	180.1
POWER DENSITY:	-63.00 (dBm/M**2)	99.00	:	176.9

\*\*\*\*\* TTP TIREM RESULTS [VERSION: 1.0 ] \*\*\*\*\*

STEPPING PARAMETER: FREQUENCY CURRENT VALUE: 4500.00 (MHZ)  
 INCRMT/DECRMT VALUE: 250.00 (MHZ) INCRMT/DECRMT TYPE: [+]

OUTPUT PARAMETERS:		POWER FADING STATISTICS:		
PROPAGATION MODE: DIFFRACTION			(%)	BASIC LOSS
TX TAKE-OFF ANGLE:	.0 (DEG)			
RX TAKE-OFF ANGLE:	-.1 (DEG)			
NEAR FLD BOUNDARY-TX:	916.422 (FT)	0.01	:	156.9
NEAR FLD BOUNDARY-RX:	916.422 (FT)	0.10	:	159.6
PATH LENGTH:	50.0000 (SM)	1.00	:	162.9
PROPAGATION LOSS:	172.1 (dB)	10.00	:	167.5
FREE-SPACE LOSS:	143.6 (dB)	50.00	:	172.0
ABSORPTION LOSS:	1.0 (dB)	90.00	:	175.0
BEARING (TX-RX):	.000000 (DEG)	99.00	:	177.4
SCATTERING ANGLE:	.355193 (DEG)	99.90	:	179.1
FIELD STRENGTH:	.00063 (V/M)	99.99	:	180.5
POWER DENSITY:	-63.00 (dBm/M**2)	99.00	:	177.4

\*\*\*\*\* TTP TIREM RESULTS [VERSION: 1.0 ] \*\*\*\*\*

STEPPING PARAMETER: FREQUENCY CURRENT VALUE: ~~4750.00~~ (MHZ)  
 INCRMT/DECRMT VALUE: 250.00 (MHZ) INCRMT/DECRMT TYPE: [+]

OUTPUT PARAMETERS:		POWER FADING STATISTICS:		
PROPAGATION MODE:	DIFFRACTION			
TX TAKE-OFF ANGLE:	.0 (DEG)	(%)	:	BASIC LOSS
RX TAKE-OFF ANGLE:	-.1 (DEG)			
NEAR FLD BOUNDARY-TX:	967.335 (FT)	0.01	:	157.2
NEAR FLD BOUNDARY-RX:	967.335 (FT)	0.10	:	160.0
PATH LENGTH:	50.0000 (SM)	1.00	:	163.3
PROPAGATION LOSS:	<del>172.5</del> (dB)	10.00	:	167.9
FREE-SPACE LOSS:	144.1 (dB)	50.00	:	172.4
ABSORPTION LOSS:	1.0 (dB)	90.00	:	175.4
BEARING (TX-RX):	.000000 (DEG)	99.00	:	177.8
SCATTERING ANGLE:	.355193 (DEG)	99.90	:	179.5
FIELD STRENGTH:	.00063 (V/M)	99.99	:	181.0
POWER DENSITY:	-63.00 (dBm/M**2)	99.00	:	177.8

\*\*\*\*\* TTP TIREM RESULTS [VERSION: 1.0 ] \*\*\*\*\*

STEPPING PARAMETER: FREQUENCY CURRENT VALUE: ~~5000.00~~ (MHZ)  
 INCRMT/DECRMT VALUE: 250.00 (MHZ) INCRMT/DECRMT TYPE: [+]

OUTPUT PARAMETERS:		POWER FADING STATISTICS:		
PROPAGATION MODE:	DIFFRACTION			
TX TAKE-OFF ANGLE:	.0 (DEG)	(%)	:	BASIC LOSS
RX TAKE-OFF ANGLE:	-.1 (DEG)			
NEAR FLD BOUNDARY-TX:	1018.247 (FT)	0.01	:	157.6
NEAR FLD BOUNDARY-RX:	1018.247 (FT)	0.10	:	160.3
PATH LENGTH:	50.0000 (SM)	1.00	:	163.7
PROPAGATION LOSS:	<del>172.9</del> (dB)	10.00	:	168.2
FREE-SPACE LOSS:	144.5 (dB)	50.00	:	172.8
ABSORPTION LOSS:	1.1 (dB)	90.00	:	175.8
BEARING (TX-RX):	.000000 (DEG)	99.00	:	178.2
SCATTERING ANGLE:	.355193 (DEG)	99.90	:	179.9
FIELD STRENGTH:	.00064 (V/M)	99.99	:	181.4
POWER DENSITY:	-63.00 (dBm/M**2)	99.00	:	178.2

\*\*\*\*\* TTF TIREM RESULTS [VERSION: 1.0 ] \*\*\*\*\*

STEPPING PARAMETER: FREQUENCY CURRENT VALUE: ~~5250.00~~ (MHZ)  
 INCRMT/DECRMT VALUE: 250.00 (MHZ) INCRMT/DECRMT TYPE: [+]

OUTPUT PARAMETERS:		POWER FADING STATISTICS:		
PROPAGATION MODE:	DIFFRACTION			
TX TAKE-OFF ANGLE:	.0 (DEG)	(%)	:	BASIC LOSS
RX TAKE-OFF ANGLE:	-.1 (DEG)			
NEAR FLD BOUNDARY-TX:	1069.159 (FT)	0.01	:	157.8
NEAR FLD BOUNDARY-RX:	1069.159 (FT)	0.10	:	160.6
PATH LENGTH:	50.0000 (SM)	1.00	:	164.0
PROPAGATION LOSS:	<del>173.2</del> (dB)	10.00	:	168.5
FREE-SPACE LOSS:	145.0 (dB)	50.00	:	173.1
ABSORPTION LOSS:	1.1 (dB)	90.00	:	176.1
BEARING (TX-RX):	.000000 (DEG)	99.00	:	178.5
SCATTERING ANGLE:	.355193 (DEG)	99.90	:	180.3
FIELD STRENGTH:	.00064 (V/M)	99.99	:	181.7
POWER DENSITY:	-63.00 (dBm/M**2)	99.00	:	178.5

\*\*\*\*\* TTF TIREM RESULTS [VERSION: 1.0 ] \*\*\*\*\*

STEPPING PARAMETER: FREQUENCY CURRENT VALUE: ~~5500.00~~ (MHZ)  
 INCRMT/DECRMT VALUE: 250.00 (MHZ) INCRMT/DECRMT TYPE: [+]

OUTPUT PARAMETERS:		POWER FADING STATISTICS:		
PROPAGATION MODE:	DIFFRACTION			
TX TAKE-OFF ANGLE:	.0 (DEG)	(%)	:	BASIC LOSS
RX TAKE-OFF ANGLE:	-.1 (DEG)			
NEAR FLD BOUNDARY-TX:	1120.072 (FT)	0.01	:	158.3
NEAR FLD BOUNDARY-RX:	1120.072 (FT)	0.10	:	161.1
PATH LENGTH:	50.0000 (SM)	1.00	:	164.5
PROPAGATION LOSS:	<del>173.7</del> (dB)	10.00	:	169.1
FREE-SPACE LOSS:	145.4 (dB)	50.00	:	173.7
ABSORPTION LOSS:	1.1 (dB)	90.00	:	176.6
BEARING (TX-RX):	.000000 (DEG)	99.00	:	179.1
SCATTERING ANGLE:	.355193 (DEG)	99.90	:	180.8
FIELD STRENGTH:	.00063 (V/M)	99.99	:	182.3
POWER DENSITY:	-63.00 (dBm/M**2)	99.00	:	179.1

\*\*\*\*\* TTP TIREM RESULTS [VERSION: 1.0 ] \*\*\*\*\*

STEPPING PARAMETER: FREQUENCY CURRENT VALUE: ~~5750.00~~ (MHZ)  
 INCRMT/DECRMT VALUE: 250.00 (MHZ) INCRMT/DECRMT TYPE: [+]

OUTPUT PARAMETERS:		POWER FADING STATISTICS:	
PROPAGATION MODE:	DIFFRACTION		
TX TAKE-OFF ANGLE:	.0 (DEG)	(%)	BASIC LOSS
RX TAKE-OFF ANGLE:	-.1 (DEG)		
NEAR FLD BOUNDARY-TX:	1170.984 (FT)	0.01	158.9
NEAR FLD BOUNDARY-RX:	1170.984 (FT)	0.10	161.7
PATH LENGTH:	50.0000 (SM)	1.00	165.0
PROPAGATION LOSS:	<del>174.3</del> 145.8 (dB)	10.00	169.7
FREE-SPACE LOSS:	145.8 (dB)	50.00	174.3
ABSORPTION LOSS:	1.2 (dB)	90.00	177.2
BEARING (TX-RX):	.000000 (DEG)	99.00	179.7
SCATTERING ANGLE:	.355193 (DEG)	99.90	181.5
FIELD STRENGTH:	.00061 (V/M)	99.99	182.9
POWER DENSITY:	-63.00 (dBm/M**2)	99.00	179.7

\*\*\*\*\* TTP TIREM RESULTS [VERSION: 1.0 ] \*\*\*\*\*

STEPPING PARAMETER: FREQUENCY CURRENT VALUE: 6000.00 (MHZ)  
 INCRMT/DECRMT VALUE: 250.00 (MHZ) INCRMT/DECRMT TYPE: [+]

OUTPUT PARAMETERS:		POWER FADING STATISTICS:	
PROPAGATION MODE:	DIFFRACTION		
TX TAKE-OFF ANGLE:	.0 (DEG)	(%)	BASIC LOSS
RX TAKE-OFF ANGLE:	-.1 (DEG)		
NEAR FLD BOUNDARY-TX:	1221.896 (FT)	0.01	159.4
NEAR FLD BOUNDARY-RX:	1221.896 (FT)	0.10	162.2
PATH LENGTH:	50.0000 (SM)	1.00	165.6
PROPAGATION LOSS:	174.9 (dB)	10.00	170.2
FREE-SPACE LOSS:	146.1 (dB)	50.00	174.8
ABSORPTION LOSS:	1.2 (dB)	90.00	177.8
BEARING (TX-RX):	.000000 (DEG)	99.00	180.3
SCATTERING ANGLE:	.355193 (DEG)	99.90	182.1
FIELD STRENGTH:	.00060 (V/M)	99.99	183.5
POWER DENSITY:	-64.00 (dBm/M**2)	99.00	180.3

\*\*\*\*\* TTP TIREM RESULTS [VERSION: 1.0 ] \*\*\*\*\*

STEPPING PARAMETER: FREQUENCY CURRENT VALUE: ~~6250.00~~ (MHZ)  
 INCRMT/DECRMT VALUE: 250.00 (MHZ) INCRMT/DECRMT TYPE: [+]

OUTPUT PARAMETERS:		POWER FADING STATISTICS:	
PROPAGATION MODE:	DIFFRACTION		
TX TAKE-OFF ANGLE:	.0 (DEG)	(%)	BASIC LOSS
RX TAKE-OFF ANGLE:	-.1 (DEG)		
NEAR FLD BOUNDARY-TX:	1272.809 (FT)	0.01	160.0
NEAR FLD BOUNDARY-RX:	1272.809 (FT)	0.10	162.8
PATH LENGTH:	50.0000 (SM)	1.00	166.1
PROPAGATION LOSS:	<del>175.5</del> (dB)	10.00	170.8
FREE-SPACE LOSS:	146.5 (dB)	50.00	175.4
ABSORPTION LOSS:	1.2 (dB)	90.00	178.4
BEARING (TX-RX):	.000000 (DEG)	99.00	180.9
SCATTERING ANGLE:	.355193 (DEG)	99.90	182.6
FIELD STRENGTH:	.00058 (V/M)	99.99	184.1
POWER DENSITY:	-64.00 (dBm/M**2)	99.00	180.9

\*\*\*\*\* TTP TIREM RESULTS [VERSION: 1.0 ] \*\*\*\*\*

STEPPING PARAMETER: FREQUENCY CURRENT VALUE: ~~6500.00~~ (MHZ)  
 INCRMT/DECRMT VALUE: 250.00 (MHZ) INCRMT/DECRMT TYPE: [+]

OUTPUT PARAMETERS:		POWER FADING STATISTICS:	
PROPAGATION MODE:	DIFFRACTION		
TX TAKE-OFF ANGLE:	.0 (DEG)	(%)	BASIC LOSS
RX TAKE-OFF ANGLE:	-.1 (DEG)		
NEAR FLD BOUNDARY-TX:	1323.721 (FT)	0.01	160.5
NEAR FLD BOUNDARY-RX:	1323.721 (FT)	0.10	163.3
PATH LENGTH:	50.0000 (SM)	1.00	166.7
PROPAGATION LOSS:	<del>176.0</del> (dB)	10.00	171.3
FREE-SPACE LOSS:	146.8 (dB)	50.00	175.9
ABSORPTION LOSS:	1.2 (dB)	90.00	178.9
BEARING (TX-RX):	.000000 (DEG)	99.00	181.4
SCATTERING ANGLE:	.355193 (DEG)	99.90	183.2
FIELD STRENGTH:	.00057 (V/M)	99.99	184.7
POWER DENSITY:	-64.00 (dBm/M**2)	99.00	181.4

\*\*\*\*\* TTP TIREM RESULTS [VERSION: 1.0 ] \*\*\*\*\*

STEPPING PARAMETER: FREQUENCY CURRENT VALUE: ~~6750.00~~ 7000.00 (MHZ)  
 INCRMT/DECRMT VALUE: 250.00 (MHZ) INCRMT/DECRMT TYPE: [+]

OUTPUT PARAMETERS:		POWER FADING STATISTICS:		
PROPAGATION MODE:	DIFFRACTION			
TX TAKE-OFF ANGLE:	.0 (DEG)	(%)	:	BASIC LOSS
RX TAKE-OFF ANGLE:	-.1 (DEG)			
NEAR FLD BOUNDARY-TX:	1374.633 (FT)	0.01	:	161.0
NEAR FLD BOUNDARY-RX:	1374.633 (FT)	0.10	:	163.8
PATH LENGTH:	50.0000 (SM)	1.00	:	167.2
PROPAGATION LOSS:	<del>176.5</del> 177.0 (dB)	10.00	:	171.8
FREE-SPACE LOSS:	147.1 (dB)	50.00	:	176.5
ABSORPTION LOSS:	1.3 (dB)	90.00	:	179.5
BEARING (TX-RX):	.000000 (DEG)	99.00	:	181.9
SCATTERING ANGLE:	.355193 (DEG)	99.90	:	183.7
FIELD STRENGTH:	.00056 (V/M)	99.99	:	185.2
POWER DENSITY:	-64.00 (dBm/M**2)	99.00	:	181.9

\*\*\*\*\* TTP TIREM RESULTS [VERSION: 1.0 ] \*\*\*\*\*

STEPPING PARAMETER: FREQUENCY CURRENT VALUE: ~~7000.00~~ 7000.00 (MHZ)  
 INCRMT/DECRMT VALUE: 250.00 (MHZ) INCRMT/DECRMT TYPE: [+]

OUTPUT PARAMETERS:		POWER FADING STATISTICS:		
PROPAGATION MODE:	DIFFRACTION			
TX TAKE-OFF ANGLE:	.0 (DEG)	(%)	:	BASIC LOSS
RX TAKE-OFF ANGLE:	-.1 (DEG)			
NEAR FLD BOUNDARY-TX:	1425.546 (FT)	0.01	:	161.4
NEAR FLD BOUNDARY-RX:	1425.546 (FT)	0.10	:	164.2
PATH LENGTH:	50.0000 (SM)	1.00	:	167.6
PROPAGATION LOSS:	177.0 (dB)	10.00	:	172.3
FREE-SPACE LOSS:	147.5 (dB)	50.00	:	177.0
ABSORPTION LOSS:	1.3 (dB)	90.00	:	180.0
BEARING (TX-RX):	.000000 (DEG)	99.00	:	182.5
SCATTERING ANGLE:	.355193 (DEG)	99.90	:	184.2
FIELD STRENGTH:	.00054 (V/M)	99.99	:	185.7
POWER DENSITY:	-65.00 (dBm/M**2)	99.00	:	182.5



\*\*\*\*\* TTP TIREM RESULTS [VERSION: 1.0 ] \*\*\*\*\*

STEPPING PARAMETER: FREQUENCY CURRENT VALUE: ~~7500.00~~ (MHZ)  
 INCRMT/DECRMT VALUE: 250.00 (MHZ) INCRMT/DECRMT TYPE: [+]

OUTPUT PARAMETERS:		POWER FADING STATISTICS:	
PROPAGATION MODE:	DIFFRACTION		
TX TAKE-OFF ANGLE:	.0 (DEG)	(%)	BASIC LOSS
RX TAKE-OFF ANGLE:	-.1 (DEG)		
NEAR FLD BOUNDARY-TX:	1476.458 (FT)	0.01	161.9
NEAR FLD BOUNDARY-RX:	1476.458 (FT)	0.10	164.7
PATH LENGTH:	50.0000 (SM)	1.00	168.1
PROPAGATION LOSS:	<del>177.5</del> (dB)	10.00	172.8
FREE-SPACE LOSS:	147.8 (dB)	50.00	177.4
ABSORPTION LOSS:	1.3 (dB)	90.00	180.5
BEARING (TX-RX):	.000000 (DEG)	99.00	183.0
SCATTERING ANGLE:	.355193 (DEG)	99.90	184.7
FIELD STRENGTH:	.00053 (V/M)	99.99	186.2
POWER DENSITY:	-65.00 (dBm/M**2)	99.00	183.0

\*\*\*\*\* TTP TIREM RESULTS [VERSION: 1.0 ] \*\*\*\*\*

STEPPING PARAMETER: FREQUENCY CURRENT VALUE: ~~7500.00~~ (MHZ)  
 INCRMT/DECRMT VALUE: 250.00 (MHZ) INCRMT/DECRMT TYPE: [+]

OUTPUT PARAMETERS:		POWER FADING STATISTICS:	
PROPAGATION MODE:	DIFFRACTION		
TX TAKE-OFF ANGLE:	.0 (DEG)	(%)	BASIC LOSS
RX TAKE-OFF ANGLE:	-.1 (DEG)		
NEAR FLD BOUNDARY-TX:	1527.370 (FT)	0.01	162.3
NEAR FLD BOUNDARY-RX:	1527.370 (FT)	0.10	165.1
PATH LENGTH:	50.0000 (SM)	1.00	168.6
PROPAGATION LOSS:	<del>178.0</del> (dB)	10.00	173.2
FREE-SPACE LOSS:	148.1 (dB)	50.00	177.9
ABSORPTION LOSS:	1.4 (dB)	90.00	180.9
BEARING (TX-RX):	.000000 (DEG)	99.00	183.4
SCATTERING ANGLE:	.355193 (DEG)	99.90	185.2
FIELD STRENGTH:	.00052 (V/M)	99.99	186.7
POWER DENSITY:	-65.00 (dBm/M**2)	99.00	183.4

\*\*\*\*\* TTP TIREM RESULTS [VERSION: 1.0 ] \*\*\*\*\*

STEPPING PARAMETER: FREQUENCY CURRENT VALUE: ~~7750490~~ (MHZ)  
 INCRMT/DECRMT VALUE: 250.00 (MHZ) INCRMT/DECRMT TYPE: [+]

OUTPUT PARAMETERS:		POWER FADING STATISTICS:		
PROPAGATION MODE:	DIFFRACTION			
TX TAKE-OFF ANGLE:	.0 (DEG)	(%)	:	BASIC LOSS
RX TAKE-OFF ANGLE:	-.1 (DEG)			
NEAR FLD BOUNDARY-TX:	1578.283 (FT)	0.01	:	162.8
NEAR FLD BOUNDARY-RX:	1578.283 (FT)	0.10	:	165.6
PATH LENGTH:	50.0000 (SM)	1.00	:	169.0
PROPAGATION LOSS:	178.4 (dB)	10.00	:	173.7
FREE-SPACE LOSS:	148.3 (dB)	50.00	:	178.4
ABSORPTION LOSS:	1.4 (dB)	90.00	:	181.4
BEARING (TX-RX):	.000000 (DEG)	99.00	:	183.9
SCATTERING ANGLE:	.355193 (DEG)	99.90	:	185.7
FIELD STRENGTH:	.00051 (V/M)	99.99	:	187.2
POWER DENSITY:	-65.00 (dBm/M**2)	99.00	:	183.9

\*\*\*\*\* TTP TIREM RESULTS [VERSION: 1.0 ] \*\*\*\*\*

STEPPING PARAMETER: FREQUENCY CURRENT VALUE: ~~8000.00~~ (MHZ)  
 INCRMT/DECRMT VALUE: 250.00 (MHZ) INCRMT/DECRMT TYPE: [+]

OUTPUT PARAMETERS:		POWER FADING STATISTICS:		
PROPAGATION MODE:	DIFFRACTION			
TX TAKE-OFF ANGLE:	.0 (DEG)	(%)	:	BASIC LOSS
RX TAKE-OFF ANGLE:	-.1 (DEG)			
NEAR FLD BOUNDARY-TX:	1629.195 (FT)	0.01	:	163.2
NEAR FLD BOUNDARY-RX:	1629.195 (FT)	0.10	:	166.0
PATH LENGTH:	50.0000 (SM)	1.00	:	169.4
PROPAGATION LOSS:	178.9 (dB)	10.00	:	174.1
FREE-SPACE LOSS:	148.6 (dB)	50.00	:	178.8
ABSORPTION LOSS:	1.4 (dB)	90.00	:	181.9
BEARING (TX-RX):	.000000 (DEG)	99.00	:	184.4
SCATTERING ANGLE:	.355193 (DEG)	99.90	:	186.2
FIELD STRENGTH:	.00050 (V/M)	99.99	:	187.6
POWER DENSITY:	-65.00 (dBm/M**2)	99.00	:	184.4

\*\*\*\*\* TTP TIREM INPUT PARAMETERS \*\*\*\*\*  
 [ VERSION: 1.0 ]

GENERAL PARAMETERS:

TOPOGRAPHIC DATA FILE: USER-ENTERED	PERMITTIVITY: 13.0831
DATUM CODE: 0	CONDUCTIVITY: 1.14280 (SIEMEN/M)
CLIMATIC ZONE: 1	REFRACTIVITY: 350.0 (N-UNITS)
VARIABILITY PERCENT: 99.00 (%)	HUMIDITY: 10. (GM/M**3)

TRANSMITTER PARAMETERS:

IDENTIFIER: [ TRANSMIT ]  
 ANTENNA HEIGHT: 100.00 (FT)  
 SITE ELEVATION: 3000.00 (FT)  
 LOCATION: - - - - -  
 MAXIMUM ANT DIM: 10.00 (FT)  
 ANTENNA GAIN: 30.00 (dBi)  
 FREQUENCY: 8250.00 (MHZ)  
 TX POWER: 100.00 ( W )  
 POLARIZATION: [V]

RECEIVER PARAMETERS:

IDENTIFIER: [ RECEIVER ]  
 ANTENNA HEIGHT: 100.00 (FT)  
 SITE ELEVATION: 3000.00 (FT)  
 LOCATION: - - - - -  
 MAXIMUM ANT DIM: 10.00 (FT)  
 ANTENNA GAIN: 30.00 (dBi)

\*\*\*\*\* TTP TIREM RESULTS [VERSION: 1.0 ] \*\*\*\*\*

STEPPING PARAMETER: FREQUENCY CURRENT VALUE: 8250.00 (MHZ)  
 INCRMT/DECRMT VALUE: 250.00 (MHZ) INCRMT/DECRMT TYPE: [+]

OUTPUT PARAMETERS:

PROPAGATION MODE: DIFFRACTION  
 TX TAKE-OFF ANGLE: .0 (DEG)  
 RX TAKE-OFF ANGLE: -.1 (DEG)  
 NEAR FLD BOUNDARY-TX: 1680.107 (FT)  
 NEAR FLD BOUNDARY-RX: 1680.107 (FT)  
 PATH LENGTH: 50.0000 (SM)  
 PROPAGATION LOSS: .179.3 (dB)  
 FREE-SPACE LOSS: 148.9 (dB)  
 ABSORPTION LOSS: 1.4 (dB)  
 BEARING (TX-RX): .000000 (DEG)  
 SCATTERING ANGLE: .355193 (DEG)  
 FIELD STRENGTH: .00049 (V/M)  
 POWER DENSITY: -65.00 (dBm/M\*\*2)

POWER FADING STATISTICS:

(%)	:	BASIC LOSS
0.01	:	163.6
0.10	:	166.4
1.00	:	169.8
10.00	:	174.5
50.00	:	179.2
90.00	:	182.3
99.00	:	184.8
99.90	:	186.6
99.99	:	188.1
99.00	:	184.8

\*\*\*\*\* TTP TIREM RESULTS [VERSION: 1.0 ] \*\*\*\*\*

STEPPING PARAMETER: FREQUENCY CURRENT VALUE: ~~8500.00~~ (MHZ)  
 INCRMT/DECRMT VALUE: 250.00 (MHZ) INCRMT/DECRMT TYPE: [+]

OUTPUT PARAMETERS:		POWER FADING STATISTICS:	
PROPAGATION MODE:	DIFFRACTION		
TX TAKE-OFF ANGLE:	.0 (DEG)	(%)	BASIC LOSS
RX TAKE-OFF ANGLE:	-.1 (DEG)		
NEAR FLD BOUNDARY-TX:	1731.020 (FT)	0.01	164.0
NEAR FLD BOUNDARY-RX:	1731.020 (FT)	0.10	166.8
PATH LENGTH:	50.0000 (SM)	1.00	170.2
PROPAGATION LOSS:	<del>179.97</del> (dB)	10.00	174.9
FREE-SPACE LOSS:	149.1 (dB)	50.00	179.7
ABSORPTION LOSS:	1.5 (dB)	90.00	182.7
BEARING (TX-RX):	.000000 (DEG)	99.00	185.2
SCATTERING ANGLE:	.355193 (DEG)	99.90	187.0
FIELD STRENGTH:	.00048 (V/M)	99.99	188.5
POWER DENSITY:	-66.00 (dBm/M**2)	99.00	185.2

\*\*\*\*\* TTP TIREM RESULTS [VERSION: 1.0 ] \*\*\*\*\*

STEPPING PARAMETER: FREQUENCY CURRENT VALUE: ~~8750.00~~ (MHZ)  
 INCRMT/DECRMT VALUE: 250.00 (MHZ) INCRMT/DECRMT TYPE: [+]

OUTPUT PARAMETERS:		POWER FADING STATISTICS:	
PROPAGATION MODE:	DIFFRACTION		
TX TAKE-OFF ANGLE:	.0 (DEG)	(%)	BASIC LOSS
RX TAKE-OFF ANGLE:	-.1 (DEG)		
NEAR FLD BOUNDARY-TX:	1781.932 (FT)	0.01	164.4
NEAR FLD BOUNDARY-RX:	1781.932 (FT)	0.10	167.2
PATH LENGTH:	50.0000 (SM)	1.00	170.6
PROPAGATION LOSS:	180.1 (dB)	10.00	175.3
FREE-SPACE LOSS:	149.4 (dB)	50.00	180.1
ABSORPTION LOSS:	1.5 (dB)	90.00	183.1
BEARING (TX-RX):	.000000 (DEG)	99.00	185.6
SCATTERING ANGLE:	.355193 (DEG)	99.90	187.4
FIELD STRENGTH:	.00047 (V/M)	99.99	188.9
POWER DENSITY:	-66.00 (dBm/M**2)	99.00	185.6

\*\*\*\*\* TTP TIREM RESULTS [VERSION: 1.0 ] \*\*\*\*\*

STEPPING PARAMETER: FREQUENCY CURRENT VALUE: ~~9000.00~~ (MHZ)  
 INCRMT/DECRMT VALUE: 250.00 (MHZ) INCRMT/DECRMT TYPE: [+]

OUTPUT PARAMETERS:		POWER FADING STATISTICS:	
PROPAGATION MODE:	DIFFRACTION		
TX TAKE-OFF ANGLE:	.0 (DEG)	(%)	BASIC LOSS
RX TAKE-OFF ANGLE:	-.1 (DEG)		
NEAR FLD BOUNDARY-TX:	1832.844 (FT)	0.01	164.7
NEAR FLD BOUNDARY-RX:	1832.844 (FT)	0.10	167.6
PATH LENGTH:	50.0000 (SM)	1.00	171.0
PROPAGATION LOSS:	<del>180.5</del> (dB)	10.00	175.7
FREE-SPACE LOSS:	149.6 (dB)	50.00	180.5
ABSORPTION LOSS:	1.5 (dB)	90.00	183.5
BEARING (TX-RX):	.000000 (DEG)	99.00	186.0
SCATTERING ANGLE:	.355193 (DEG)	99.90	187.8
FIELD STRENGTH:	.00046 (V/M)	99.99	189.4
POWER DENSITY:	-66.00 (dBm/M**2)	99.00	186.0

\*\*\*\*\* TTP TIREM RESULTS [VERSION: 1.0 ] \*\*\*\*\*

STEPPING PARAMETER: FREQUENCY CURRENT VALUE: 9250.00 (MHZ)  
 INCRMT/DECRMT VALUE: 250.00 (MHZ) INCRMT/DECRMT TYPE: [+]

OUTPUT PARAMETERS:		POWER FADING STATISTICS:	
PROPAGATION MODE:	DIFFRACTION		
TX TAKE-OFF ANGLE:	.0 (DEG)	(%)	BASIC LOSS
RX TAKE-OFF ANGLE:	-.1 (DEG)		
NEAR FLD BOUNDARY-TX:	1883.757 (FT)	0.01	165.1
NEAR FLD BOUNDARY-RX:	1883.757 (FT)	0.10	167.9
PATH LENGTH:	50.0000 (SM)	1.00	171.4
PROPAGATION LOSS:	<del>180.9</del> (dB)	10.00	176.1
FREE-SPACE LOSS:	149.9 (dB)	50.00	180.8
ABSORPTION LOSS:	1.5 (dB)	90.00	183.9
BEARING (TX-RX):	.000000 (DEG)	99.00	186.4
SCATTERING ANGLE:	.355193 (DEG)	99.90	188.2
FIELD STRENGTH:	.00046 (V/M)	99.99	189.8
POWER DENSITY:	-66.00 (dBm/M**2)	99.00	186.4

\*\*\*\*\* TTP TIREM RESULTS [VERSION: 1.0 ] \*\*\*\*\*

STEPPING PARAMETER: FREQUENCY CURRENT VALUE: ~~3500.00~~ (MHZ)  
 INCRMT/DECRMT VALUE: 250.00 (MHZ) INCRMT/DECRMT TYPE: [+]

OUTPUT PARAMETERS:		POWER FADING STATISTICS:	
PROPAGATION MODE:	DIFFRACTION		
TX TAKE-OFF ANGLE:	.0 (DEG)	(%)	BASIC LOSS
RX TAKE-OFF ANGLE:	-.1 (DEG)		
NEAR FLD BOUNDARY-TX:	1934.669 (FT)	0.01	165.4
NEAR FLD BOUNDARY-RX:	1934.669 (FT)	0.10	168.3
PATH LENGTH:	50.0000 (SM)	1.00	171.7
PROPAGATION LOSS:	<del>181.3</del> (dB)	10.00	176.5
FREE-SPACE LOSS:	150.1 (dB)	50.00	181.2
ABSORPTION LOSS:	1.6 (dB)	90.00	184.3
BEARING (TX-RX):	.000000 (DEG)	99.00	186.8
SCATTERING ANGLE:	.355193 (DEG)	99.90	188.6
FIELD STRENGTH:	.00045 (V/M)	99.99	190.1
POWER DENSITY:	-66.00 (dBm/M**2)	99.00	186.8

\*\*\*\*\* TTP TIREM RESULTS [VERSION: 1.0 ] \*\*\*\*\*

STEPPING PARAMETER: FREQUENCY CURRENT VALUE: ~~3750.00~~ (MHZ)  
 INCRMT/DECRMT VALUE: 250.00 (MHZ) INCRMT/DECRMT TYPE: [+]

OUTPUT PARAMETERS:		POWER FADING STATISTICS:	
PROPAGATION MODE:	DIFFRACTION		
TX TAKE-OFF ANGLE:	.0 (DEG)	(%)	BASIC LOSS
RX TAKE-OFF ANGLE:	-.1 (DEG)		
NEAR FLD BOUNDARY-TX:	1985.582 (FT)	0.01	165.8
NEAR FLD BOUNDARY-RX:	1985.582 (FT)	0.10	168.6
PATH LENGTH:	50.0000 (SM)	1.00	172.1
PROPAGATION LOSS:	<del>181.6</del> (dB)	10.00	176.8
FREE-SPACE LOSS:	150.3 (dB)	50.00	181.6
ABSORPTION LOSS:	1.6 (dB)	90.00	184.7
BEARING (TX-RX):	.000000 (DEG)	99.00	187.2
SCATTERING ANGLE:	.355193 (DEG)	99.90	189.0
FIELD STRENGTH:	.00044 (V/M)	99.99	190.5
POWER DENSITY:	-66.00 (dBm/M**2)	99.00	187.2

\*\*\*\*\* TTP TIREM RESULTS [VERSION: 1.0 ] \*\*\*\*\*

STEPPING PARAMETER: FREQUENCY CURRENT VALUE: 10000.00 (MHZ)  
 INCRMT/DECRMT VALUE: 250.00 (MHZ) INCRMT/DECRMT TYPE: [+]

OUTPUT PARAMETERS:		POWER FADING STATISTICS:	
PROPAGATION MODE:	DIFFRACTION		
TX TAKE-OFF ANGLE:	.0 (DEG)	(%)	BASIC LOSS
RX TAKE-OFF ANGLE:	-.1 (DEG)		
NEAR FLD BOUNDARY-TX:	2036.494 (FT)	0.01	166.1
NEAR FLD BOUNDARY-RX:	2036.494 (FT)	0.10	169.0
PATH LENGTH:	50.0000 (SM)	1.00	172.4
PROPAGATION LOSS:	182.0 (dB)	10.00	177.2
FREE-SPACE LOSS:	150.6 (dB)	50.00	181.9
ABSORPTION LOSS:	1.6 (dB)	90.00	185.0
BEARING (TX-RX):	.000000 (DEG)	99.00	187.6
SCATTERING ANGLE:	.355193 (DEG)	99.90	189.4
FIELD STRENGTH:	.00043 (V/M)	99.99	190.9
POWER DENSITY:	-67.00 (dBm/M**2)	99.00	187.6

\*\*\*\*\* TTP TIREM RESULTS [VERSION: 1.0 ] \*\*\*\*\*

STEPPING PARAMETER: FREQUENCY CURRENT VALUE: 10250.00 (MHZ)  
 INCRMT/DECRMT VALUE: 250.00 (MHZ) INCRMT/DECRMT TYPE: [+]

OUTPUT PARAMETERS:		POWER FADING STATISTICS:	
PROPAGATION MODE:	DIFFRACTION		
TX TAKE-OFF ANGLE:	.0 (DEG)	(%)	BASIC LOSS
RX TAKE-OFF ANGLE:	-.1 (DEG)		
NEAR FLD BOUNDARY-TX:	2087.406 (FT)	0.01	166.5
NEAR FLD BOUNDARY-RX:	2087.406 (FT)	0.10	169.4
PATH LENGTH:	50.0000 (SM)	1.00	172.8
PROPAGATION LOSS:	182.4 (dB)	10.00	177.6
FREE-SPACE LOSS:	150.8 (dB)	50.00	182.3
ABSORPTION LOSS:	1.7 (dB)	90.00	185.4
BEARING (TX-RX):	.000000 (DEG)	99.00	188.0
SCATTERING ANGLE:	.355193 (DEG)	99.90	189.8
FIELD STRENGTH:	.00042 (V/M)	99.99	191.3
POWER DENSITY:	-67.00 (dBm/M**2)	99.00	188.0

\*\*\*\*\* TTP TIREM RESULTS [VERSION: 1.0 ] \*\*\*\*\*

STEPPING PARAMETER: FREQUENCY CURRENT VALUE: 45500.00 (MHZ)  
 INCRMT/DECRMT VALUE: 250.00 (MHZ) INCRMT/DECRMT TYPE: [+]

OUTPUT PARAMETERS:		POWER FADING STATISTICS:	
PROPAGATION MODE:	DIFFRACTION		
TX TAKE-OFF ANGLE:	.0 (DEG)	(%)	BASIC LOSS
RX TAKE-OFF ANGLE:	-.1 (DEG)		
NEAR FLD BOUNDARY-TX:	2138.319 (FT)	0.01	166.9
NEAR FLD BOUNDARY-RX:	2138.319 (FT)	0.10	169.7
PATH LENGTH:	50.0000 (SM)	1.00	173.2
PROPAGATION LOSS:	182.8 (dB)	10.00	178.0
FREE-SPACE LOSS:	151.0 (dB)	50.00	182.7
ABSORPTION LOSS:	1.8 (dB)	90.00	185.8
BEARING (TX-RX):	.000000 (DEG)	99.00	188.3
SCATTERING ANGLE:	.355193 (DEG)	99.90	190.2
FIELD STRENGTH:	.00041 (V/M)	99.99	191.7
POWER DENSITY:	-67.00 (dBm/M**2)	99.00	188.3

\*\*\*\*\* TTP TIREM RESULTS [VERSION: 1.0 ] \*\*\*\*\*

STEPPING PARAMETER: FREQUENCY CURRENT VALUE: 50750.00 (MHZ)  
 INCRMT/DECRMT VALUE: 250.00 (MHZ) INCRMT/DECRMT TYPE: [+]

OUTPUT PARAMETERS:		POWER FADING STATISTICS:	
PROPAGATION MODE:	DIFFRACTION		
TX TAKE-OFF ANGLE:	.0 (DEG)	(%)	BASIC LOSS
RX TAKE-OFF ANGLE:	-.1 (DEG)		
NEAR FLD BOUNDARY-TX:	2189.231 (FT)	0.01	167.2
NEAR FLD BOUNDARY-RX:	2189.231 (FT)	0.10	170.1
PATH LENGTH:	50.0000 (SM)	1.00	173.6
PROPAGATION LOSS:	183.2 (dB)	10.00	178.3
FREE-SPACE LOSS:	151.2 (dB)	50.00	183.1
ABSORPTION LOSS:	1.8 (dB)	90.00	186.2
BEARING (TX-RX):	.000000 (DEG)	99.00	188.7
SCATTERING ANGLE:	.355193 (DEG)	99.90	190.6
FIELD STRENGTH:	.00041 (V/M)	99.99	192.1
POWER DENSITY:	-67.00 (dBm/M**2)	99.00	188.7



\*\*\*\*\* TTP TIREM RESULTS [VERSION: 1.0 ] \*\*\*\*\*

STEPPING PARAMETER: FREQUENCY CURRENT VALUE: ~~11000.00~~ (MHZ)  
 INCRMT/DECRMT VALUE: 250.00 (MHZ) INCRMT/DECRMT TYPE: [+]

OUTPUT PARAMETERS:		POWER FADING STATISTICS:		
PROPAGATION MODE:	DIFFRACTION			
TX TAKE-OFF ANGLE:	.0 (DEG)	(%)	:	BASIC LOSS
RX TAKE-OFF ANGLE:	-.1 (DEG)			
NEAR FLD BOUNDARY-TX:	2240.143 (FT)	0.01	:	167.6
NEAR FLD BOUNDARY-RX:	2240.143 (FT)	0.10	:	170.4
PATH LENGTH:	50.0000 (SM)	1.00	:	173.9
PROPAGATION LOSS:	183.5 (dB)	10.00	:	178.7
FREE-SPACE LOSS:	151.4 (dB)	50.00	:	183.5
ABSORPTION LOSS:	1.9 (dB)	90.00	:	186.6
BEARING (TX-RX):	.000000 (DEG)	99.00	:	189.1
SCATTERING ANGLE:	.355193 (DEG)	99.90	:	190.9
FIELD STRENGTH:	.00040 (V/M)	99.99	:	192.5
POWER DENSITY:	-67.00 (dBm/M**2)	99.00	:	189.1

\*\*\*\*\* TTP TIREM RESULTS [VERSION: 1.0 ] \*\*\*\*\*

STEPPING PARAMETER: FREQUENCY CURRENT VALUE: 11250.00 (MHZ)  
 INCRMT/DECRMT VALUE: 250.00 (MHZ) INCRMT/DECRMT TYPE: [+]

OUTPUT PARAMETERS:		POWER FADING STATISTICS:		
PROPAGATION MODE:	DIFFRACTION			
TX TAKE-OFF ANGLE:	.0 (DEG)	(%)	:	BASIC LOSS
RX TAKE-OFF ANGLE:	-.1 (DEG)			
NEAR FLD BOUNDARY-TX:	2291.056 (FT)	0.01	:	167.9
NEAR FLD BOUNDARY-RX:	2291.056 (FT)	0.10	:	170.8
PATH LENGTH:	50.0000 (SM)	1.00	:	174.3
PROPAGATION LOSS:	183.9 (dB)	10.00	:	179.1
FREE-SPACE LOSS:	151.6 (dB)	50.00	:	183.8
ABSORPTION LOSS:	2.0 (dB)	90.00	:	186.9
BEARING (TX-RX):	.000000 (DEG)	99.00	:	189.5
SCATTERING ANGLE:	.355193 (DEG)	99.90	:	191.3
FIELD STRENGTH:	.00039 (V/M)	99.99	:	192.8
POWER DENSITY:	-67.00 (dBm/M**2)	99.00	:	189.5

\*\*\*\*\* TTP TIREM RESULTS [VERSION: 1.0 ] \*\*\*\*\*

STEPPING PARAMETER: FREQUENCY CURRENT VALUE: ~~14500.00~~ (MHZ)  
 INCRMT/DECRMT VALUE: 250.00 (MHZ) INCRMT/DECRMT TYPE: [+]

OUTPUT PARAMETERS:		POWER FADING STATISTICS:	
PROPAGATION MODE:	DIFFRACTION		
TX TAKE-OFF ANGLE:	.0 (DEG)	(%)	BASIC LOSS
RX TAKE-OFF ANGLE:	-.1 (DEG)		
NEAR FLD BOUNDARY-TX:	2341.968 (FT)	0.01	168.3
NEAR FLD BOUNDARY-RX:	2341.968 (FT)	0.10	171.1
PATH LENGTH:	50.0000 (SM)	1.00	174.6
PROPAGATION LOSS:	<del>184.6</del> (dB)	10.00	179.4
FREE-SPACE LOSS:	151.8 (dB)	50.00	184.2
ABSORPTION LOSS:	2.1 (dB)	90.00	187.3
BEARING (TX-RX):	.000000 (DEG)	99.00	189.8
SCATTERING ANGLE:	.355193 (DEG)	99.90	191.7
FIELD STRENGTH:	.00038 (V/M)	99.99	193.2
POWER DENSITY:	-68.00 (dBm/M**2)	99.00	189.8

\*\*\*\*\* TTP TIREM RESULTS [VERSION: 1.0 ] \*\*\*\*\*

STEPPING PARAMETER: FREQUENCY CURRENT VALUE: ~~14750.00~~ (MHZ)  
 INCRMT/DECRMT VALUE: 250.00 (MHZ) INCRMT/DECRMT TYPE: [+]

OUTPUT PARAMETERS:		POWER FADING STATISTICS:	
PROPAGATION MODE:	DIFFRACTION		
TX TAKE-OFF ANGLE:	.0 (DEG)	(%)	BASIC LOSS
RX TAKE-OFF ANGLE:	-.1 (DEG)		
NEAR FLD BOUNDARY-TX:	2392.880 (FT)	0.01	168.6
NEAR FLD BOUNDARY-RX:	2392.880 (FT)	0.10	171.5
PATH LENGTH:	50.0000 (SM)	1.00	175.0
PROPAGATION LOSS:	184.6 (dB)	10.00	179.8
FREE-SPACE LOSS:	152.0 (dB)	50.00	184.5
ABSORPTION LOSS:	2.1 (dB)	90.00	187.6
BEARING (TX-RX):	.000000 (DEG)	99.00	190.2
SCATTERING ANGLE:	.355193 (DEG)	99.90	192.0
FIELD STRENGTH:	.00037 (V/M)	99.99	193.6
POWER DENSITY:	-68.00 (dBm/M**2)	99.00	190.2

\*\*\*\*\* TTP TIREM RESULTS [VERSION: 1.0 ] \*\*\*\*\*

STEPPING PARAMETER: FREQUENCY CURRENT VALUE: ~~2000.00~~ (MHZ)  
INCRMT/DECRMT VALUE: 250.00 (MHZ) INCRMT/DECRMT TYPE: [+]

OUTPUT PARAMETERS:		POWER FADING STATISTICS:		
PROPAGATION MODE:	DIFFRACTION			
TX TAKE-OFF ANGLE:	.0 (DEG)	(%)	:	BASIC LOSS
RX TAKE-OFF ANGLE:	-.1 (DEG)			
NEAR FLD BOUNDARY-TX:	2443.793 (FT)	0.01	:	168.9
NEAR FLD BOUNDARY-RX:	2443.793 (FT)	0.10	:	171.8
PATH LENGTH:	50.0000 (SM)	1.00	:	175.3
PROPAGATION LOSS:	185.0 (dB)	10.00	:	180.1
FREE-SPACE LOSS:	152.1 (dB)	50.00	:	184.9
ABSORPTION LOSS:	2.2 (dB)	90.00	:	188.0
BEARING (TX-RX):	1.000000 (DEG)	99.00	:	190.6
SCATTERING ANGLE:	.355193 (DEG)	99.90	:	192.4
FIELD STRENGTH:	.00037 (V/M)	99.99	:	193.9
POWER DENSITY:	-68.00 (dBm/M**2)	99.00	:	190.6

### 1.2.1.2 Example 2

This is an example on MIXPATH. This model is primarily used when there are discontinuities in the earth surface, i.e., rivers and lakes between ground. In this case, the characteristics of the terrain profile vary so much that only smooth profiles can be used. This model also includes any effects from surface waves. The model is based on Millington's method and it does not consider any effects due to ducting or rain attenuation.

Input Parameters :

Both transmitting and receiving antennas are horizontal dipoles.

Frequency range = 1 to 10 GHz.

Pages 38 to 46 show the input and output data formats for MIXPATH. The input data are supplied to the computer in the format that appears in screens 1.1 to 34.1. The results are given in the format shown in screen 36.1 .

===== SCREEN NUMBER 1.1 =====\*\*\* UNCLASSIFIED \*\*\*

\*\*\* MIXED PATH MODEL \*\*\*

THE MIXED PATH MODEL (MIXPATH) PROVIDES PROPAGATION LOSS PREDICTIONS FOR PATHS OVER TWO OR MORE TYPES OF EARTH. THE MODEL IS INTENDED PRIMARILY FOR USE AT FREQUENCIES AND ANTENNA HEIGHTS WHERE SURFACE-WAVE EFFECTS CAUSE THE AMOUNT OF TRANSMISSION LOSS OVER THE PROPAGATION PATH TO BE HIGHLY DEPENDENT ON THE ELECTRICAL CHARACTERISTICS OF THE EARTH SURFACE INVOLVED. THE MODEL IS BASED ON MILLINGTON'S METHOD, WHICH APPLIES ONLY WHEN THE EARTH SURFACE IS SMOOTH (ELEVATION IRREGULARITIES ARE SMALL COMPARED WITH THE WAVELENGTH). THE MIXED PATH MODEL IS NOT APPLICABLE TO TROPOSCATTER OR SKYWAVE PROPAGATION, NOR DOES IT CONSIDER THE EFFECTS OF ATMOSPHERIC ABSORPTION, RAIN ATTENUATION, DUCTING PHENOMENA, DETAILED TOPOGRAPHY, OR FOLIAGE.

TRANSMIT TO CONTINUE

===== SCREEN NUMBER 2.1 =====\*\*\* UNCLASSIFIED \*\*\*

-----  
MIXPATH CALCULATION OPTIONS SCREEN  
-----

ENTER AN X IN THE DESIRED BOXES:

- X] - RELIABLE GROUND WAVE COMMUNICATION CALCULATIONS
- X] - MIXPATH USING NON-HERTZIAN ANTENNAS
- ] - DISTANCE INCREMENT OPTION

GROUND CONSTANTS / TYPE OPTION (ENTER AN X IN ONE BOX):

- ] - USER ENTERS GROUND CONSTANTS FOR EACH SEGMENT  
- OR -
- X] - USER ENTERS CCIR GROUND TYPE FOR EACH SEGMENT

===== SCREEN NUMBER 3.1 =====\*\*\* UNCLASSIFIED \*\*\*

-----  
GENERAL INPUT SCREEN  
-----

PATH ID: [ SAMPLE ]  
 PATH DISTANCE: [ 100 ]  
 DISTANCE UNITS: [ S ] K - KILOMETERS  
   S - STATUTE MILES  
   N - NAUTICAL MILES

HEIGHT OF TX ABOVE SMOOTH EARTH: [ 50 ]  
 HEIGHT OF RX ABOVE SMOOTH EARTH: [ 50 ]  
 HEIGHT UNITS: [ M ] F - FEET  
   M - METERS

TRANSMITTER POLARIZATION: [ H ] V - VERTICAL  
   H - HORIZONTAL

TRANSMITTER TITLE: [ TX HOR. DIPOLE ]  
 RECEIVER TITLE: [ RX HOR. DIPOLE ]

COMMENT TO BE PRINTED IN HEADING: [ MIX PATH SAMPLE ]

===== SCREEN NUMBER 4.1 =====\*\*\* UNCLASSIFIED \*\*\*

-----  
FREQUENCY INPUT SCREEN  
-----

ENTER TRANSMITTER FREQUENCIES (MHz):

1. [ 10 ]	2. [ 30 ]	3. [ 60 ]	4. [ 100 ]
5. [ 200 ]	6. [ 400 ]	7. [ 700 ]	8. [ 1000 ]
[ 2000 ]	10. [ 4000 ]	11. [ 6000 ]	12. [ 10000 ]
[ ]	14. [ ]	15. [ ]	16. [ ]
7. [ ]	18. [ ]	19. [ ]	20. [ ]
[ ]	22. [ ]	23. [ ]	24. [ ]
[ ]	26. [ ]	27. [ ]	28. [ ]
9. [ ]	30. [ ]	31. [ ]	32. [ ]
[ ]	34. [ ]	35. [ ]	36. [ ]
[ ]	38. [ ]	39. [ ]	40. [ ]
1. [ ]	42. [ ]	43. [ ]	44. [ ]
5. [ ]	46. [ ]	47. [ ]	48. [ ]
[ ]	50. [ ]	[ ]	[ ]

\*\*\* MUST ENTER AT LEAST ONE FREQUENCY \*\*\*

===== SCREEN NUMBER 6.1 =====\*\*\* UNCLASSIFIED \*\*\*

-----  
SEGMENT INPUT SCREEN  
-----

SEGMENT NO. (1-9)	LENGTH (SM)	REFRACTIVITY (N-UNITS)	CCIR GROUND TYPE
1	[ 5 ]	[ 301. ]	[ D ]
2	[ 30 ]	[ 301 ]	[ A ]
3	[ 65 ]	[ 301 ]	[ D ]
4	[ ]	[ ]	[ ]
5	[ ]	[ ]	[ ]
6	[ ]	[ ]	[ ]
7	[ ]	[ ]	[ ]
8	[ ]	[ ]	[ ]
9	[ ]	[ ]	[ ]

GROUND TYPE: A - SEA WATER (20 DEG C)      E - VERY DRY GROUND  
 B - WET GROUND      F - PURE WATER (NOT USED)  
 C - FRESH WATER (20 DEG C)      G - ICE (FRESH WATER, -1 DEG C)  
 D - MEDIUM WET GROUND      H - ICE (FRESH WATER, -10 DEG C)

\*\*\* MUST ENTER AT LEAST ONE SEGMENT \*\*\*

===== SCREEN NUMBER 9.1 =====\*\*\* UNCLASSIFIED \*\*\*

-----  
TRANSMITTER ANTENNA TYPE SELECTION  
-----

ENTER THE NUMBER OF THE TRANSMITTER ANTENNA TYPE: [ 2 ]

1 - VERTICAL MONOPOLE	2 - HORIZONTAL DIPOLE
3 - HORIZONTAL YAGI-UDA	4 - VERTICAL DIPOLE
5 - CURTAIN ARRAY	6 - TERMINATED SLOPING VEE
7 - INVERTED L	8 - TERMINATED SLOPING RHOMBIC
9 - SLOPING LONG WIRE	10 - HORIZONTAL LOG-PERIODIC
11 - ARBITRARILY TILTED DIPOLE	12 - HALF RHOMBIC
13 - SLOPING DOUBLE RHOMBIC	14 - VERTICAL LOG-PERIODIC
15 - HERTZIAN DIPOLE	16 - MANUALLY-ENTERED GAIN/ISOTROPIC
17 - TERMINATED SLOPING LONG WIRE	18 - INVERTED-VEE

===== SCREEN NUMBER 13.1 =====\*\*\* UNCLASSIFIED \*\*\*

-----  
HORIZONTAL DIPOLE ANTENNA  
-----

ANTENNA TITLE: TX HOR. DIPOLE

ANTENNA FEED HEIGHT: [ .5 ] UNITS: [ ] M -OR- [ X ] WAVELENGTHS

ANTENNA LENGTH: [ .5 ] UNITS: [ ] M -OR- [ X ] WAVELENGTHS

RETURN TO ANTENNA SELECTION SCREEN [ ]

===== SCREEN NUMBER 8.1 =====\*\*\* UNCLASSIFIED \*\*\*

-----  
BEARING INPUT SCREEN  
-----

MAINBEAM BEARING INPUT OPTION (ENTER AN X IN ONE BOX):

- 1. [ X ] - ANTENNA MAINBEAM BEARING IS ALONG GREAT-CIRCLE PATH BETWEEN THE SITES (NOT NECESSARY TO ENTER A BEARING)  
- OR -
- 2. [ ] - ANTENNA MAINBEAM BEARING IS RELATIVE TO TRUE NORTH  
- OR -
- 3. [ ] - ANTENNA MAINBEAM BEARING IS RELATIVE TO THE GREAT-CIRCLE PATH BETWEEN THE SITES

ANTENNA BEARING: [ ] (DEG)  
(ENTERED ONLY IF 2 OR 3 CHOSEN ABOVE)



===== SCREEN NUMBER 10.1 =====\*\*\* UNCLASSIFIED \*\*\*

-----  
RECEIVER ANTENNA TYPE SELECTION  
-----

ENTER THE NUMBER OF THE RECEIVER ANTENNA TYPE: [ 2 ]

- |                                      |                                      |
|--------------------------------------|--------------------------------------|
| 1 - VERTICAL MONOPOLE                | 2 - HORIZONTAL DIPOLE                |
| 3 - HORIZONTAL YAGI-UDA              | 4 - VERTICAL DIPOLE                  |
| 5 - CURTAIN ARRAY                    | 6 - TERMINATED SLOPING VEE           |
| 7 - INVERTED L                       | 8 - TERMINATED SLOPING RHOMBIC       |
| 9 - SLOPING LONG WIRE                | 10 - HORIZONTAL LOG-PERIODIC         |
| 11 - ARBITRARILY TILTED DIPOLE       | 12 - HALF RHOMBIC                    |
| 13 - SLOPING DOUBLE RHOMBIC          | 14 - VERTICAL LOG-PERIODIC           |
| 15 - HERTZIAN DIPOLE                 | 16 - MANUALLY-ENTERED GAIN/ISOTROPIC |
| 17 - TERMINATED SLOPING LONG<br>WIRE | 18 - INVERTED-VEE                    |

===== SCREEN NUMBER 13.2 =====\*\*\* UNCLASSIFIED \*\*\*

-----  
HORIZONTAL DIPOLE ANTENNA  
-----

ANTENNA TITLE: RX HOR. DIPOLE

ANTENNA FEED HEIGHT: [ .5 ] UNITS: [ ] M -OR- [ X ] WAVELENGTHS

ANTENNA LENGTH: [ .5 ] UNITS: [ ] M -OR- [ X ] WAVELENGTHS

RETURN TO ANTENNA SELECTION SCREEN [ ]

===== SCREEN NUMBER 8.2 =====\*\*\* UNCLASSIFIED \*\*\*

-----  
BEARING INPUT SCREEN  
-----

MAINBEAM BEARING INPUT OPTION (ENTER AN X IN ONE BOX):

- 1.  - ANTENNA MAINBEAM BEARING IS ALONG GREAT-CIRCLE PATH  
BETWEEN THE SITES (NOT NECESSARY TO ENTER A BEARING)  
- OR -
- 2.  - ANTENNA MAINBEAM BEARING IS RELATIVE TO TRUE NORTH  
- OR -
- 3.  - ANTENNA MAINBEAM BEARING IS RELATIVE TO THE GREAT-  
CIRCLE PATH BETWEEN THE SITES

ANTENNA BEARING: [ ] (DEG)  
(ENTERED ONLY IF 2 OR 3 CHOSEN ABOVE)

===== SCREEN NUMBER 11.1 =====\*\*\* UNCLASSIFIED \*\*\*

-----  
RELIABLE GROUND WAVE COMMUNICATION CALCULATIONS INPUTS  
-----

DATE: [ 12 ] (mm) [ 1991 ] (yyyy)  
 HOUR START: [ 11 ] (1-24)  
 HOUR END: [ 13 ] (1-24)  
 STEP IN HOURS: [ 1 ] (1-23)

TIME ZONE (PLACE X IN ONE BOX): LOCAL  - OR - UNIVERSAL

ENTER MAN-MADE NOISE DENSITY: [ ] (dBW/HZ) (INTEGER)  
 - OR -

ENTER NOISE TYPE: [ 3 ] TYPES: 1: INDUSTRIAL (-125 dBW/HZ)  
 2: RESIDENTIAL (-136 dBW/HZ)  
 3: RURAL (-148 dBW/HZ)  
 4: REMOTE (-164 dBW/HZ)

REQUIRED SIGNAL-TO-NOISE RATIO: [ 48. ]

TRANSMITTER POWER: [ 400 ]  
 POWER UNITS: [ W ] W - WATTS  
 K - KILOWATTS

===== SCREEN NUMBER 33.1 =====\*\*\* UNCLASSIFIED \*\*\*

-----  
RECEIVER LATITUDE / LONGITUDE INPUT  
-----

RECEIVER TITLE: RX HOR. DIPOLE  
RECEIVER LATITUDE: [ 39- 09- 00- N] (DD-MM-SS-H)  
RECEIVER LONGITUDE: [ 075- 32- 00- W] (DDD-MM-SS-H)

===== SCREEN NUMBER 34.1 =====\*\*\* UNCLASSIFIED \*\*\*

-----  
OUTPUT OPTIONS  
-----

OUTPUT TO THE SCREEN FOR RUNS WITHOUT RELIABLE GROUND-WAVE COMMUNICATIONS CALCULATIONS WILL OCCUR 14 FREQUENCIES AND 10 DISTANCE INCREMENTS AT A TIME. OUTPUT TO THE SCREEN FOR RUNS WITH RELIABLE GROUND-WAVE COMMUNICATIONS CALCULATIONS WILL OCCUR 12 FREQUENCIES AND 5 DISTANCE INCREMENTS AT A TIME. THESE OPTIONS ARE RECOMMENDED FOR RUNS WITH FEWER THAN THESE SPECIFIED NUMBERS OF FREQUENCIES AND DISTANCE INCREMENTS.

OUTPUT TO A USER SPECIFIED FILE IN PRINTED FORMAT WILL OCCUR IN 132 COLUMN FORMAT FOR ALL FREQUENCIES AND DISTANCES SPECIFIED. THIS CAN THEN BE PRINTED OR EXAMINED AT A LATER TIME. THIS OPTION IS RECOMMENDED FOR MULTIPLE FREQUENCY RUNS.

ANY COMBINATION OF OUTPUTS MAY BE SELECTED.  
ENTER AN X IN THE DESIRED BOXES.

- [ X ] OUTPUT RESULTS TO SCREEN IN FULL-SCREEN FORMAT
- [ X ] OUTPUT RESULTS TO FILE: [ mix3c.OUT ]
- [ ] OUTPUT RESULTS TO FILE IN AUTODIN FORMAT: [ mix3c.AUD ]

===== SCREEN NUMBER: 36.1

\*\*\*\*\* UNCLASSIFIED \*\*\*

RESULTS

REQ(MHz)	SYSTEM LOSS	ANTENNA POWER GAIN (dBI)		DAILY NOISE (dBW/Hz)		RELIABLE DISTANCE (SM)	
		TX	RX	MIN	MAX	MIN	MAX
10.0-148.9		2.3	2.3	-161.7	-161.8	76.2	76.2
30.0-158.3		2.3	2.3	-175.7	-175.7	91.0	91.0
60.0-167.0		2.3	2.3	-183.9	-183.9	91.8	91.8
100.0-175.3		2.3	2.3	-190.0	-190.0	90.2	90.2
200.0-189.3		2.3	2.3	-198.1	-198.1	85.5	85.5
400.0-207.2		2.3	2.3	-206.1	-206.1	80.1	80.1
700.0-224.8		2.3	2.3	-212.5	-212.5	74.6	74.6
1000.0-237.7		2.3	2.3	-216.5	-216.5	72.3	72.3
2000.0-267.3		2.3	2.3	-224.1	-224.1	66.0	66.0
4000.0-303.5		2.3	2.3	-231.5	-231.5	61.3	61.3
6000.0-328.5		2.3	2.3	-235.8	-235.8	58.2	58.2
10000.0-364.7		2.3	2.3	-241.1	-241.1	55.1	55.1

-----  
DIST(SM) 100.0

\*\*\* TRANSMIT TO CONTINUE \*\*\*

===== SCREEN NUMBER 36.1

=====**\*\*\* UNCLASSIFIED \*\*\***

RESULTS  
-----

FREQ(MHz)	SYSTEM LOSS	ANTENNA POWER GAIN (dBI)		DAILY NOISE (dBW/Hz)		RELIABLE DISTANCE (SM)	
		TX	RX	MIN	MAX	MIN	MAX
10.0-148.9		2.3	2.3	-161.7	-161.8	76.2	76.2
30.0-158.3		2.3	2.3	-175.7	-175.7	91.0	91.0
60.0-167.0		2.3	2.3	-183.9	-183.9	91.8	91.8
100.0-175.3		2.3	2.3	-190.0	-190.0	90.2	90.2
200.0-189.3		2.3	2.3	-198.1	-198.1	85.5	85.5
400.0-207.2		2.3	2.3	-206.1	-206.1	80.1	80.1
700.0-224.8		2.3	2.3	-212.5	-212.5	74.6	74.6
1000.0-237.7		2.3	2.3	-216.5	-216.5	72.3	72.3
2000.0-267.3		2.3	2.3	-224.1	-224.1	66.0	66.0
4000.0-303.5		2.3	2.3	-231.5	-231.5	61.3	61.3
6000.0-328.5		2.3	2.3	-235.8	-235.8	58.2	58.2
10000.0-364.7		2.3	2.3	-241.1	-241.1	55.1	55.1

-----  
DIST(SM) 100.0

**\*\*\* TRANSMIT TO CONTINUE \*\*\***

### 1.3 RESULTS-Antenna Platform Effects

In this section the capability of "GAUGE" and "GEMACS" computer models to input complicated platforms and predict near fields is presented. Various examples were run for low (method of moments) and high (Geometrical Theory of Diffraction) frequencies. Figure 1.4 explains the organization of GAUGE and GEMACS programs.

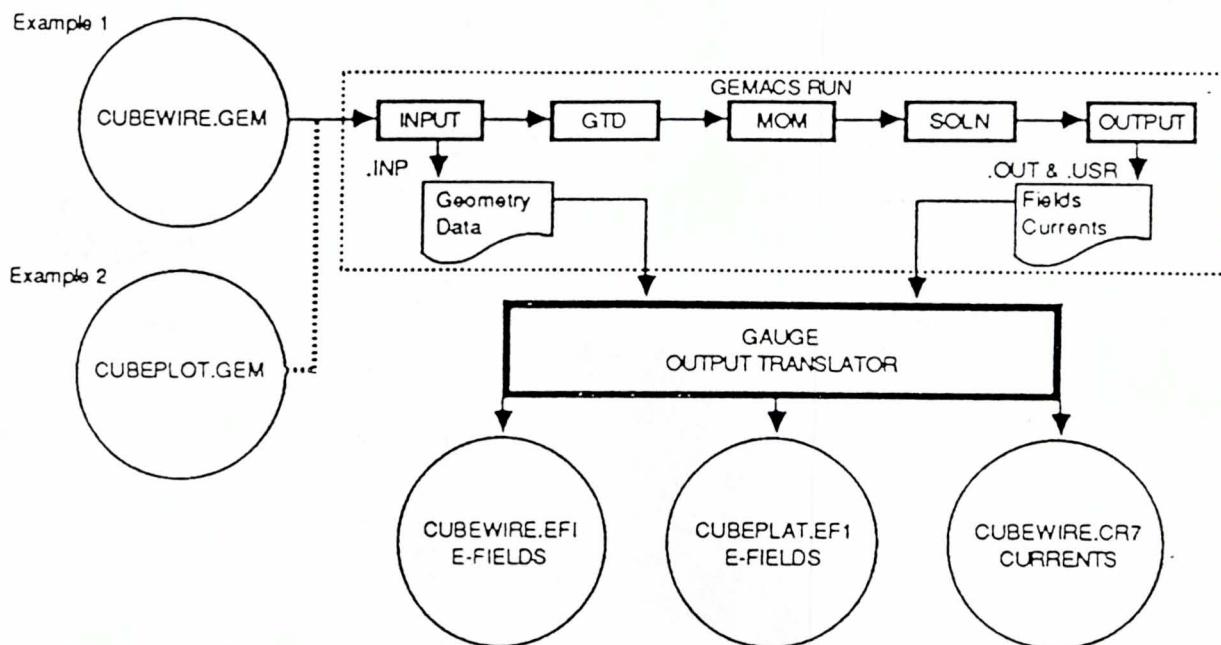


Fig. 1.4 Example of GAUGE/GEMACS file interaction

### 1.3.1 Examples

#### 1.3.1.1 Example 1

Figure 1.5 depicts the geometry of the cube whose scattered fields were evaluated by GEMACS. The moment method was utilized in this example at a frequency of operation of 300 MHz. The result is shown in Figure 1.6. Table 1.1 shows the input-format for the cube geometry for GAUGE and Table 1.2 shows the input file for GEMACS at 300 MHz for the same cube.

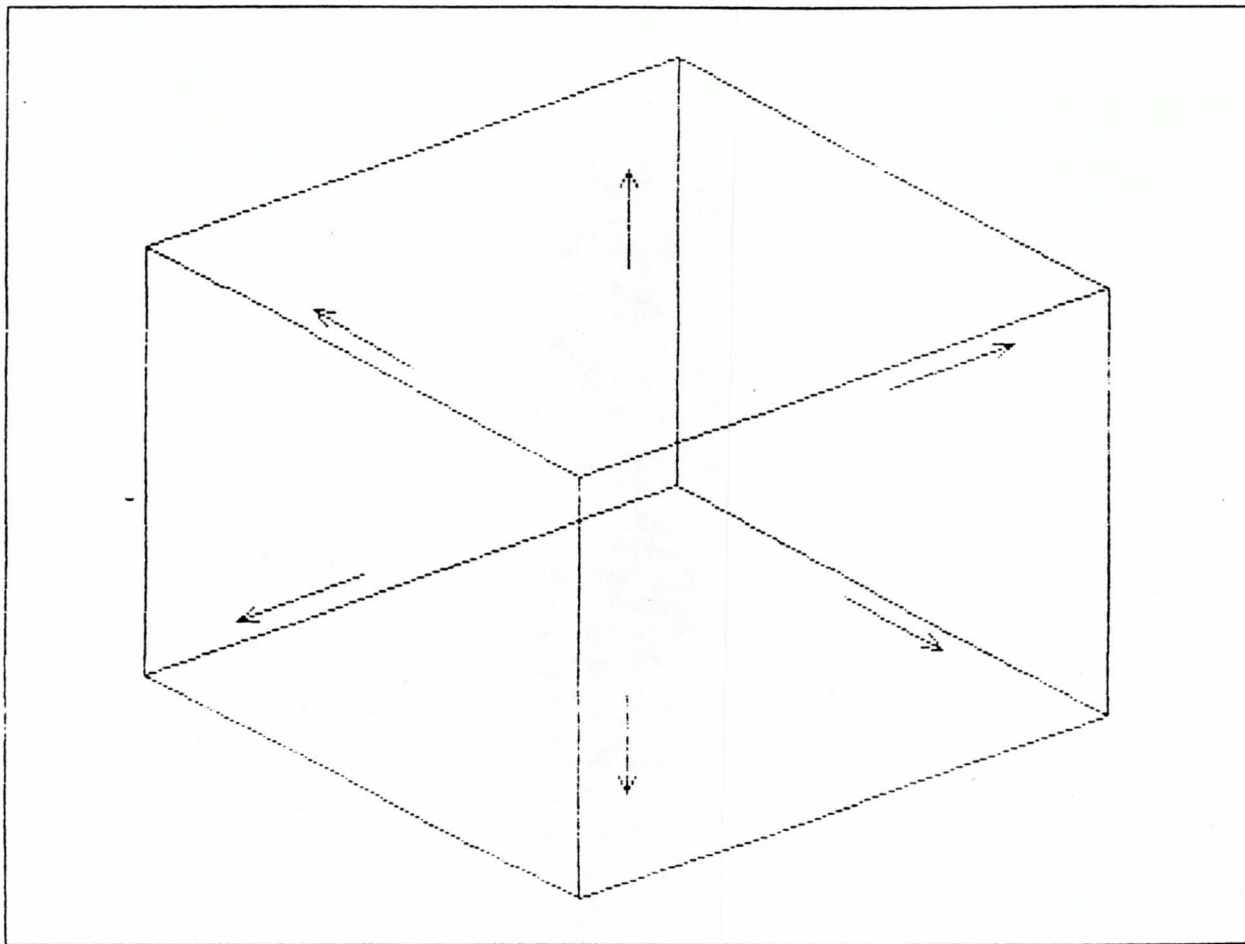


Fig. 1.5 Example of a cube geometry and the normals on each face

PT	1	-.5000E-01		-.5000E-01		-.5000E-01
PT	2	.5000E-01		-.5000E-01		-.5000E-01
PT	3	.5000E-01		.5000E-01		-.5000E-01
PT	4	-.5000E-01		.5000E-01		-.5000E-01
PT	5	-.5000E-01		-.5000E-01		.5000E-01
PT	6	.5000E-01		-.5000E-01		.5000E-01
PT	7	.5000E-01		.5000E-01		.5000E-01
PT	8	-.5000E-01		.5000E-01		.5000E-01
CP	1	2	1	1	1	
CP	1	4	1	2	1	
CP	1	5	1	3	1	
CP	2	3	1	4	1	
CP	2	6	1	5	1	
CP	3	4	1	6	1	
CP	3	7	1	7	1	
CP	4	8	1	8	1	
CP	5	6	1	9	1	
CP	5	8	1	10	1	
CP	6	7	1	11	1	
CP	7	8	1	12	1	

END

Table 1.1 Input geometry for a cube to be processed by GAUGE at 300 MHz in a wire form.



```

$
$ GEMACS COMMANDS TO CALCULATE BISCATTERING FROM A CUBE
$ AT 300 MHZ BY METHOD OF MOMENTS.
$
NUMFIL=17
TITLE "WIRE GRID OF A CUBE"
FRQ=300.
SETINT MOM
GMDATA=CUBE
ZGEN GMDATA=CUBE ZMATRX=ZIJ
SRC=ESRC(CUBE) SW=-1.,0. THETA=90. PHI=0.
SOLVE ZIJ*I=SRC
PRINT I
FFLD1=EFIELD(CUBE) T1=90. P1=0. DP=1. P2=180.
PRINT FFLD1
END OF COMMANDS

$
$ GEMACS GEOMETRY WIRE GRID REPRESENTATION OF CUBE
$
RA .10000E-02
PT 1 -.5000E-01 -.5000E-01 -.5000E-01
PT 2 .5000E-01 -.5000E-01 -.5000E-01
PT 3 .5000E-01 .5000E-01 -.5000E-01
PT 4 -.5000E-01 .5000E-01 -.5000E-01
PT 5 -.5000E-01 -.5000E-01 .5000E-01
PT 6 .5000E-01 -.5000E-01 .5000E-01
PT 7 .5000E-01 .5000E-01 .5000E-01
PT 8 -.5000E-01 .5000E-01 .5000E-01
CP 1 2 1 1 1
CP 1 4 1 2 1
CP 1 5 1 3 1
CP 2 3 1 4 1
CP 2 6 1 5 1
CP 3 4 1 6 1
CP 3 7 1 7 1
CP 4 8 1 8 1
CP 5 6 1 9 1
CP 5 8 1 10 1
CP 6 7 1 11 1
CP 7 8 1 12 1
END

```

GEMACS Commands  
that have to be  
added before the  
cube geometry

Geometry of cube  
stored in wire form

Table 1.2 GEMACS input file for a cube to be run using MOM  
at 300 MHz

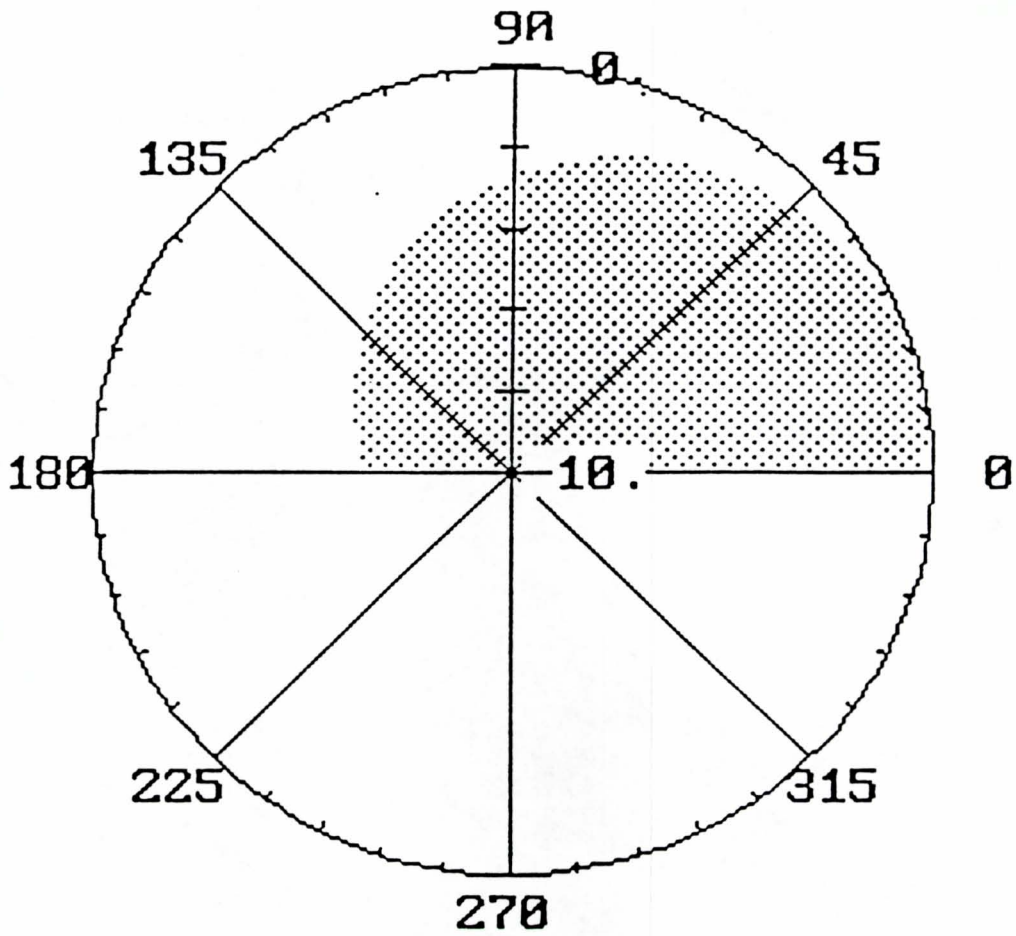


Fig. 1.6 Far Field polar plot using the output file  
 "cubewire.efl" (Scattered field from a cube)

### 1.3.1.2 Example 2

Example 2 uses the same cube shown in Figure 1.5, except the Geometrical Theory of Diffraction (GTD) was used at a frequency of 9 GHz. In this case the faces of the cube are modelled as plates instead of a wire structure used in Example 1. The evaluated scattered field from the cube in Figure 1.7. Table 1.3 shows the input-format for GAUGE using GTD, whereas Table 1.4 depicts the GEMACS input file at 9 GHz.

PT	1	-.5000E-01		-.5000E-01		-.5000E-01	
PT	2	.5000E-01		-.5000E-01		-.5000E-01	
PT	3	.5000E-01		.5000E-01		-.5000E-01	
PT	4	-.5000E-01		.5000E-01		-.5000E-01	
PT	5	-.5000E-01		-.5000E-01		.5000E-01	
PT	6	.5000E-01		-.5000E-01		.5000E-01	
PT	7	.5000E-01		.5000E-01		.5000E-01	
PT	8	-.5000E-01		.5000E-01		.5000E-01	
PL	1	4	4	3	2	1	0
PL	2	4	5	6	7	8	0
PL	3	4	1	2	6	5	0
PL	4	4	2	3	7	6	0
PL	5	4	3	4	8	7	0
PL	6	4	4	1	5	8	0
END							

Table 1.3 Input geometry for a cube to be processed by GAUGE at 9 GHz

```

$
$ GEMACS COMMANDS TO CALCULATE BISSCATTERING FROM A CUBE
$ AT 9 GHZ USING GTD
$
NUMFIL=17
TITLE "GTD PLATE MODEL OF A CUBE"
FRQ=9000.
SETINT PL EI
GMDATA=CUBE
SRC=ESRC(CUBE) SW=-1.,0. R=0.2 THETA=90. PHI=0.
FFLD1=EFIELD(CUBE) T1=90. P1=0. DP=1. P2=180.
END OF COMMANDS
$
$ GEMACS GEOMETRY REPRESENTING CUBE PLATE MODEL
$
PT 1 -.5000E-01 -.5000E-01 -.5000E-01
PT 2 .5000E-01 -.5000E-01 -.5000E-01
PT 3 -.5000E-01 .5000E-01 -.5000E-01
PT 4 .5000E-01 .5000E-01 -.5000E-01
PT 5 -.5000E-01 -.5000E-01 .5000E-01
PT 6 .5000E-01 -.5000E-01 .5000E-01
PT 7 -.5000E-01 .5000E-01 .5000E-01
PT 8 .5000E-01 .5000E-01 .5000E-01
PL 1 4 3 4 2 1 0
PL 2 4 5 6 8 7 0
PL 3 4 1 2 6 5 0
PL 4 4 2 4 8 6 0
PL 5 4 4 3 7 8 0
PL 6 4 3 1 5 7 0
END

```

GEMACS Commands  
for a cube  
geometry to  
be used with  
GTD

Geometry of cube  
stored in plate  
form

Table 1.4 GEMACS input file for a cube to be run using GTD  
at 9 GHz

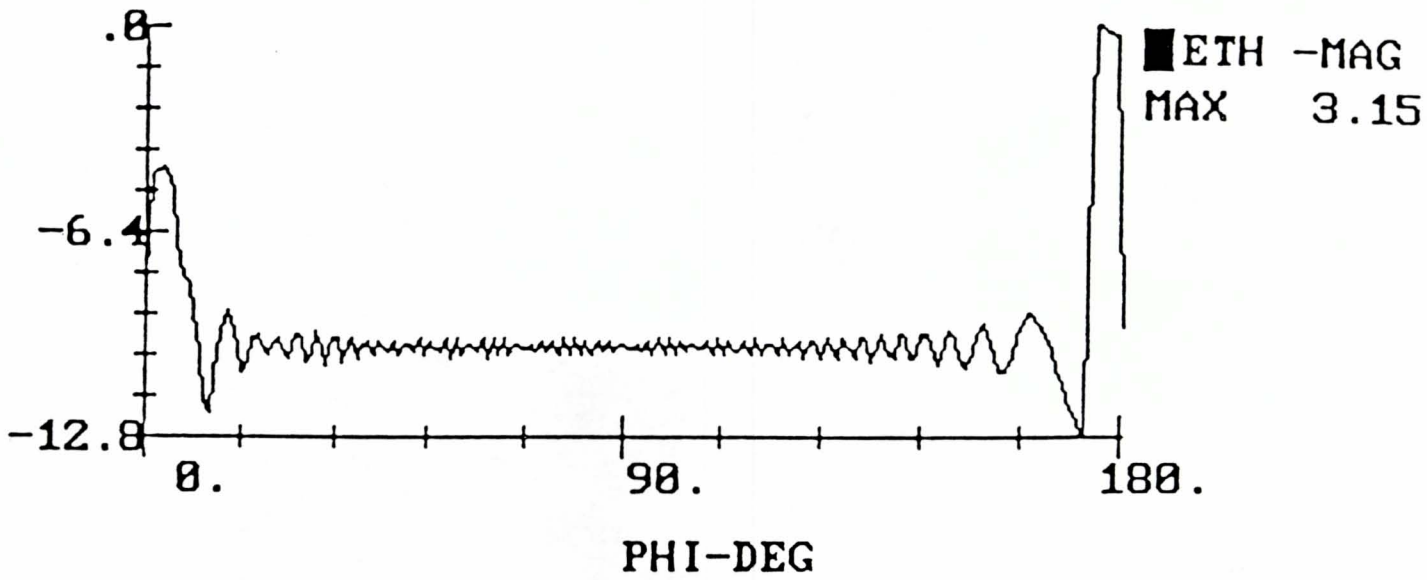
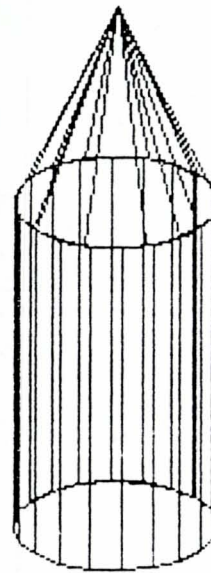
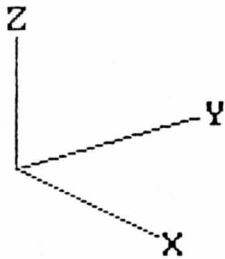


Fig.1.7 Rectangular dB plot of Cubeplat.efl data (Scattered field from a cube)

### 1.3.1.3 Example 3 - A rocket model

This is a model of a rocket formed by merging a cylinder and a cone.

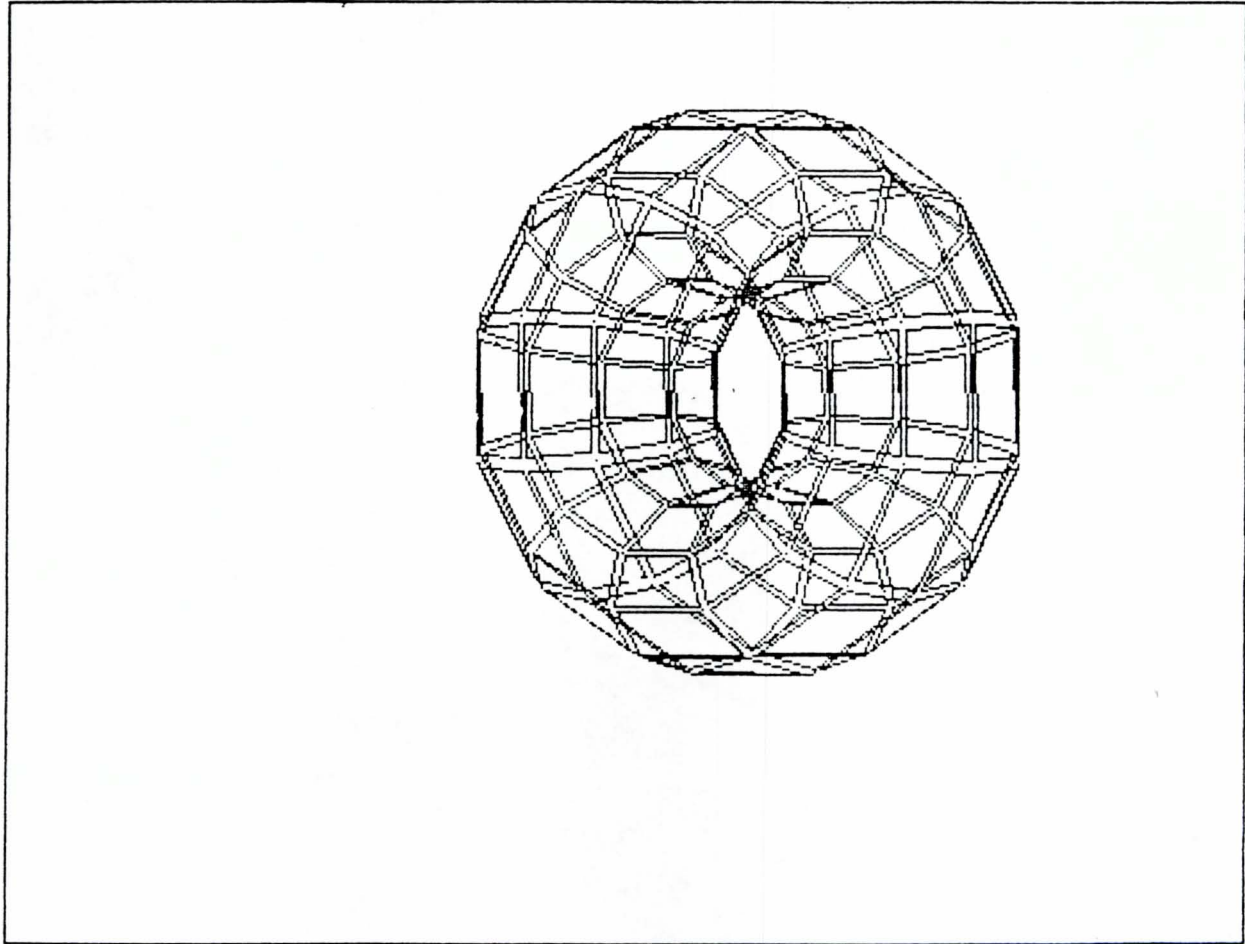
This rocket is form  
by "merge" option.  
Connect a cone to  
a cylinder.



Model of rocket by  
cylinder + cone

#### 1.3.1.4 Example 4 - A Torrus model

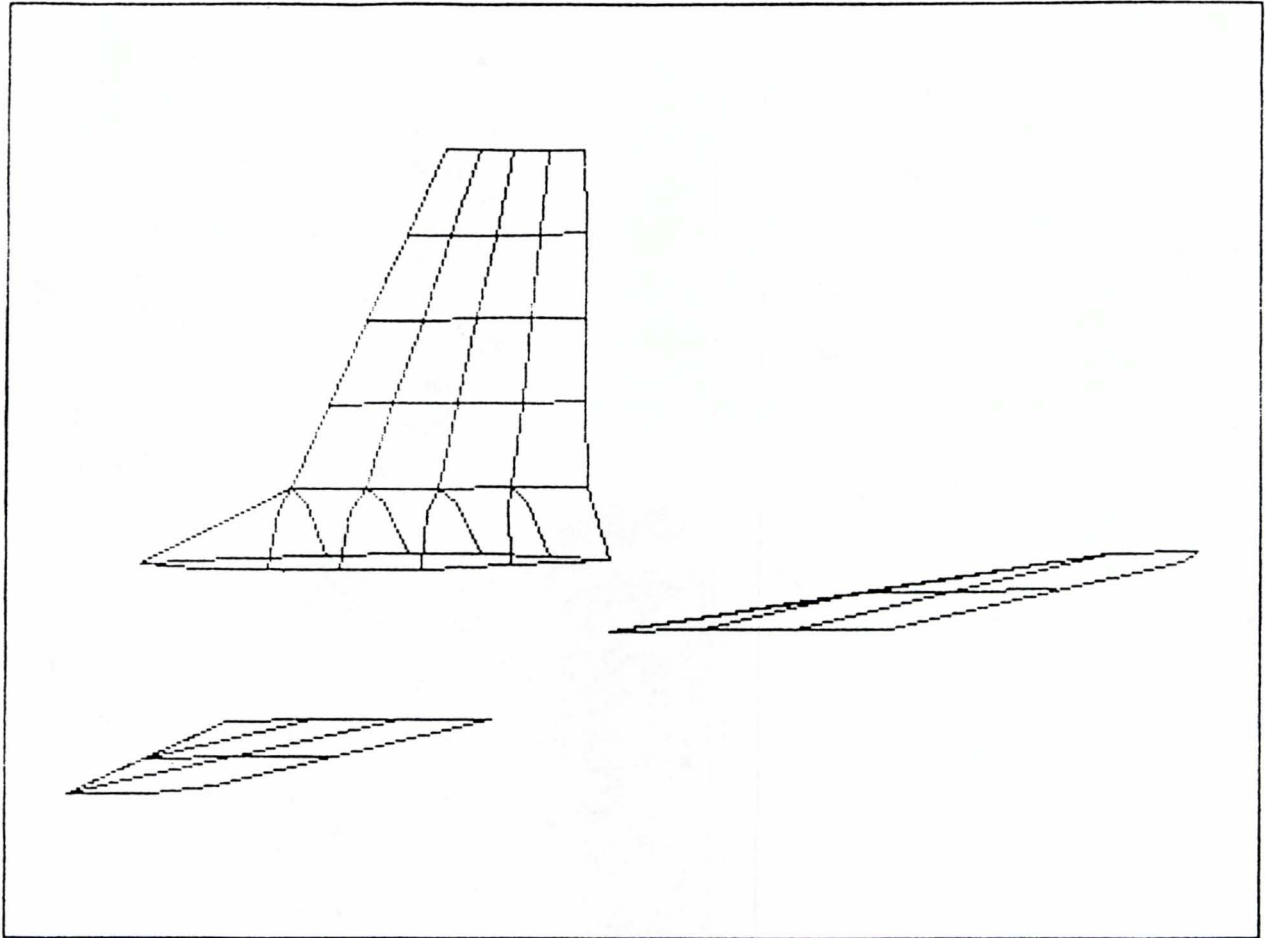
This is a torrus model generated by rotating and translating a circle along a 360-degree path .

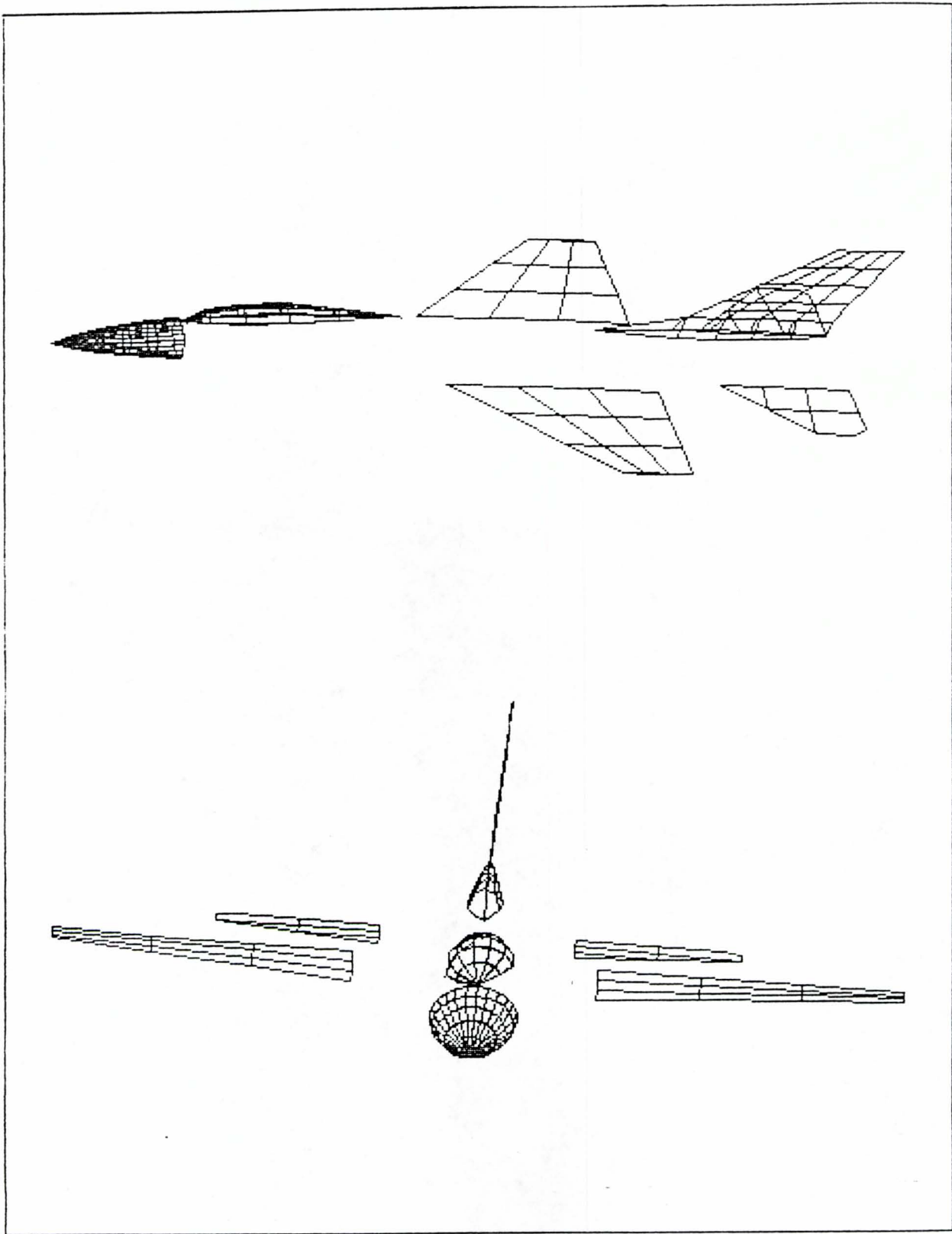


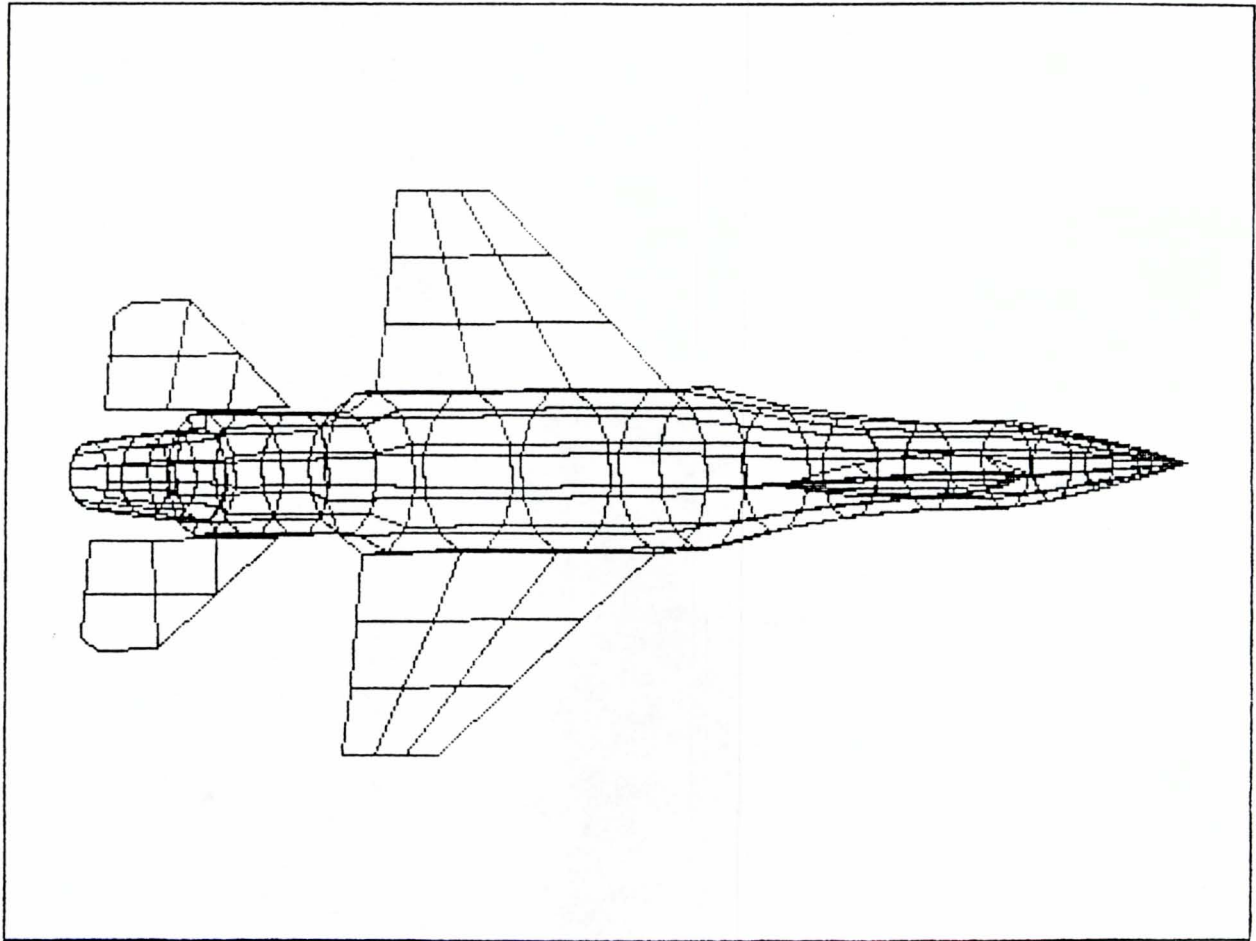


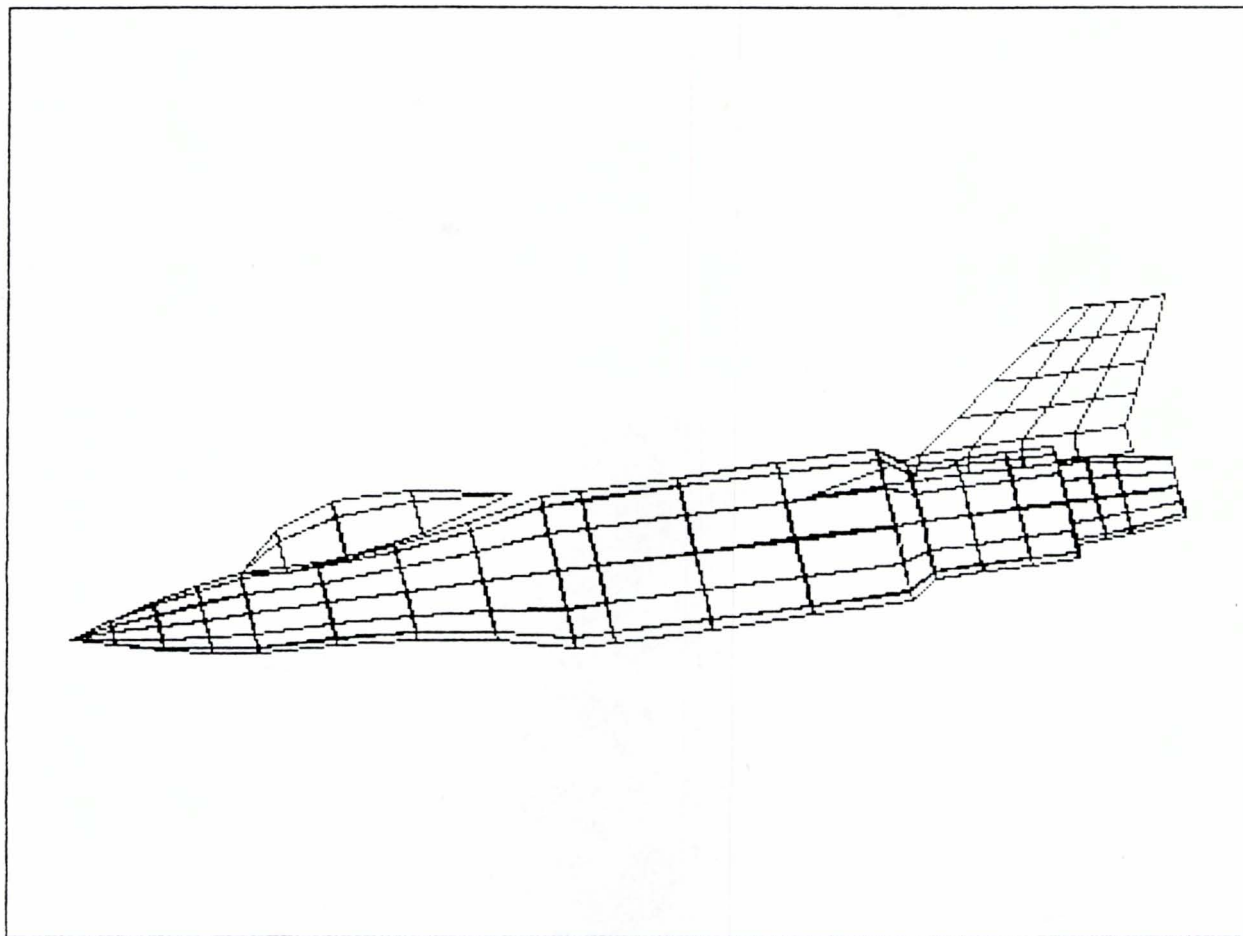
### 1.3.1.5 Example 5 - Airplane Geometry

The following pages show a sequence of airplane-parts modelling.









#### 1.4 CONCLUSIONS

There is still a lot of work that should be done in the areas of multipath effects and antenna platform effects. Regarding the multipath effects, the models that have been tested do not consider pulse signals and their dispersion through the atmosphere. The models only give the attenuation of the signal between two communication points. Also, the models are restricted to a number of specific types of antennas. That means that an antenna radiation pattern that includes all platform effects should be entered in this code to simulate real life signals.

As far as the antenna platform effects are concerned, there is still a need for more work with GEMACS to identify the limits of this software package. We have mastered GAUGE and we believe that once the user builds a good library of various canonical geometries, i.e. cones, cylinders etc. and various parts of airplane geometries, then the user can build complicated structures in a short period of time.

# **IFF Tactical Electronic Simulation and Test System**

## **2. Signal Generation**

Dr. D.C. Malocha

## 2.1 INTRODUCTION

There are many approaches to consider when designing a signal conditioner system. Ideally, we would like to require infinite dynamic control on all of the variables, including amplitude, delay, dispersion, and bandwidth. Unfortunately, it is unrealistic to require these types of constraints, since they are non-realizable. And, therefore, we are left with a less than ideal signal conditioner system. It becomes important then to specify the correct operating ranges for the system and the dynamic range that is available on all of the variables. The signal conditioner should modify the input signal in a way that is controlled by the simulation tools and add a minimum distortion which is both measurable and acceptable to the system under test.

Upon reviewing what might be required for an arbitrary comm-link system, we set some preliminary design goals, including dynamic amplitude control of approximately 150 dB, dynamic delay control between zero and one millisecond, variable amplitude dispersion to less than 11 dB dynamic range over the fractional bandwidth of interest, and variable phase dispersion in the range of tens of nanoseconds. We did not specify any switching delay times because these will be limited by the technology of choice for each of the components to accomplish the signal conditioning.

The approach we have taken is to not limit the input signal to any particular format. Therefore, if a signal conditioner box can be defined and implemented, it should be able to accommodate signals having a range of center frequencies with an acceptable range of fractional bandwidths. This approach is most general in that it can handle conventional AM, FM, or digital transmissions as well as handling spread spectrum system transmissions.

The following sections describe what we have accomplished in this past month. We compiled the information from the vendors (sent to us in the previous month) in this report. We continued to work on quadrature modulation approaches. And finally, we have presented a

briefing to the Navy at UCF's Institute of Simulation and Training on September 12, 1991.

During this time, we briefed the Navy personnel on our initial findings and also presented the theoretical work as well as a hardware demonstration of our quadrature modulation research.

## **2.2 DELAY**

Producing variable delay at RF frequencies over a large dynamic range is extremely challenging. The principle motivating factor requiring the use of RF frequencies is the fact that a large absolute bandwidth is necessary for state-of-the-art communication systems. Because of the fairly large RF bandwidths, it is very difficult or impossible to obtain digital-to-analog or analog-to-digital converters that will sample at the required rates.

There are two principle limiting situations with respect to the dynamic range on delay. The direct transmission signal delay is dependent on the distance between transmitter and receiver. This could be a very short distance, as in an air squadron, or very long distances, as in air-to-ground base communication link. The second delay range of interest corresponds to dispersion, which creates a very minor delay variation versus frequency.

Based on the previous months' reports, the delay time between two transponders at a separation distance of one hundred miles is approximately six hundred microseconds. To simulate this delay at RF frequencies is very difficult. Since the velocity of an electromagnetic wave is approximately the same as that in free space, it would require an enormously and prohibitively long delay line to achieve six hundred microseconds of delay. A common approach to obtaining relatively long delays is to convert the electrical signal into acoustic energy. An acoustic wave travels approximately ten thousand times slower than an electromagnetic wave, which condenses the required path length implemented in a given device. An electromagnetic wave delay of miles can be simulated on an acoustic device in inches.



There are several technologies that have been previously used for obtaining various delays acoustically. These include bulk acoustic wave delay lines, surface acoustic wave devices, and the launching of acoustic waves on other types of materials. Depending on the exact requirement, we might include investigation of all of these technologies.

In order to simulate the very long delays, it is proposed at the present time to modify the effective trigger at the signal generation source. This approach allows for digital control of the delay of the generated transmission signal. This has the advantage of achieving very long delays, which are simulated through clocks and gates, easily digitally. The disadvantage of this approach is that the simulation hardware and software tool must be able to be integrated into the actual transmitter hardware. This will require some thought on the hardware layout and the approach to software simulation and hardware drivers from the simulator. However, it is our belief that there presently is no good approach to simulation of variable long delay paths at RF frequencies and bandwidths.

Surface acoustic wave devices have been built with tens of microseconds of delay. Actual device lengths of up to six inches have been previously reported. It would be possible to simulate delays in the tens of microseconds. However, in the simulation process, it would not be possible to achieve an arbitrary variable delay. In a typical surface wave device, there would be multiple outputs that would be spaced at a predetermined interval. For long delays, in the tens of microseconds, it would probably be reasonable to expect four to ten outputs. It would be technically feasible to have more than this number of fixed outputs; however, the cost may increase and a reasonable amount of research might be required.

Another approach for obtaining variable delays may be to use an acoustic charge transport (ACT) device. Acoustic charge transport devices represent a relatively new technology. There have been reports of using these devices for memory applications. The approach uses a surface acoustic wave as a clock to move electronic charge. The only purpose of the surface wave is to provide the clock; it does not do any signal processing. The charge moves in potential wells at

the acoustic velocity. There has been previous work and reports on using an ACT device in a memory configuration. The approach is to freeze the charge into potential wells for the required length of time, and then to dump the charge back into the moving potential wells for clocking out of the signal at the appropriate time. This is a research device and is not commercially available (to our knowledge). There may also be limitations in terms of requirements for cooling of the device to hold the charge for relatively long periods of time. This would be an area for further investigation and research.

In addition to obtaining the long delays, it would also be required to provide relatively short delays as well as phase dispersion, which is a frequency dependent delay. Relatively short delays are feasible with surface acoustic wave devices. A surface wave device can have multiple tapped outputs which are externally controlled via PIN attenuators on each tap. The delay time between taps is on the order of tens of nanoseconds to as low as five nanoseconds. The minimum delay spacing in a single in-line device is proportional to center frequency. Such a device has been previously used in production for proximity fuses. These devices may be off-the-shelf and available, but may not meet the system requirements.

Another approach would be to use parallel devices with a slight fixed delay offset such that the relative delay between taps of two devices would be slightly different. This would allow the minimum delay between taps to be divided by  $N$ , where  $N$  is the number of parallel devices.

Another technique is to again use acoustic charge transport devices. There are commercially available ACT devices that have programmable taps. The number of taps currently available is 128 with a time delay separation of approximately ten nanoseconds. The device is fully programmable, and, therefore, it would be possible to have 128 discrete delay steps that are relatively close together.

It is believed that using a combination of an external trigger and one or more of the mentioned technologies for simulation of a reasonable set of delayed signal responses is feasible. Although the proposed implementations would not allow for continuous delay steps, it is

believed that the choice of the steps could be judiciously made such that reasonable simulations over a wide range of operating scenarios could be tested. For instance, it may only be possible to test a scenario based on a separation distance of ten miles, fifty miles, one hundred miles, one hundred and fifty miles, etc., in quantized steps. However, it would seem reasonable that interpolation could be accomplished, based on these results, via computer to provide a smooth fit of the data. The exact step size and the system requirements would be integrated into an overall simulator requirement.

### **2.3 AMPLITUDE CONTROL**

We have primarily investigated two different approaches to control of amplitude of the signal. The first has been the use of programmable attenuators. Programmable attenuators may be switched either mechanically or electronically. The second is the use of a voltage variable attenuator. The results of both approaches are presented in Appendices A and B, which describes much of the hardware considerations.

The variable attenuator approach has distinct advantages in its simplicity, low cost, and wide bandwidth. It basically uses electrically controlled mechanical devices, or electronic switches, to switch in a variable amount of attenuation in a fixed impedance transmission line. Attenuation is available from tens of dBs to half dB steps. There are several issues that would require further research even after seeing the manufacturer's specifications. The first issue is the range of accuracy and the reproducibility of the attenuators. Absolute accuracy is desirable; however, software could compensate for known deviations in the amplitude control. Although the attenuation steps may not be exact, if they are reproducible, it would be possible to compensate for these effects in software. However, if these effects are non-reproducible, it would be required a limit be placed on the accuracy of the simulation itself. If mechanical devices are used, the reproducibility of switching is certainly a major question to be investigated.

A second issue is the lifetime of the switches themselves. If they are mechanical devices, the meantime to failure may not be long enough to be practical for real world simulations. The lifetime for mechanical devices might be increased by using a "smart" approach to minimize the required number of switches. Electronic switching should have a much longer lifetime and is probably the preferred approach for long lifetimes and fast switching speeds.

Finally, the attenuators for which we had requested information have a rather long settling time of several milliseconds. This time would be unacceptable for most simulations. Therefore, it may be required to buy faster switching attenuators which, more than likely, would increase the cost of the components.

We also investigated a voltage controllable attenuator. This has some distinct advantages because it is non-mechanical and, therefore, should have a very long lifetime and possibly very fast switching time capabilities. However, there is a disadvantage in that the dynamic range of the attenuator is approximately ten dB. This would require the cascading of many attenuators together. This could raise serious problems in terms of feedback in the system, which would cause spurious oscillations and concern for the amount of signal distortion and noise that may be introduced into the system using this approach. This would certainly be an area for further study.

## **2.4 AMPLITUDE DISPERSION**

Because of the transmitter and receiver operating frequency, it may be necessary to model the effects of the signal propagation through the atmosphere. One effect will be frequency dependent attenuation versus frequency. This amplitude dispersion is caused by frequency dependent atmospheric absorption. Figure 2 of Monthly Report #1 showed the path loss versus frequency around a center frequency of 1 GHz and at a distance of  $d=150$  miles. The plot shows a linear attenuation (in dB) versus frequency and approximately 2 dB variation over 320 MHz. The slope of the line will decrease as the path length decreases and increase as the path length increases. This should be quite easy to model and simulate in software.

There are several approaches to simulate amplitude dispersion in hardware. One approach is to use a linear, programmable, wideband filter, and another approach is to use multiple linear, fixed, narrow band filters in parallel with a programmable attenuator in series with each filter. The first approach is both elegant and simple in concept; however, it may be very difficult to implement in hardware and may be costly. One device which is programmable at RF frequencies and with reasonable bandwidths is an acoustic charge transport (ACT) programmable filter. Devices operate at center frequencies between approximately 300-400 MHz and have a fractional bandwidth of at least 50%. Current devices provide a 128 tap finite impulse response (FIR) in which each tap can be reprogrammed. Issues would include cost, programming speed, tap weight accuracy, and spurious response generation.

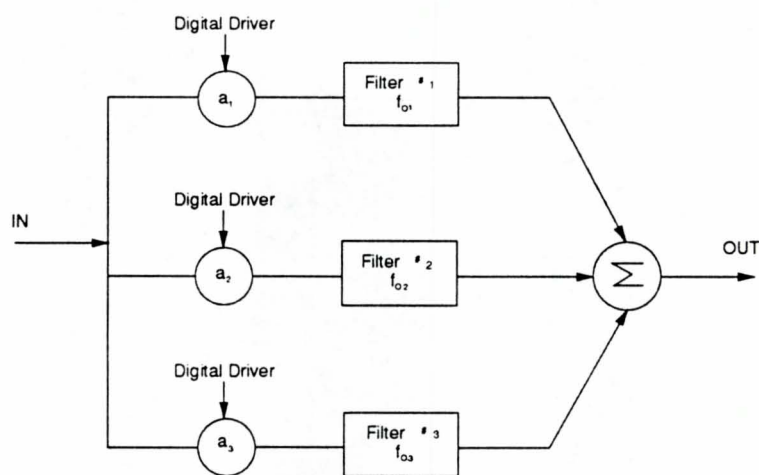


Figure 1. Programmable Amplitude Dispersive Filter

The second approach may be implemented as shown in Figure 2.1. The signal is input to three parallel branches. Each branch contains a programmable attenuator ( $a_1, a_2, a_3$ ) and a fixed filter with differing center frequencies. The attenuators can be programmed for the small frequency-dependent-path-loss variations and may also include the required center frequency attenuation. This approach requires more hardware, but may be more easily attainable and have lower risk. The filters must be linear to minimize unwanted distortion. At these RF frequencies,

surface acoustic wave (SAW) filters would probably yield the best performance for the filters. The parallel branches are similar to a conventional filter bank. Since the dynamic range of the attenuator is small, the best component choice would probably be variable, linear amplifiers. Issues would include the power splitter, the relative filter match between components and the filter bandwidth and impulse response length.

## 2.5 CONCLUSIONS

During these last three months, we have examined the requirements for a signal conditioner system. The signal conditioner that is proposed would not be limited to any particular data format. Rather, the signal conditioner system would be able to input any arbitrary waveform within a given range of center frequencies and within a given range of fractional bandwidths, and the output of the signal conditioner would be a distorted waveform that would include the simulated effects of transmission through a given environment between the transmitter and receiver.

Based on this work, it does appear feasible to build a signal conditioning unit. There are some technical difficulties that would need further study; however, the basic feasibility does appear to be available at the present time.

The primary approach we have taken assumes an intermediate frequency type receiver, which will introduce amplitude and phase dispersion, a variable delay with moderate delay times available, and a variable attenuator to simulate the effects of distance between transmitter and receiver. This approach is based on the fact that current limitations in digital technology do not allow for the required sampling rates of hundreds of megahertz needed to process bandwidths in the tens of megahertz. The signal conditioner box will have limitations with regards to the fractional bandwidth of the transmitted signal and the level of distortion which the signal conditioner may introduce. Details of these effects are dependent on the choice of technology

for implementing the signal conditioner components as well as the center frequency and bandwidth of the signal under test. It is believed that this approach to system implementation will meet a broad class of communications currently used by the Navy.

If a wide range of digital hardware begins to operate at hundreds of megahertz clock frequencies, it may be possible to go to a digital hardware implementation. Digital hardware is primarily limited by the fractional bandwidth of the communication system. If digital techniques provide sampling of analog signals at the rate of one hundred megahertz or more, then it may be possible to use a digital receiver approach to capturing the signal, mixing it to base-band, sampling it, and then breaking the channel into in-phase and quadrature channels for introducing the controlled conditioning of the input signal. The signal would then be digital-to-analog converted and mixed back and re-transmitted at the original carrier frequency. Advantages include adding long delay times via the clock and gates, using relatively inexpensive digital hardware, and using I-Q processing for adding distortion effects.

Considering the limited amount of time and resources which have been allocated to signal conditioning research, it is clearly an area for further research. In addition to the design problems discussed, there are technical problems that will become apparent only when trying to implement the actual hardware. The design approach appears, at this time, to be a direct trade-off between a signal conditioner hardware cost versus its capability. Some components that are available can provide simple functions at a very low cost. However, some of the functions (such as delay) require sophisticated hardware approaches to implement the probable required delay specifications; these approaches use new technologies that currently have a rather high cost. As always, it is anticipated that the cost of these technologies will continue to decrease as time progresses. Therefore, it can be concluded that the possibility of building a signal conditioner hardware system to measure a broad range of communication system formats is possible. However, considerably more research is necessary to accomplish the task.

During this research, we have investigated various quadrature modulation techniques for confining spectral energy while maintaining a uniform modulated time envelope. The spectral confinement reduces out-of-band energy which decreases noise and co-channel interference. In addition, we have demonstrated actual hardware which generates the quadrature modulation, PN sequence for spread spectrum applications. The results obtained compared very well with theoretical predictions. These approaches help to eliminate system filtering which degrades the modulated signal by causing AM and intersymbol interference. Further research will continue on attempts to fully characterize system performance.



Appendix 2.A

NAVY TESTS  
BRIEFING

September 12, 1991

Donald C. Malocha

Professor

Nancy L. Eisenhauer

Research Assistant

## What Do We Want From A Signal Conditioner?

---

- Infinite bandwidth (very wide)
- Dynamic amplitude control
  - 150dB dynamic range
- Dynamic delay control
  - 0 - 10 msec
- Variable amplitude dispersion
  - Broad band
  - 10's of dB dynamic range

## What Do We Want (cont.)

---

- Variable phase dispersion
  - Broad band
  - 10's of nsecs
- Signal conditioner is input signal independent
- Distortionless
- Zero time delay for switching components

# Path Loss v Distance

f=1000 Mhz

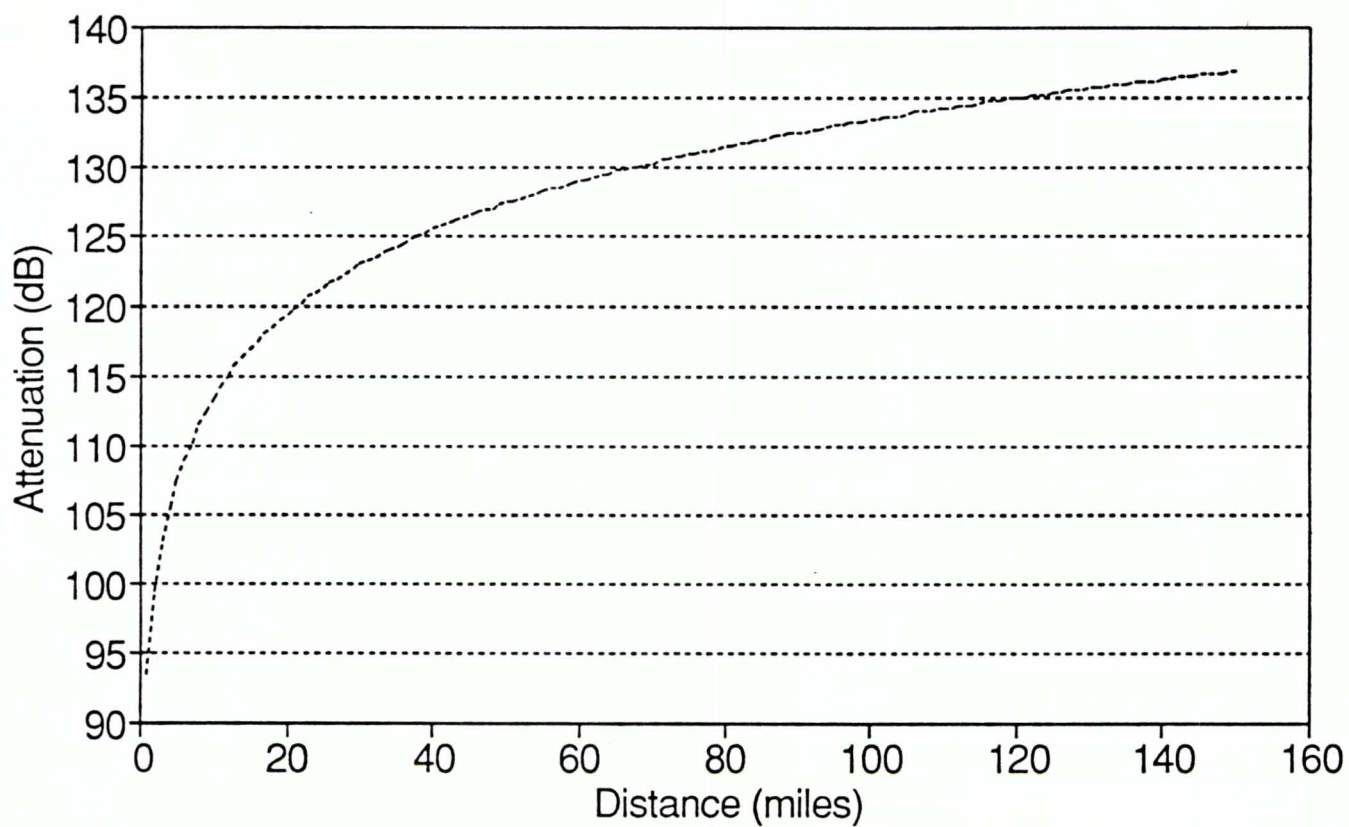


Figure 2.A.1

# Delay v Distance

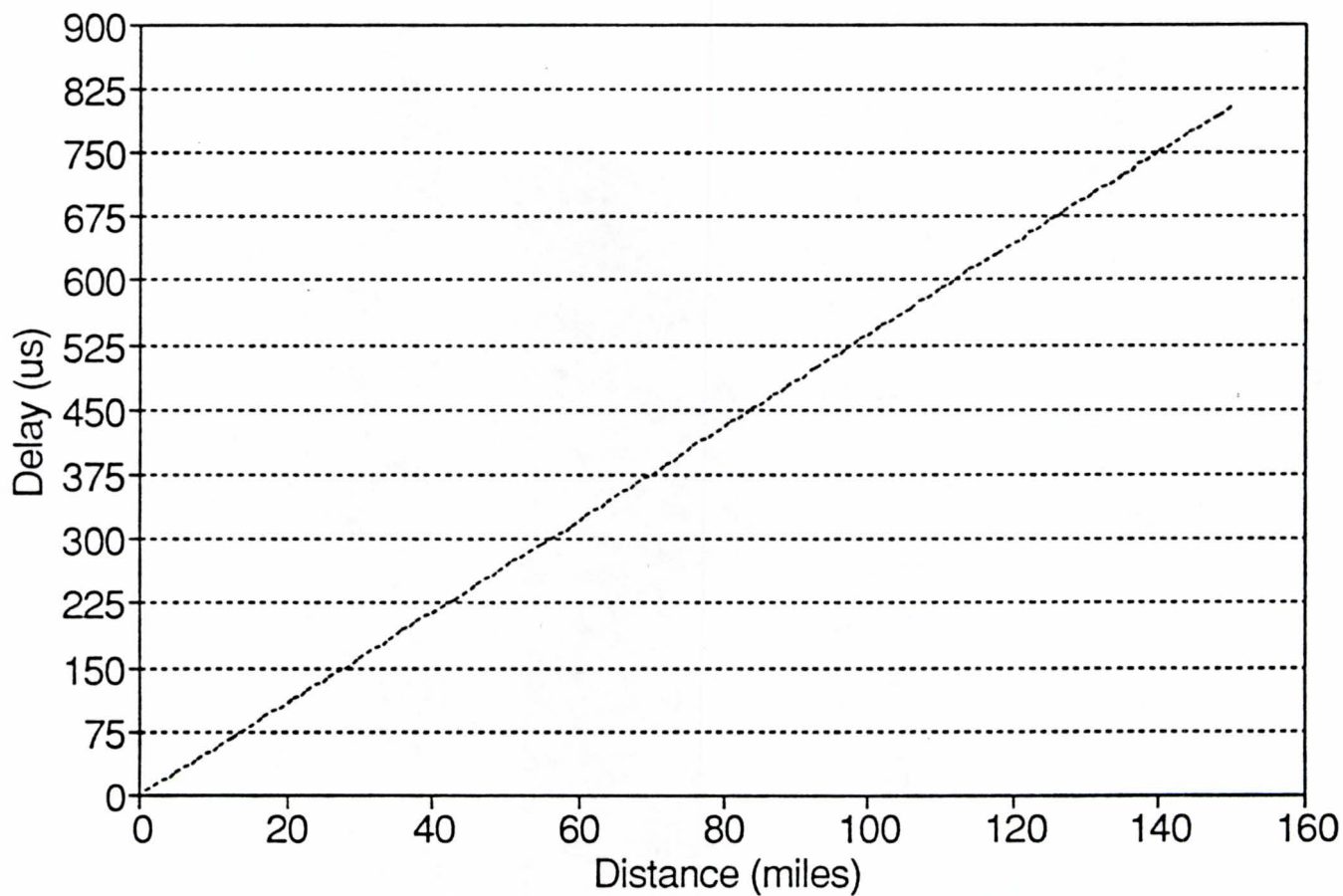
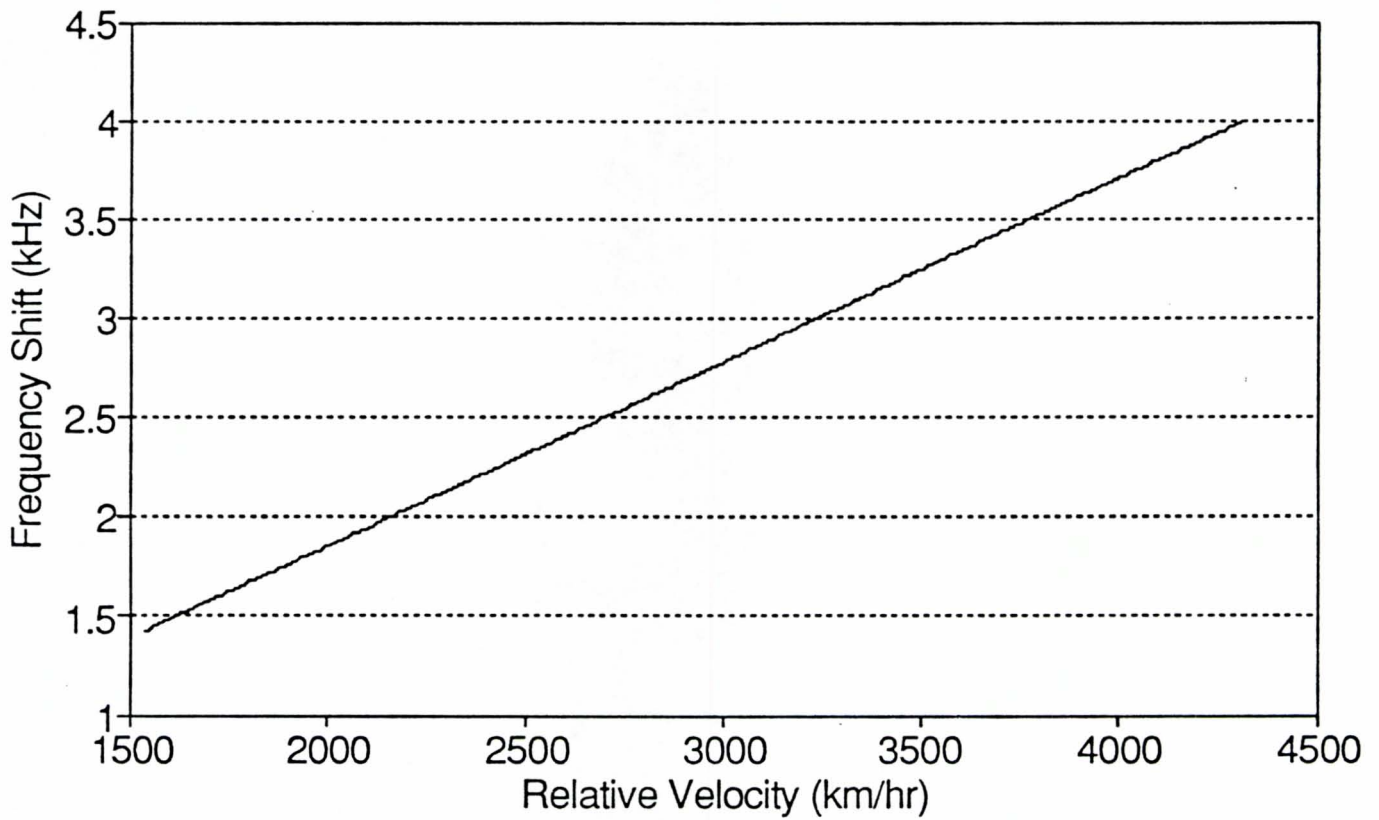


Figure 2.A.3

# Doppler Frequency Shift

$f = 1000 \text{ MHz}$



Frequency Shift Due to Doppler vs. Relative Velocity

Figure 2.A.4

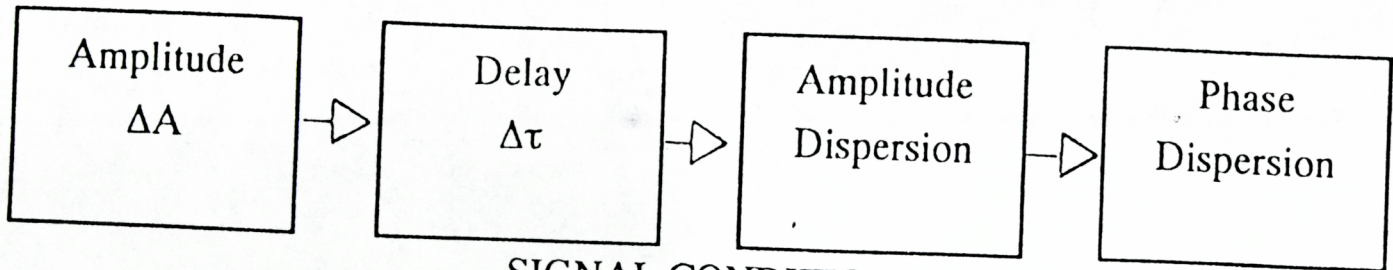
# Approaches

---

- Implement signal conditioner as a receiver/transmitter
- Passive component based ( $f_0$ , %BW)(distortion)
- I.F. signal conditioner (distortion)

- Hardware
  - Cost vs. Performance
    - Linearity
    - Accuracy
    - Speed
- Software
  - Programmed component corrections





SIGNAL CONDITIONER  
SYSTEM BLOCK DIAGRAM

Input Signal

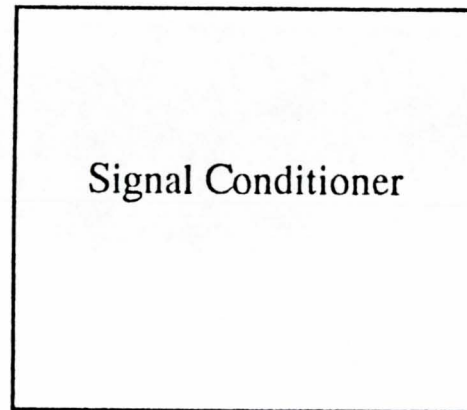
$f_o$

BW

$\tau$

$A_i(f)$

$\varphi_i(f)$



Output Signal

$f_o$

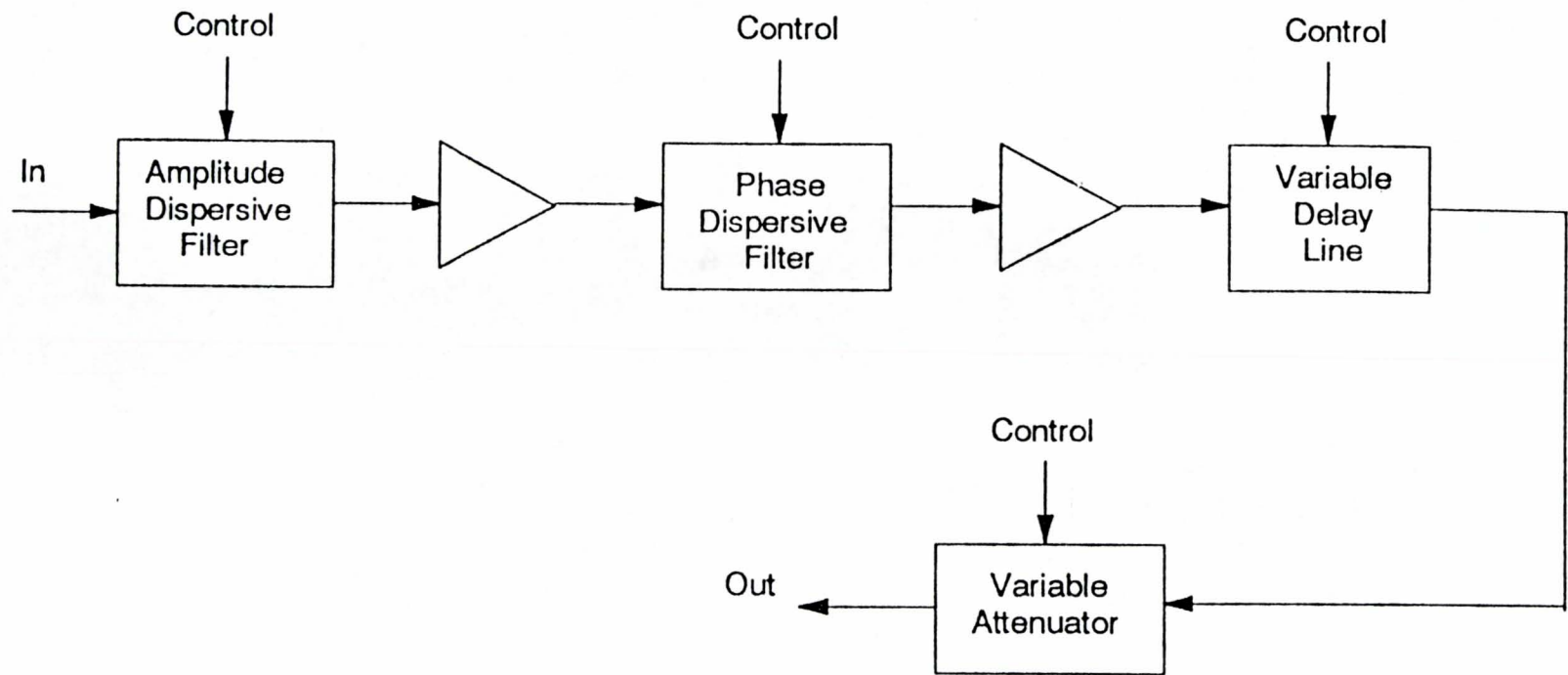
BW

$\tau_o + \Delta\tau$

$A_o(f)$

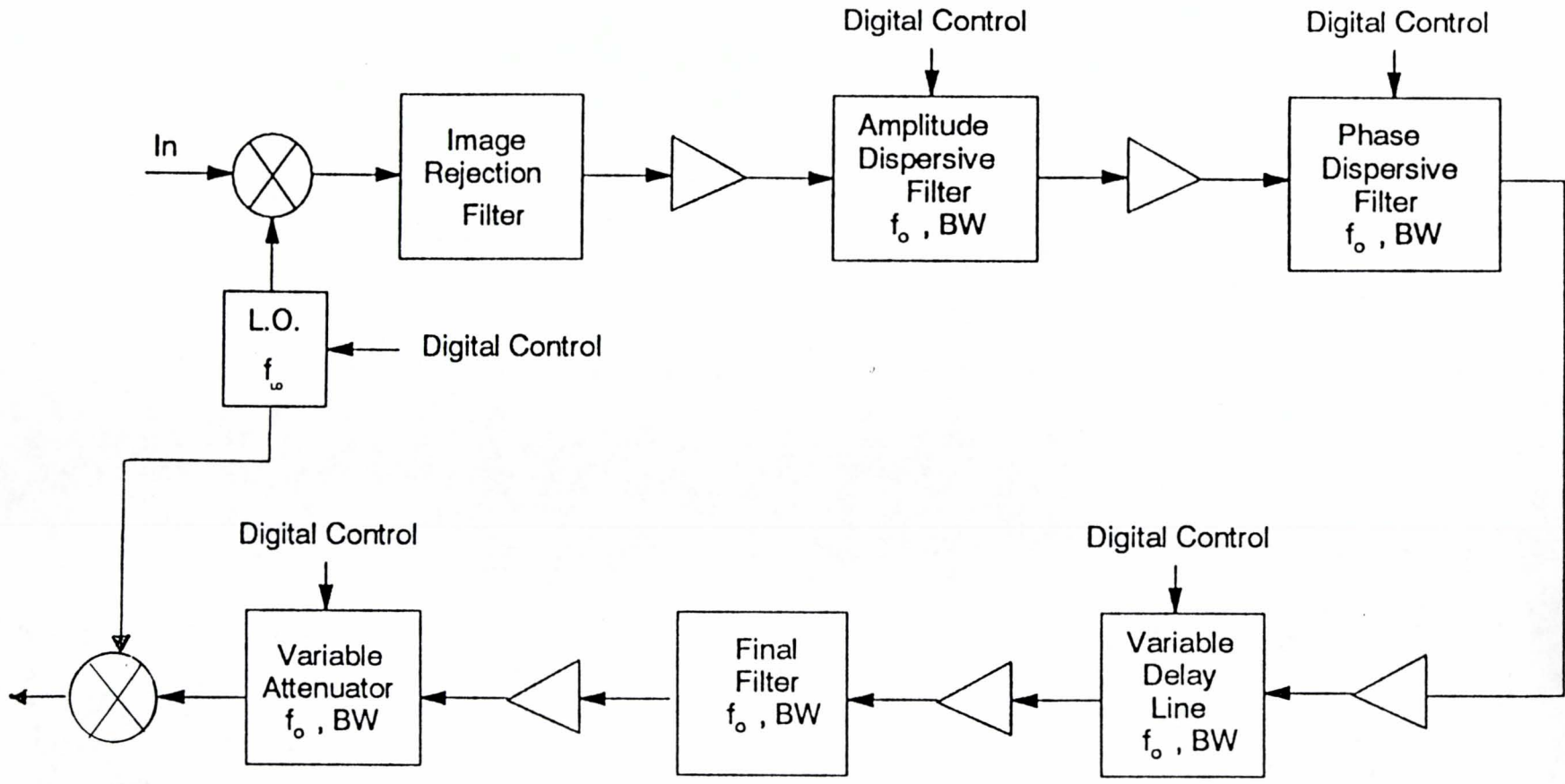
$\varphi_o(f)$

Figure 3



85

Signal Conditioner  
Component Block Diagram #1



Signal Conditioner  
Component Block Diagram #2

## Amplitude/Phase Dispersion

---

- ACT device
  - Programmable
- Multi-filter SAW
  - Amplitude only

# Delay

---

- Delay  $< 10 \mu\text{sec}$ 
  - SAW delay line
    - Proximity fuses
    - Required development
- ACT programmable delay line
  - $f_0 \sim 180 \text{ MHz}$
  - $\Delta T \cong 6 \text{ nsec}$

## Appendix 2.B

### COMPONENT SPECIFICATIONS

Donald C. Malocha

Professor

Nancy L. Eisenhauer

Research Assistant

The component specification sheets which follow are a subset of what is believed to be a good representation of devices needed to generate, transmit and detect spread spectrum signals. This is not meant to be an exhaustive set of hardware specifications. The actual hardware will be dependent on the required system specifications. However, there are available system components which allow a large class of potential communication system configurations to be built.

# Attenuators

---

- Programmable
  - 10 dB steps
    - ~ 0.7 dB accuracy
    - ~ 6 ms switching
  - 1 dB steps
    - ~ 0.1 dB accuracy
    - ~ 6 ms switching
  - 0.1 dB steps
    - ?
  - Variable amplifier
    - Dynamic range ~ 10 dB



## Linear Voltage Variable Attenuator

Purpose: To simulate fine attenuation adjustment due to distances between the transmitter and receiver.

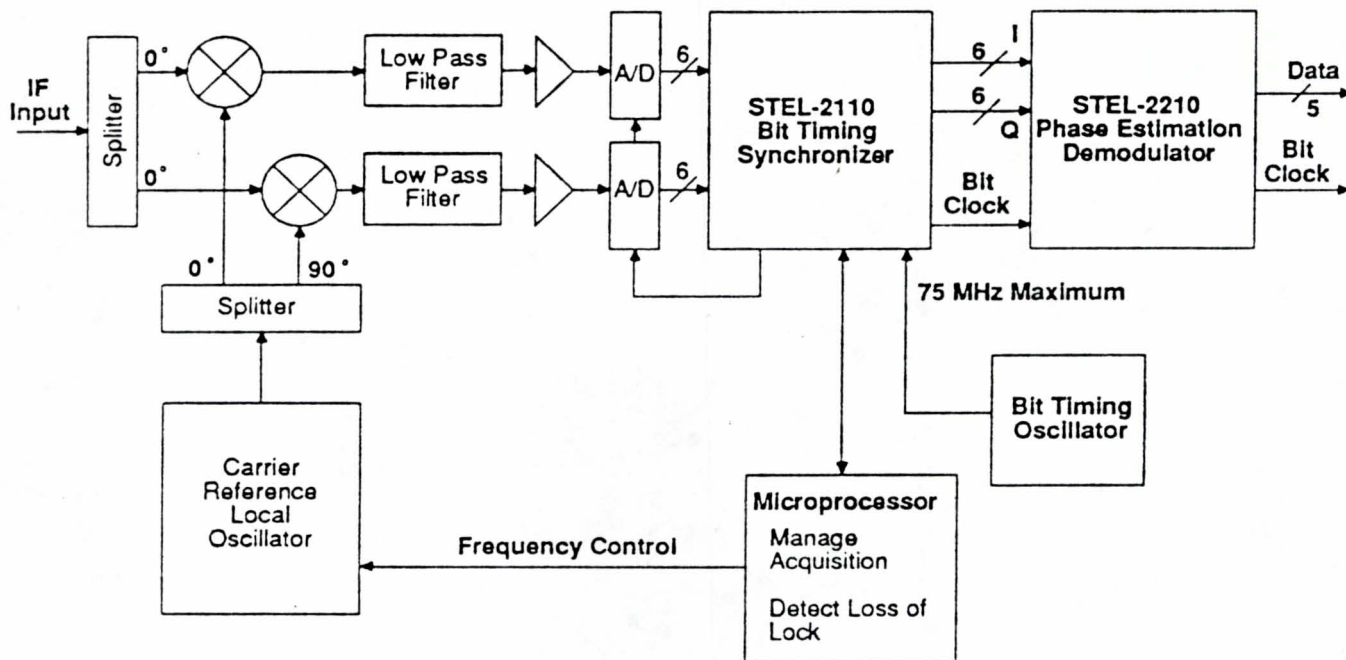
Parameters	Specification Limits	Units
Frequency Range	20 - 500	MHz
Linear Attenuation	0.0 - 11.0	dB Min
Range		
Attenuation Flatness	0.7	dB Max p-p
Input 1 dB Compression	10.0	dBm Min
Deviation from Best Fit	$\pm 1.0$	dB Max
Line		
Switching Speed	6	ms
Price	\$150.00	

## Programmable Attenuators

Purpose: To simulate rough attenuation adjustment due to distances.

Parameters	Specification Limits	Units
Frequency Range	DC - 3	GHz
Attenuation Range	0 - 85	dB (in 1 dB steps)
Attenuation Steps	1, 2, 4, 8, 10, 20, 40	dB
Attenuation Accuracy	DC - 500 MHz $\pm$ .3 or .5%	dB
	500 - 1000 MHz $\pm$ .4 or	dB
	1.0%	dB
	1000 - 2000 MHz $\pm$ .5 or	dB
	1.0%	
Attenuation Accuracy	2000 - 3000 MHz $\pm$ .6 or	
	1.5%	
Switching Speed	6	ms
Repeatability	$\pm$ .2	dB
Life (typical)	10 million	operations/relay
Price	\$872.00	

# TYPICAL APPLICATION COHERENT PSK DEMODULATOR



FOR FURTHER INFORMATION  
CALL OR WRITE  
**STANFORD TELECOMMUNICATIONS**

ASIC & Custom Products Group

Direct dial: (408)980-5684 or Operator assist: (408) 748-1010

Fax: (408) 980-1066 Telex: (910) 339-9531

2421 Mission College Blvd. • Santa Clara, CA 95054-1298

© 1988, 1989, 1990 Stanford Telecommunications, Inc. 7/90

**STANFORD  
TELECOM**

---

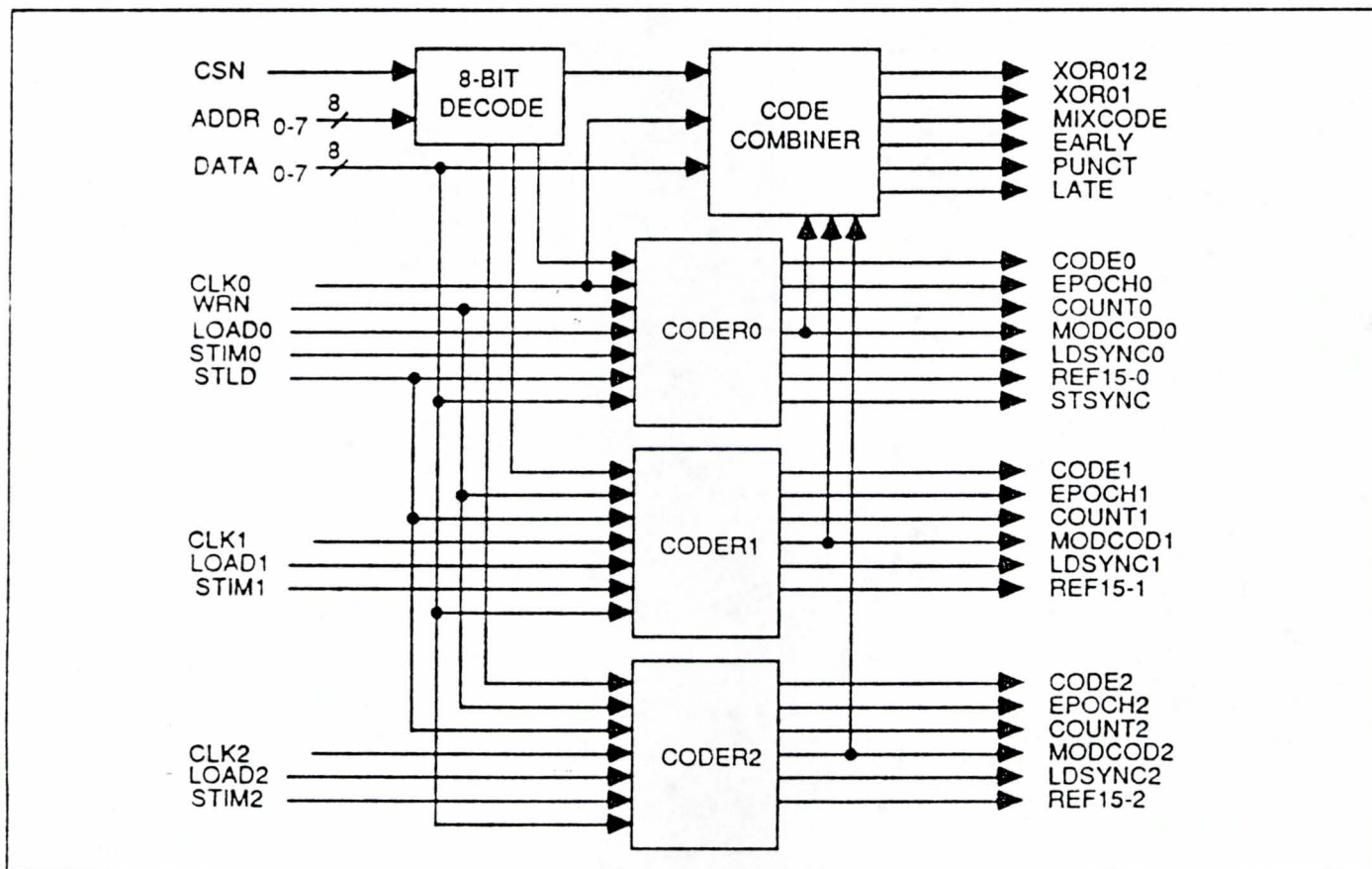
- INDEPENDENT CLOCKS, CONTROLS, AND OUTPUTS
- MICROPROCESSOR CONTROL INTERFACE
- COMPOSITE CODE GENERATION CAPABILITIES
- PUNCTUAL, LATE, AND EARLY OUTPUTS FOR CODE TRACKING
- 30 MHz OPERATION
- LOW POWER CMOS
- MILITARY AND COMMERCIAL TEMPERATURE RANGES AVAILABLE

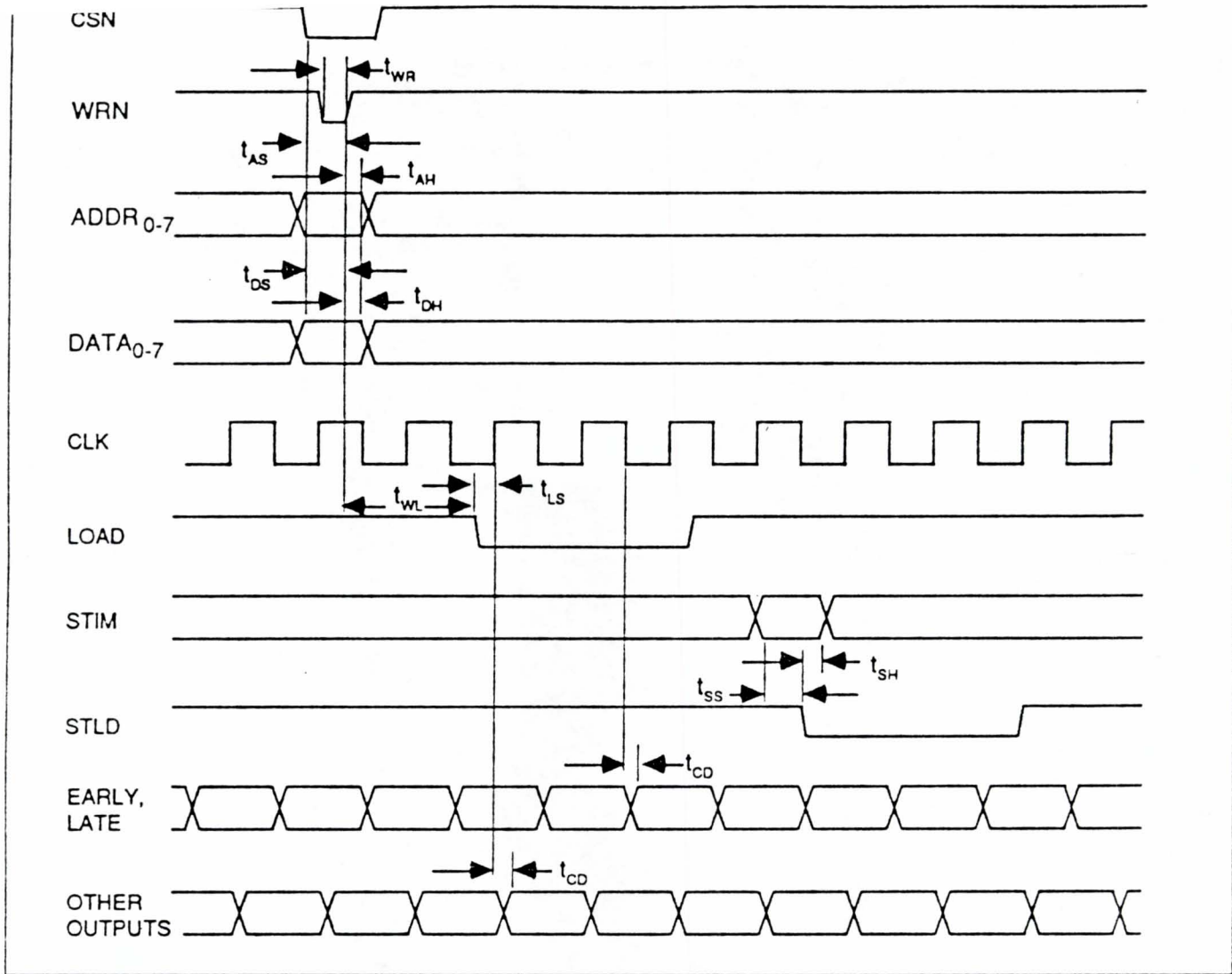
Coder provides the communications industry with a cost-effective and compact solution to code generation. The device's unique architectural design provides a power-efficient, high-speed code generator able to produce any 3 maximal or non-maximal length codes with up to 32 feedback taps per generator, and code lengths up to  $2^{32}-1$  (4,394,967,295) bits. Capabilities for modulo-2 addition (EXOR), code modulation, and non-linear composite code generation are also provided in the device. The device can be programmed very easily via the microprocessor interface.

## APPLICATIONS

- PSEUDO-RANDOM CODE GENERATION
- GOLD CODE GENERATION
- JPL RANGING CODE GENERATION
- SYNCOPATED CODE GENERATION

## BLOCK DIAGRAM





$t_{DS}$	Data Setup time	10		nsec.	
$t_{AS}$	Address Setup time	10		nsec.	
$t_{DH}$	Data Hold time	10		nsec.	
$t_{AH}$	Address Hold time	10		nsec.	
$t_{LS}$	Load Setup time	10		nsec.	
$t_{WL}$	Write to Load delay time	160		nsec.	
$t_{DH}$	STIM to STLD Setup time	10		nsec.	
$t_{AH}$	STIM to STLD Hold time	10		nsec.	
$t_{CP}$	Max. CLK frequency		30	MHz	
$t_{LS}$	CLK pulse width	10		nsec.	
$t_{WR}$	WRN pulse width	20		nsec.	
$t_{CD}$	Clock delay, CLK to any output	5	18	nsec.	Load = 20 pF

Note: The duty cycle of the  $CLK_0$  signal must be 50% in order to achieve correct timing of the **EARLY** and **LATE** signals, since these outputs are latched on the falling edge of the clock and the **PUNCT** signal is latched on the rising edge.

---

**FOR FURTHER INFORMATION  
CALL OR WRITE  
STANFORD TELECOMMUNICATIONS  
ASIC & Custom Products Group**

Direct dial: (408)980-5684 or Operator assist: (408) 748-1010

Fax: (408) 980-1066 Telex: (910) 339-9531

2421 Mission College Blvd. • Santa Clara, CA 95054-1298

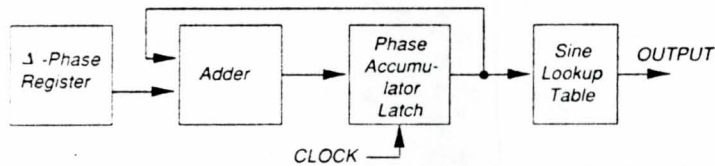
© 1989, 1990 Stanford Telecommunications, Inc. 7/90

---

# Frequency Synthesis Products

## Typical Applications

- ▼ Frequency Synthesizers
- ▼ High-Speed Frequency Hopping
- ▼ Modulators and Demodulators
- ▼ Timing Recovery Circuits
- ▼ Single Sideband Converters
- ▼ Baseband Receivers
- ▼ Digital Signal Processors
- ▼ Frequency and Phase locked Loops



Basic NCO Block Diagram

## Functional Description

The basic principle of operation of an NCO is that an accumulator is used to generate constantly incrementing phase angles, as shown in the block diagram above. These phase angles are then used to address a sine / cosine look-up table to produce the final output signal. By changing the "Δ-phase" number added to the accumulator at each cycle the rate at which the phase angle increments can be varied, thereby changing the frequency of the sine or cosine signal generated.

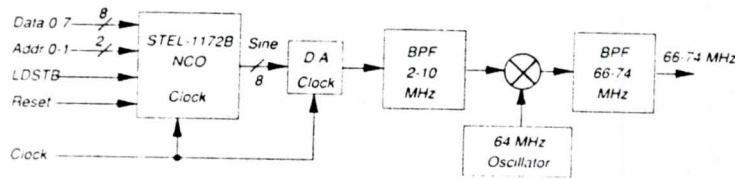
NCOs generate digitized sine and cosine signals with very fine frequency resolution to be used in digital processing applications.

They can also be used in conjunction with a D/A converter in analog frequency generation applications. Most of the NCO devices are designed to operate with an 8-bit microprocessor bus. The STEL-1176, STEL-2172 and STEL-2173 have parallel frequency control interfaces. Although the frequency change is effectively instantaneous after a new Δ-phase word is loaded, the devices all exhibit a latency period between the loading of the new Δ-phase value and the instant of frequency change. The latency periods are shown in the table .



## Typical Application

### ▼ Fast switching 66-74 MHz synthesizer



If the output of the NCO is fed into a video-speed D/A converter, a fast, phase coherent high resolution frequency synthesizer may be realized. The spurious components out of the first filter are 50 to 60 dB below the primary output. This signal can then be translated to any desired center frequency by means of a fixed frequency oscillator, a mixer and a bandpass filter.

## NCO/Direct Digital Synthesis Product Selection Guide

NCO:	STEL-1130	STEL-1172B	STEL-1173	STEL-1174	STEL-1175	STEL-1176	STEL-1177	STEL-1178	STEL-2172	STEL-2173
Technology	CMOS	CMOS	CMOS	CMOS	CMOS	CMOS	CMOS	CMOS	ECL	GaAs
Max clock (MHz)	60	50	50	50	60	80	60	50	300	1000
Frequency Resolution (Hz)	NA	$12 \times 10^{-3}$	$178 \times 10^{-9}$	763	$14 \times 10^{-3}$	0.1000	$14 \times 10^{-3}$	$12 \times 10^{-3}$	1.12	0.233
Frequency Res (bits)	NA	32	48	16	32	35(BCD)	32	32	28	32
Phase Res (bits)	NA	10	13	13	13	15(BCD)	13	13	8	10
DAC Res (bits)	12	8	12	12	12	12	12	12	8	8
Latency (clock cycles)	16/18	34	20	12	17	35	19	19	33	24
Sine and Cosine Outputs	NA	Y	N	N	N	N	Y	N	N	N
FM Res (bits)	NA	-	-	-	-	-	16	-	-	-
PM Res (bits)	NA	-	-	-	12	-	2 x 12	-	-	2
Worst case spur level (dBc)	NA	-55	-75	-75	-75	-72	-75	-75	-45	55
Standard Package	84 pin PLCC	40 pin DIP	48 pin DIP	44 pin PLCC	68 pin PLCC	84 pin PLCC	84 pin PLCC	68 pin PLCC	156 pin PGA	132 pin
(Options available)										flat pack
Board level products		STEL-1272	STEL-1273		STEL-1275 STEL-1375A	STEL-1276 STEL-1376	STEL-1277 STEL-1377		STEL-2272	STEL-2273
Chassis Products									STEL-9272	STEL-9273

# STEL-1130

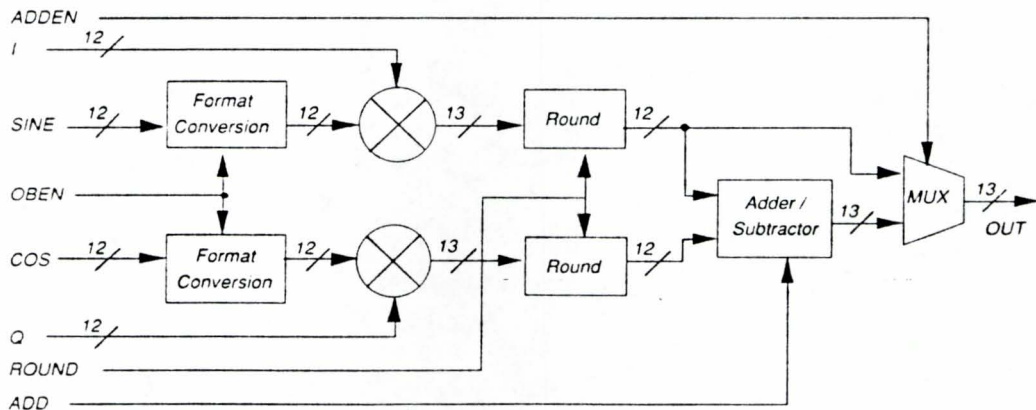
## 60 MHz CMOS Quadrature Amplitude Modulator

The STEL-1130 Quadrature Amplitude Modulator is intended to be used to amplitude modulate the output of an NCO such as the STEL-1172B and the STEL-1177. The STEL-1130 is cascaded with the outputs of the NCO, resulting in modulated digitized sine and cosine signals suitable for digital to analog conversion or digital signal processing. The STEL-1130 can be used for both unsuppressed carrier and suppressed carrier (single or double sideband) modulation.

### Features

- ▼ 60 MHz throughput capability
- ▼ 12-bit inputs
- ▼ Offset binary or two's complement inputs at NCO ports
- ▼ Two's complement or unsigned inputs at modulation ports
- ▼ Products can be added or subtracted
- ▼ 12-bit rounded or truncated products

STEL-1130 Block Diagram



# STEL-2173

## 1 GHz

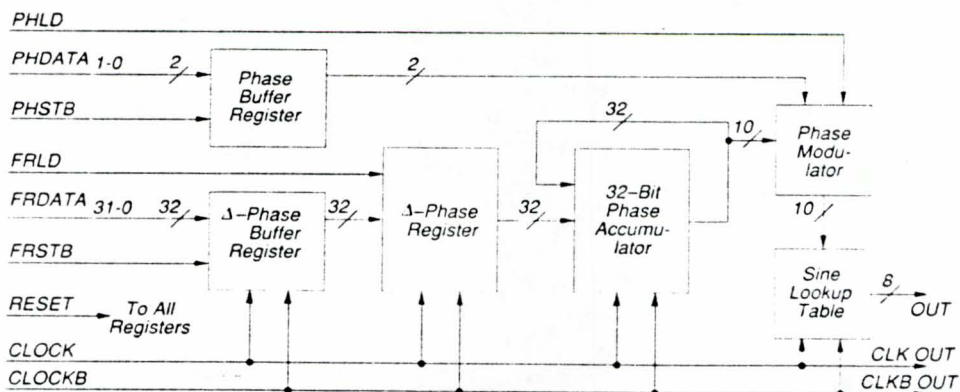
### 32-bit GaAs MNCO

The STEL-2173 GaAs NCO provides high resolution frequency synthesis with virtually instantaneous frequency switching. All I/O signals are ECL compatible to facilitate interfacing with high-speed control circuits and DACs.

#### Features

- ▼ On-chip look-up table
- ▼ 1 GHz maximum over commercial operating conditions
- ▼ 32-bit frequency resolution
- ▼ -55 dBc spurious typical
- ▼ 2-bit PM for BPSK or QPSK
- ▼ High frequency-update rate
- ▼ Evaluation board available (STEL-2273)

STEL-2173 Block Diagram



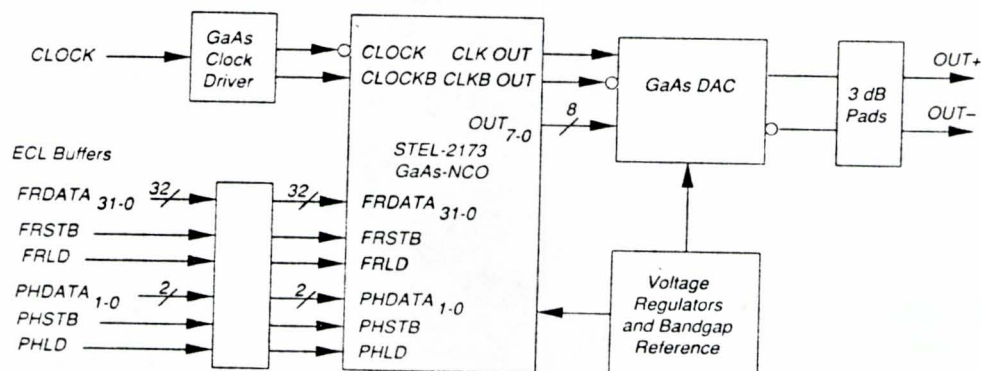
# STEL-2273 0-400 MHz DDS with 2-bit PM

The STEL-2273 is a synthesizer board assembly using the STEL-2173 GaAs Numerically Controlled Oscillator (NCO) chip. The board uses the STEL-2173 to drive a high-speed 8-bit DAC (TriQuint TQ6112) to generate complementary output signals which can then be low-pass filtered to give continuous output waveforms.

## Features

- ▼ 0-400 MHz output
- ▼ 1 GHz clock frequency guaranteed over commercial operating conditions
- ▼ 32-bit frequency resolution, 0.23 Hz @ 1 GHz clock
- ▼ 2-bit phase modulation (BPSK and QPSK)
- ▼ 8-bit parallel sine or cosine – 2 units can be used to generate quadrature output signals
- ▼ Phase coherent instantaneous frequency switching
- ▼ Up to 62.5 MHz rate for phase or frequency hopping
- ▼ ECL inputs for convenient interfacing
- ▼ 50  $\Omega$  inputs and outputs
- ▼ High-speed, low glitch GaAs DAC
- ▼ -40 dBc spurious typical
- ▼ 3.5" by 6"

STEL-2273 Block Diagram



# STEL-1023 C/A Coder

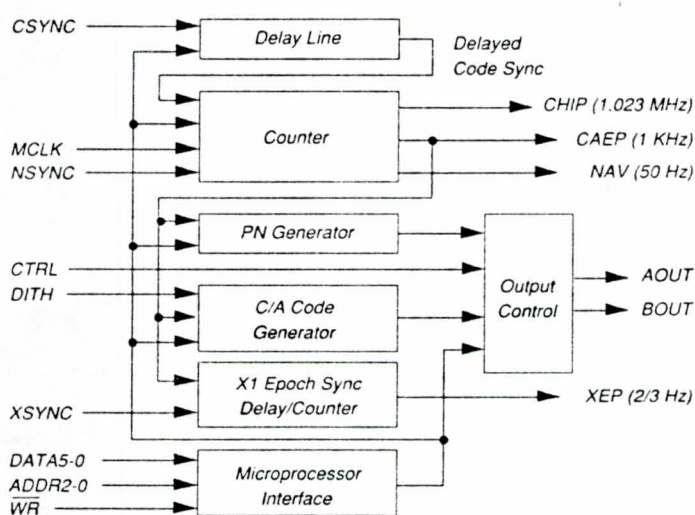
The STEL-1023 is designed to be used in GPS (Global Positioning Satellite) receivers where it generates the C/A (Clear / Acquisition) code as well as the timing for the X1 and C/A epochs, the 50 bps nav data, and other functions. The C/A code is one of the two codes used for the synchronization of the GPS receiver to the signal received from the satellites.

The codes are different for each of the satellites in the GPS constellation (for identification purposes), and the different C/A codes can be selected from the microprocessor interface.

## Features

- ▼ Generates C/A and PRN codes
- ▼ Generates all timing for GPS
- ▼ Low power CMOS – 10 mW
- ▼ Package: 28-pin DIP
- ▼ Military and commercial temperature ranges available

STEL-1023 Block Diagram



# STEL-1032 PRN Coder

The STEL-1032 Pseudo-Random Noise (PRN) Code Generator provides the communications industry with a cost effective and compact solution to code generation. The device's unique architectural design provides a power-efficient, high-speed code generator able to produce any 3 maximal or non-maximal length codes with up to 32 feedback taps per generator. The feedback taps selected are stored in the Mask Registers, and any number of taps may be selected.

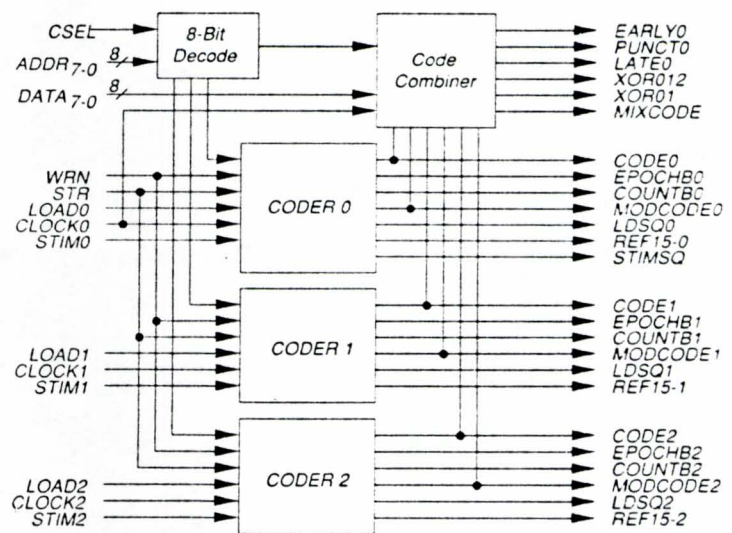
In this way all possible codes with lengths up to  $2^{32}-1$  (4,294,967,295) can be generated. The codes can be started at any selected point. Capabilities for modulo-2 addition (EXOR), code modulation, and non-linear composite code generation are also provided in the device. The output of code generator 0 is also available both late and early by one half of a clock cycle relative to the punctual code. Non-linear codes can be generated by combining 2 or 3 codes using an internal programmable lookup

table. The device can be programmed very easily via the microprocessor interface.

## Features

- ▼ 3 PRN code generators
- ▼ Independent clocks, controls, and outputs
- ▼ Microprocessor control interface
- ▼ Composite code generation capabilities
- ▼ Chip counter, initialization preset, and epoch truncation capabilities
- ▼ Punctual, late, and early outputs for code tracking
- ▼ Up to 30 MHz operation
- ▼ Military and commercial temperature ranges available
- ▼ Package: 68-pin PLCC

STEL-1032 Block Diagram



# STEL-2410 Correlator Accumulator

The STEL-2410 is a dual high-speed correlator / accumulator circuit which can be used in many data communications applications. The dual circuits, which are completely independent, can be used to correlate dual data streams such as QPSK demodulated data. The 8-bit inputs can be in either regular 2's complement code ( $00_H = \text{zero}$ ) or offset 2's complement code ( $FF_H = \text{minimum negative value}$ ,  $00_H = \text{minimum positive value}$ , no code corresponding to true zero).

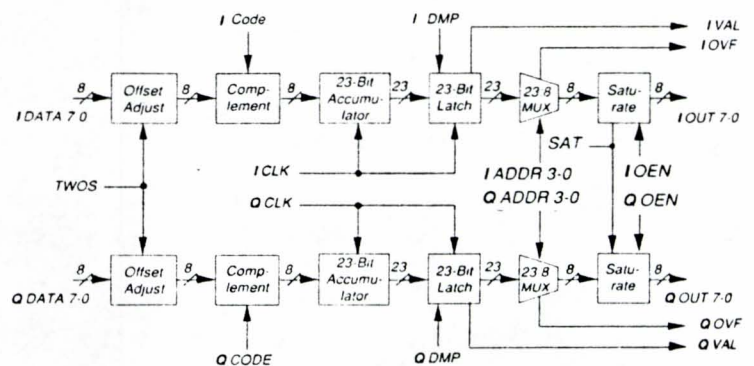
The inputs are multiplied by the reference codes and accumulated in 23-bit accumulators, thereby ensuring at least  $2^{15}$  cycles of accumulation without overflow. The outputs of the accumulators are viewed through 8-bit windows for easy microprocessor interfacing, and the significance of each window is controlled by independent multiplexers. The data dumped into each viewport can be set to saturate on overflow, thereby eliminating the

ambiguity caused when the accumulator value exceeds the range seen through the 8-bit viewport. The device may be used to digitally despread direct sequence spread spectrum signals or may be used as a digital integrate and dump filter.

## Features

- ▼ Up to 70 MHz accumulation rate
- ▼ Dual accumulators for quadrature data applications
- ▼ 32,768 cycles without overflow between dumps
- ▼ Accumulator latch and hold registers
- ▼ Saturate on overflow capability
- ▼ Two's complement or offset two's complement inputs
- ▼ Selectable 8-bit output fields
- ▼ Package: 68-pin PGA

STEL-2410 Block Diagram



# STEL-3310

## Matched Filter

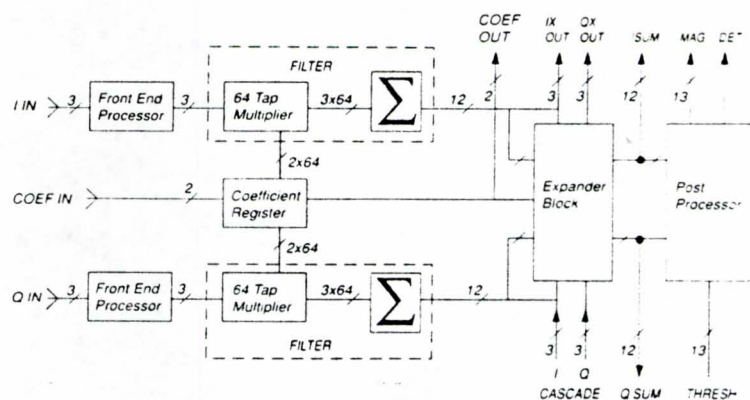
### 64-Tap, 11 Mcps

The STEL-3310 is a dual high-speed digital matched filter / correlator circuit which can be used in many spread spectrum data communications applications operating at up to 11 Mcps per second. The device is designed to be expandable up to 256 taps. The dual channels allow the device to be used directly after the baseband down-converter, the magnitude of the complex signal being computed internally with an approximation algorithm. The built-in threshold comparator allows the user to select the level at which the match is detected, permitting optimum operation over a wide range of signal conditions. The optional front-end processor function is a sliding window filter, which adds the previous data sample to each incoming one. This allows the use of non-coherent sampling at two samples per chip.

#### Features

- ▼ Up to 22 MHz sample rate
- ▼ Dual filters for quadrature channels
- ▼ Operates with BPSK and QPSK modulation
- ▼ 64 taps per device
- ▼ Up to four devices can be cascaded without overflow
- ▼ Coefficient latch and hold registers
- ▼ Ternary coefficient values (0,  $\pm 1$ )
- ▼ 3-bit offset two's complement inputs
- ▼ 12 and 13-bit two's complement outputs
- ▼ Package: 181-pin PGA

STEL-3310 Block Diagram





# **IFF Tactical Electronic Simulation and Test System**

## **3. Communications Systems Modeling**

**Dr. M. Belkerdid**

### 3.1 Introduction

This report summarizes the efforts undertaken under the IFF Tactical Electronic Simulation and Test System (TESTS) research program during the Summer 1991 semester. The research dealt with the viability of the Signal Processing Worksystem by Comdisco. SPW/BOSS is a Block Oriented Software Simulator that is a useful non-real time simulation tool for Direct Sequence Spread Spectrum (DSSS) communication link.

Last spring's reports demonstrated how SPW/BOSS can be used to model communication systems that include encoders, decoders, Pseudo-Noise (PN) generators, modulators, demodulators, and Hilbert transformers in quadrature configurations. The reports also discussed the expansion of the SPW/BOSS library via custom designed modules. These custom modules are written in the C programming language.

This report emphasizes the operation of a DSSS in a Code Division Multiple Access (CDMA) environment. The CDMA environment model, simulated using SPW/BOSS, also allows for the modeling of multipath effects, channel capacity, and the near far problem. This report also presents a technique for the generation of efficient multiple Spread Spectrum waveforms.

A sliding correlator was set up for DSSS system parameter evaluation purposes. Such a correlator is used as a test bed for all DSSS simulation scenarios.

The sliding correlator is a feedback system whose central component is an integrator in the system's feedback path. The output of this integrator for the synchronized case is given by:

$$Y_{(synch)} = Ab_i(2p-1) + \sum_{l=0}^{2p-2} n(lt_s)a_l \quad (1)$$

The equation is similar to the one developed in [2]. For the non-synchronized case, the first term is altered:

$$Y_{(no-synch)} = Ab_i \sum_{l=0}^{2p-2} a_j a_{(j+l)} + \sum_{l=0}^{2p-2} n(lt_s)a_l \quad (2)$$

where A is the signal amplitude,  $b_i$  is the  $i^{\text{th}}$  data bit at the sampler (positive or negative),  $(2p-1)$  is the number of valid samples per interval,  $l$  is the phase lag of the cross-correlated codes,  $n(lt_s)$  is

the sampled noise, and  $a_i$  is the local PN code. To avoid false synchronization, equation 2 should be small compared to equation 1.

The mean time to acquire a signal is derived in [3] as:

$$\bar{T}_{acq} = \left[ M \left( \lambda + \frac{1}{2} \right) T_c + \frac{(\lambda T_c P_F)}{(1 - P_F)^2} \right] + \left( \frac{(1 - P_D)}{P_D} \right) \left[ 2M \left( \lambda + \frac{1}{2} \right) T_c + \frac{(\lambda T_c P_F)}{(1 - P_F)^2} \right] \quad (3)$$

where  $\lambda$  is the area of integration,  $T_c$  is the period of one chip,  $P_D$  is the probability of detection,  $P_F$  is the probability of false alarms, and  $M$  is the additional chips examined for an incorrect decision. Equations for  $P_F$  and  $P_D$  are found in [4].

### 3.2 CDMA Environment

Figure 3.1 contains an arrangement of multiple transmitters with data sources and spreading mechanisms comprised of individual, maximum length PN sequence generators of different code lengths. That is, no two transmitters are alike and the orders of the polynomials range from  $n=6$  to  $n=34$ , where  $N=2^n-1$  is the length of each sequence. Table 3.1 lists specifications of the transmitters used throughout this paper. In all upcoming examples, user #1 is assumed to possess the desired message. Therefore, the local code is designed to match the spreading code of transmitter #1, except for a possible phase shift. To account for near-far conditions, on-line multipliers are mounted at each transmitting branch. The new equations describing the output of the integrator are similar to those given in [2] and are shown below:

$$Y_{(synch)}^k = A^k b_i^k (p-1) + \sum_{l=0}^{p-2} n(lt_s) a_l^k + \sum_{r=1; r \neq k}^M A^r b_{(i-1)}^r \sum_{l=0}^{p-c-1} a_l^k a_{(l+c)}^r + \sum_{r=1; r \neq k}^M A^r b_i^r \sum_{l=p-c}^{p-2} a_l^k a_{(l+c)}^r \quad (4)$$

$$Y_{(no-synch)}^k = \sum_{l=0}^{p-1} n(lt_s) a_l^k + \sum_{r=1}^M A^r b_{(i-1)}^r \sum_{l=0}^{p-c-1} a_l^k a_{(l+c)}^r + \sum_{r=1}^M A^r b_i^r \sum_{l=p-c}^{p-2} a_l^k a_{(l+c)}^r \quad (5)$$

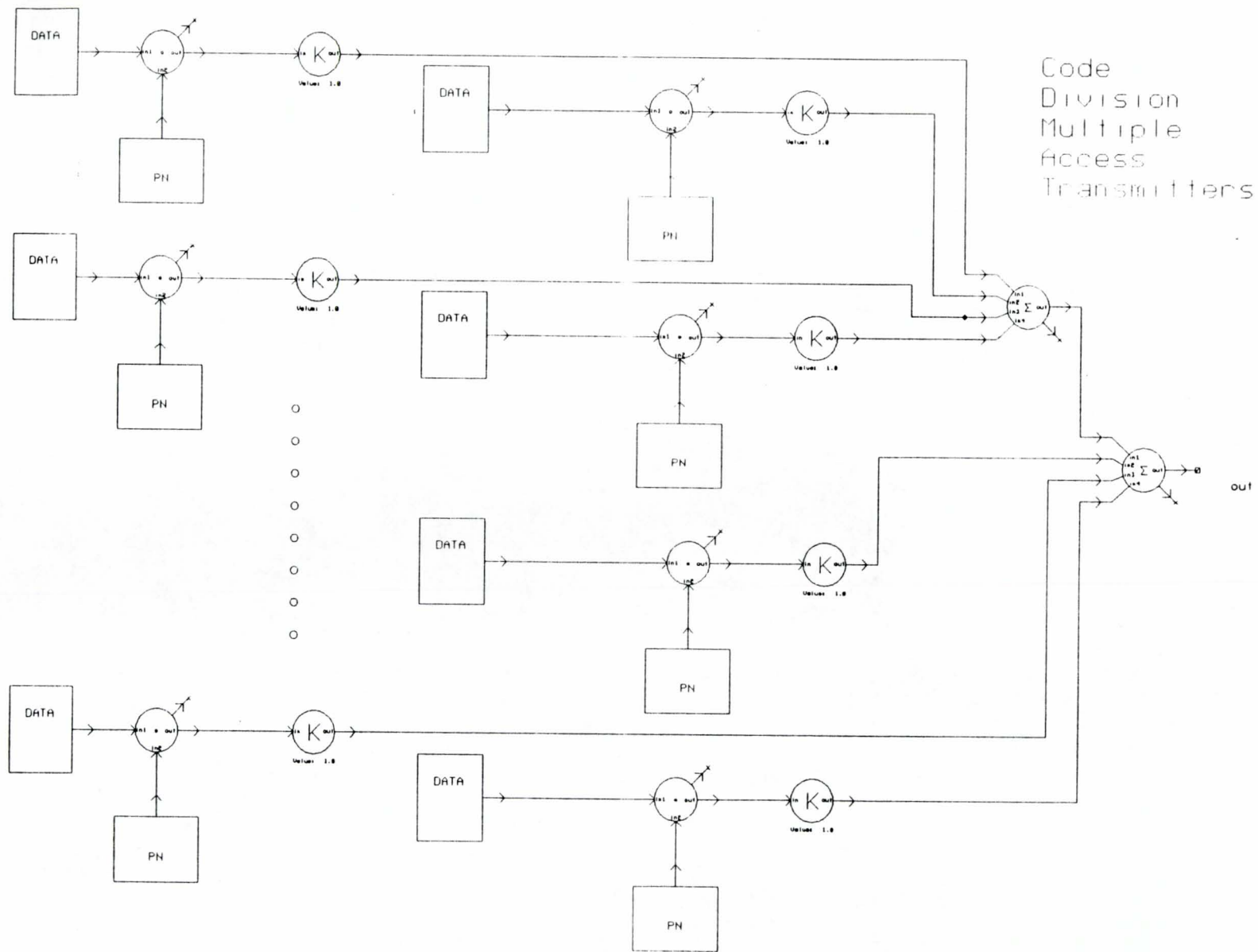


Figure 3.1 CDMA Transmitter Configuration

Table 3.1: CSC in CDMA (transmitters)

Transmitters	Data PN Order	Data Sampling Frequency	Spreader PN Order	Spreader Sampling Frequency	Processing Gain
1	21	1023	10	1	1023
2	22	1023	9	1	1023
3	23	1023	11	1	1023
4	6	1023	12	1	1023
5	8	1023	27	1	1023
6	15	1023	15	1	1023
7	19	1023	13	2	511.5
8	12	1023	34	16	63.94
9	11	512	20	1	512
10	7	1023	26	4	255.8
11	16	1023	18	1	1023
12	31	2047	8	1	2047
13	33	1023	16	1	1023
14	14	255	23	2	127.5
15	20	1023	29	1	1023
16	25	1023	31	1	1023
17	18	511	25	1	511
18	17	1023	6	1	1023
19	24	1023	30	1	1023
20	30	511	14	2	255.5
21	13	1023	19	2	511.5
22	32	2047	21	1	2047
23	27	1023	7	1	1023
24	34	1023	22	1	1023
25	28	1023	17	2	511.5
26	9	511	33	1	511
27	29	1023	24	1	1023
28	10	511	32	2	255.5

The equations reflect whole chip slippage at the receiver and one lost chip due to integrator reset. The superscript  $k$  represents the "desired" user while  $r$  depicts the  $r^{\text{th}}$  interfering transmitter. The variable  $c$  is the location of adjacent bits.

As an example, a multiple access system using the first four transmitters of Table 3.1 is modeled. System settings include: no channel noise; an integration period of 1023 chips; whole chip slippage; chip/bit/integrator alignment (with transmitter #1); and a threshold value of 675. Figure 3.2b is the despreader output for the case where the transmissions are at equal power levels. For this condition, the receiver accurately obtains synchronization and maintains it. Transmitter #3 is then boosted (via the on-line multiplier) to simulate a "near" transmitter, while the other three remain at unity as the "far" transmitters. Amplification of #3 is increased by increments until the system breaks down. Signals 3.2d and 3.2e show that with a power factor of six, the system obtains synch but eventually loses it when the integrator output drops to 670 (the threshold was set to 675). Viewing transmitter #3 as six identical users with unity power, system capacity is roughly nine users.

The nonlinear characteristic of the near-far problem is best explained mathematically. Close inspection of the last two terms of equations (4) and (5) indicate a partial cancelling in the correlation process the code sequences are dissimilar. This cancelling reduces the destructive tendencies of the interfering users. If the codes are identical, however, no cancelling occurs and the negative impact is maximized. The next section determines the number of users allowed onto the system for the ideal case of equal power. In doing so, it demonstrates (by elimination) the damaging effects of the near-far problem.

### 3.3 CDMA Equal Power Levels

Using the assumptions of the previous example (except here all transmitters have equal power), several simulations are performed. The first model has only two transmitters but an additional one is added for each subsequent simulation. As more transmitters are added, the system

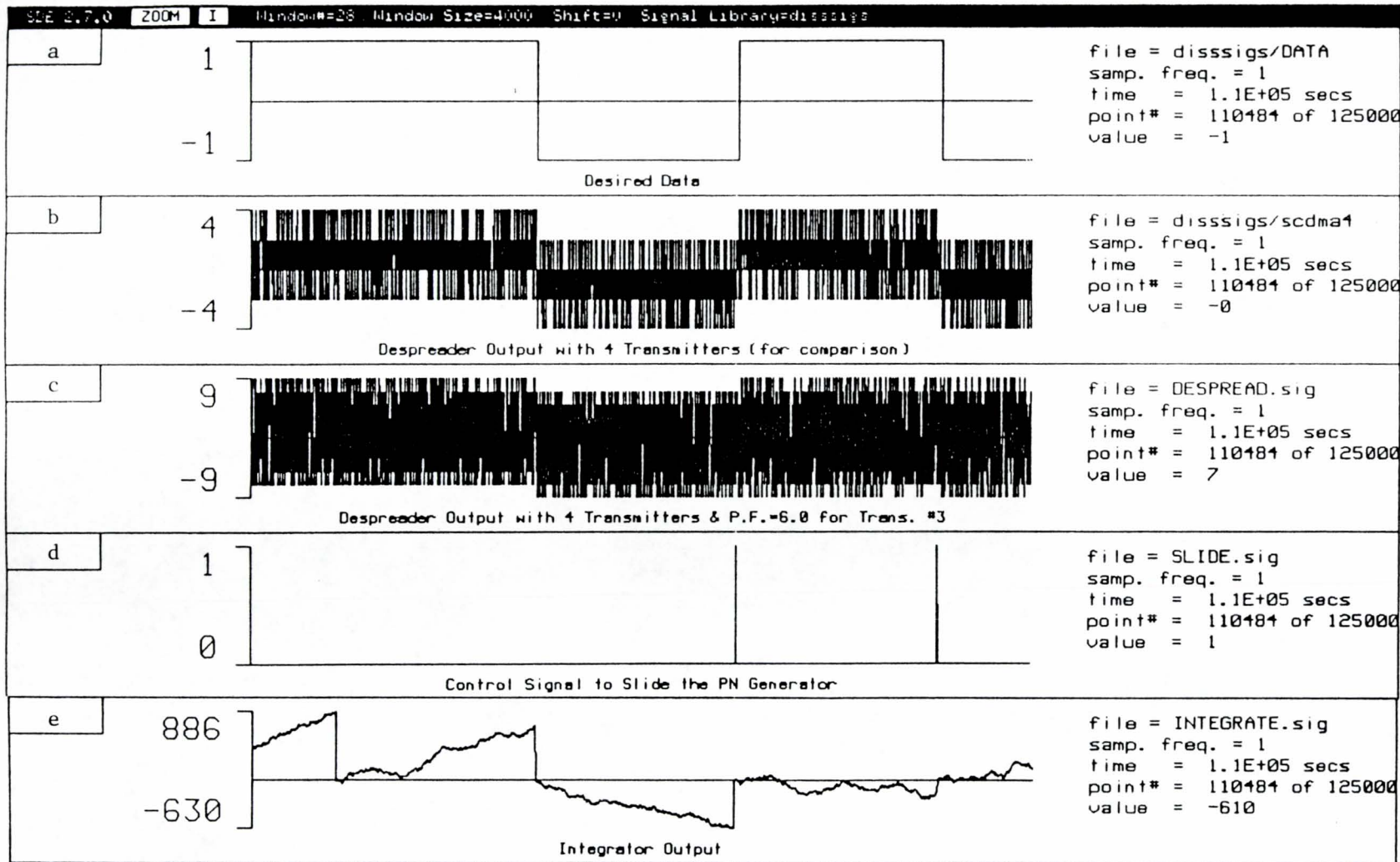


Figure 3.2 Near-Far Waveforms.

weakens until it can no longer operate effectively. The integrator output drops below threshold when the twenty-eighth transmitter is added, (see Figure 3.3). System capacity is now approximately three times larger than it was in the previous example. Nineteen more users are permitted if the near-far problem is removed. Unfortunately, this ideal case is not very realistic. Despreader outputs for various equal powered transmitter combinations are given in Figure 3.4. As predicted, the waveforms resemble noise filled sequences that worsen as the number of transmitters are increased. Zooming in on signal 3.4b, we find an M-ary type format with values  $\pm 4$ ,  $\pm 2$ , and 0, (see Figure 3.5). This is the result of summing four PN sequences. As the number of transmitters increase, so do the number of M-ary values.

### **3.4 Multiple Spread Spectrum Synthesis**

Multiple spread spectrum waveforms can be generated by specifying their unique spreading codes. These codes can be delayed versions of a single PN code generator. Phase shifted replicas are designed using a delay synthesis technique. There are many methods for creating delayed versions of a PN sequence. One method uses a parallel bank of PN generators with different initial values. Another uses strings of delay elements that are attached to the generator. An even better method (less hardware) uses polynomial theory and modulo two arithmetic to multiply the PN polynomial by the prescribed shift, and then factors it into a polynomial of degree  $n$  or less.[5] This is done for each phase shift.

An example will help to clarify the latter approach. Suppose that an eight phase PMG is desired from the following tenth order polynomial:

$$g(x) = 1 + X^2 + X^3 + X^6 + X^8 + X^9$$

The distance between neighboring sequences is calculated as  $(N+1)/L = 1024/8 = 128$ . However, one of the codes has a spacing of 127 in order to keep  $N=1023$ . Polynomials for phase shifted replicas are determined by individually multiplying  $g(x)$  by  $X^{128}$ ,  $X^{256}$ ,  $X^{384}$ ,  $X^{512}$ ,  $X^{640}$ ,  $X^{768}$ , and  $X^{896}$  and factoring until the orders of the replicated polynomials are less than or equal to 10:



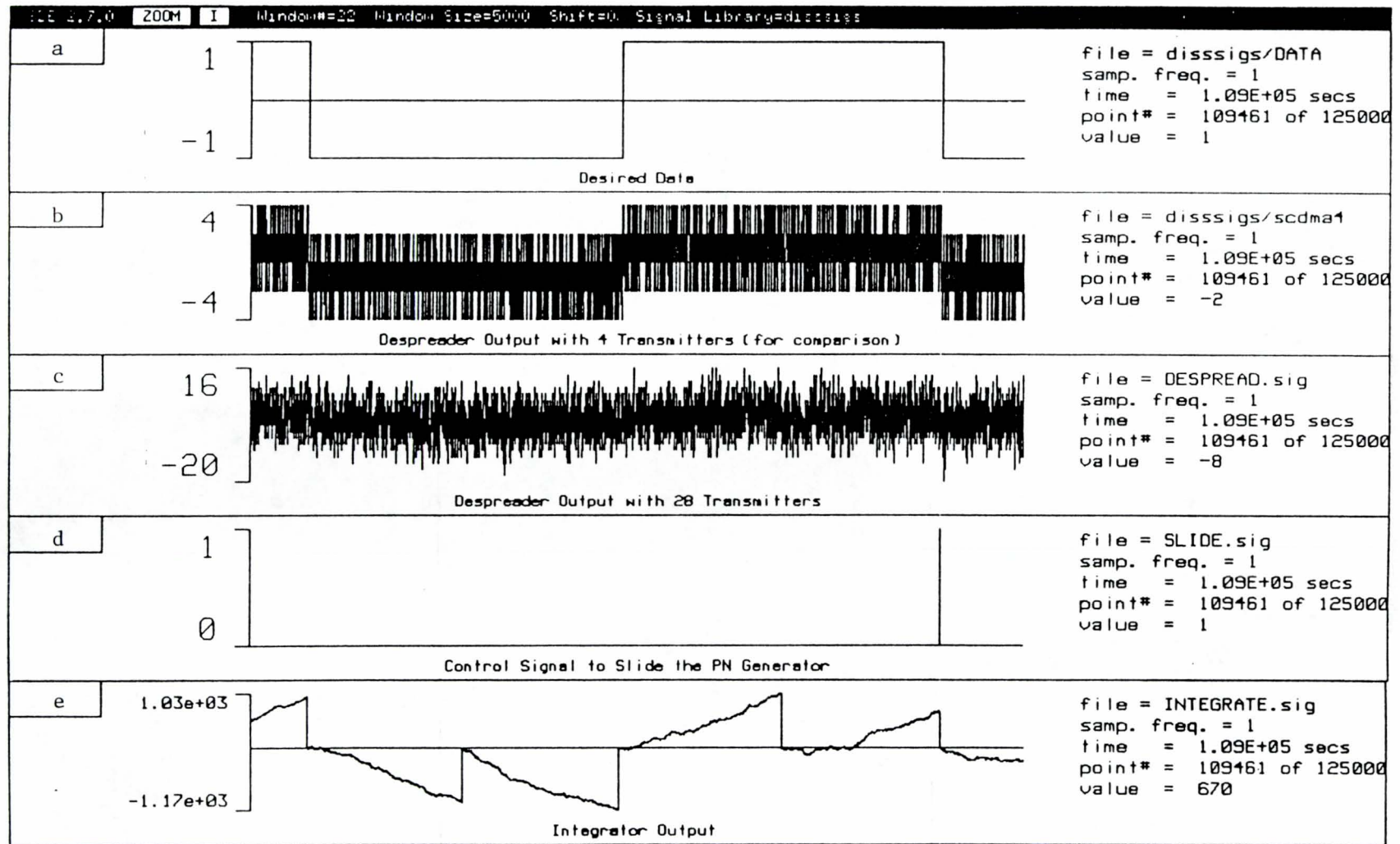


Figure 3.3 CDMA Waveforms With 28 Transmitters.

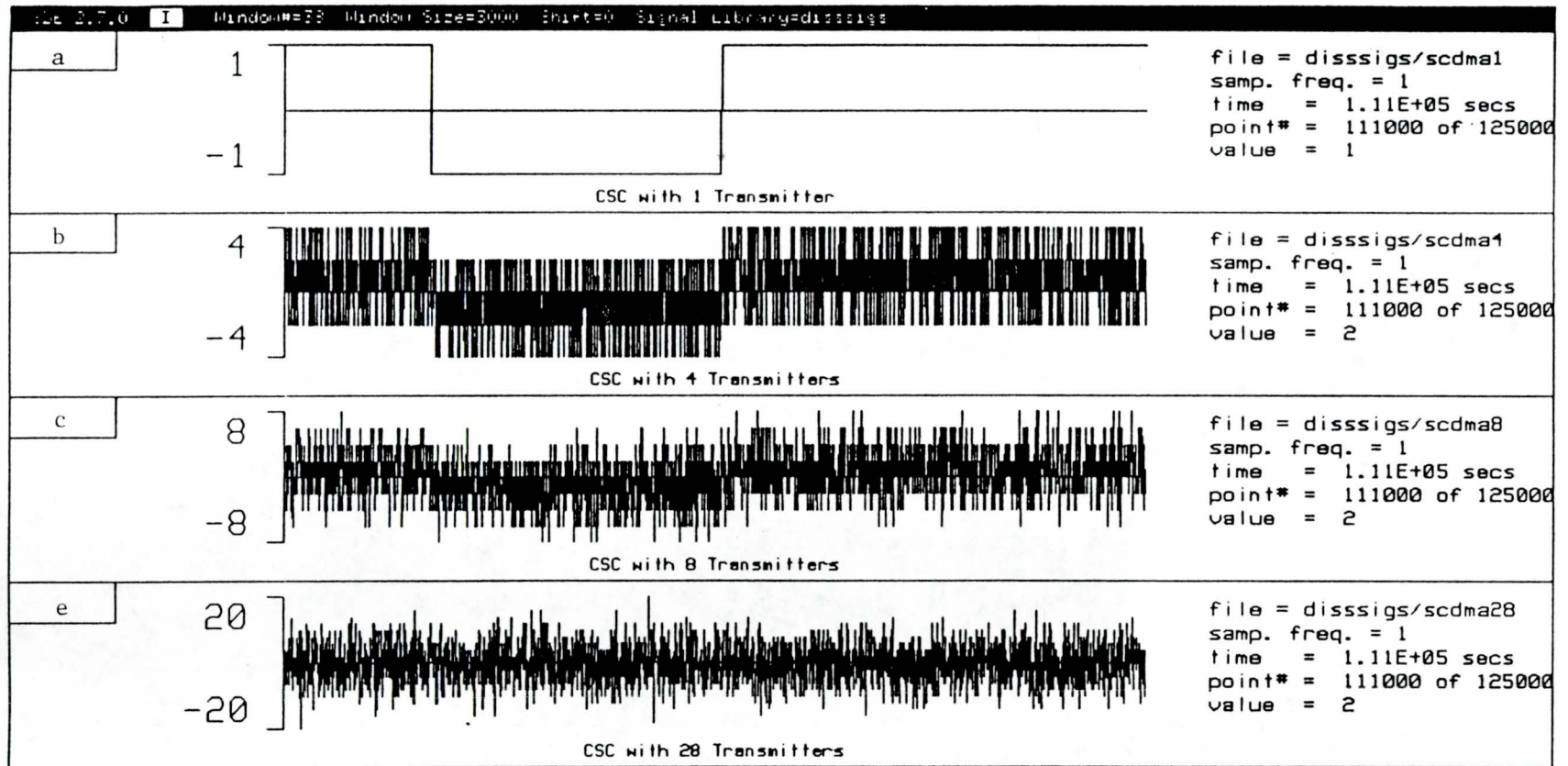


Figure 3.4 CDMA Waveforms With Multiple Transmitters

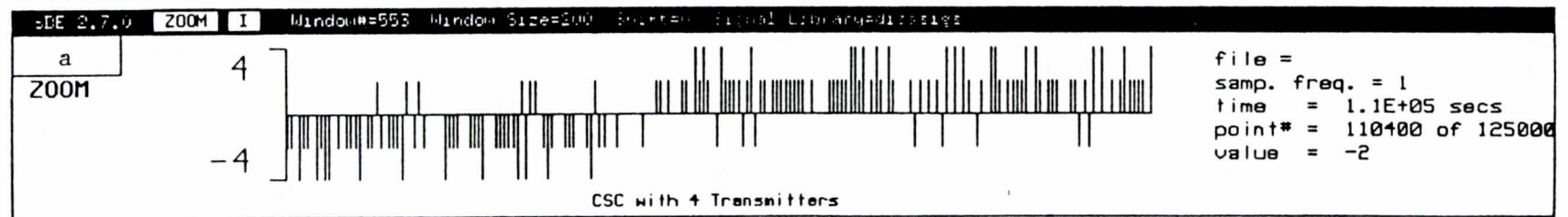


Figure 3.5 CDMA Waveform With 4 Transmitters (ZOOM)

$$g_1(x) = g(x) = 1 + X^2 + X^3 + X^6 + X^8 + X^9$$

$$g_2(x) = g(x) X^{128} = X^2 + X^4 + X^9$$

$$g_3(x) = g(x) X^{256} = X^7 + X^8$$

$$g_4(x) = g(x) X^{384} = X^2 + X^3 + X^5 + X^{10}$$

$$g_5(x) = g(x) X^{512} = X^4 + X^6$$

$$g_6(x) = g(x) X^{640} = X^3 + X^5 + X^9$$

$$g_7(x) = g(x) X^{768} = X^1 + X^2 + X^3 + X^4$$

$$g_8(x) = g(x) X^{896} = X^1 + X^7 + X^8 + X^9 + X^{10}$$

These polynomials are realized in Figure 3.6. To verify that the sequences are indeed shifted by the prescribed amounts, the cross-correlation of signal  $g(x)$  with the output of the phase multiplexed generator is shown in Figure 3.7. Note that the correlation peaks occur for lags of 0, 128, 256, 384, 512, 640, 768, and 896, as expected.

### 3.5 Conclusion

The following features were not modeled: individual carrier frequencies for all users; random alignments between chips, bits, and the integration process; and differing chip sizes among the spreaders. Inclusion of these items would make the results more realistic, but, would not change performance trends. For simplicity, they were omitted. To graphically illustrate system tendencies for various scenarios, many examples were given. Near-far considerations drop the efficiency even further, as shown in Figure 3.2.

As a final comment, this paper confirms that SPW/BOSS is well suited for spread spectrum simulation. It is now ready to be used as a DSSS simulation test bed for parameter sensitivity analysis. Appendix 3.A contains a paper that is similar to the one published and presented at the 1991 RF Expo (East).

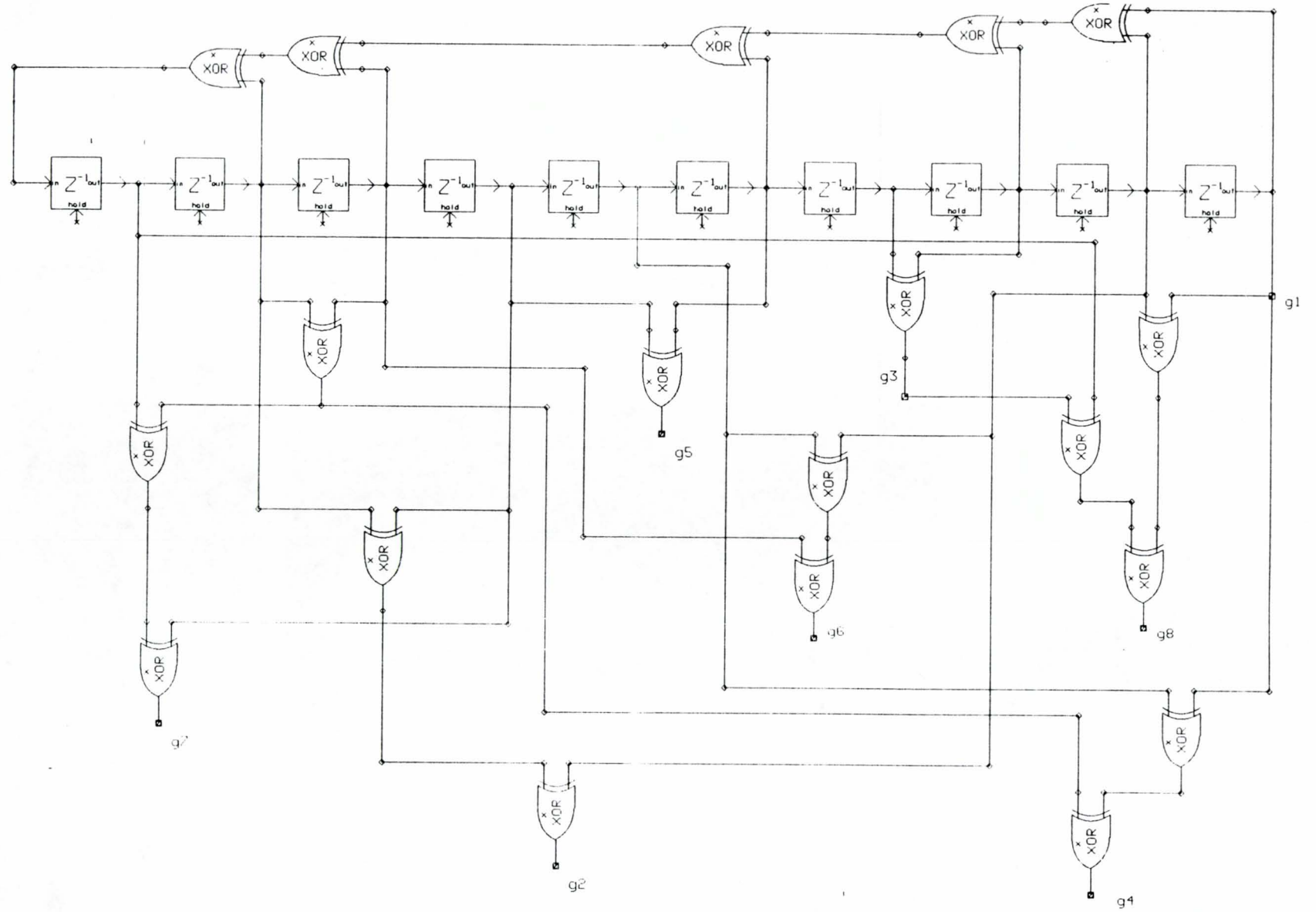


Figure 3.6 Multiple PN Sequence Generator.

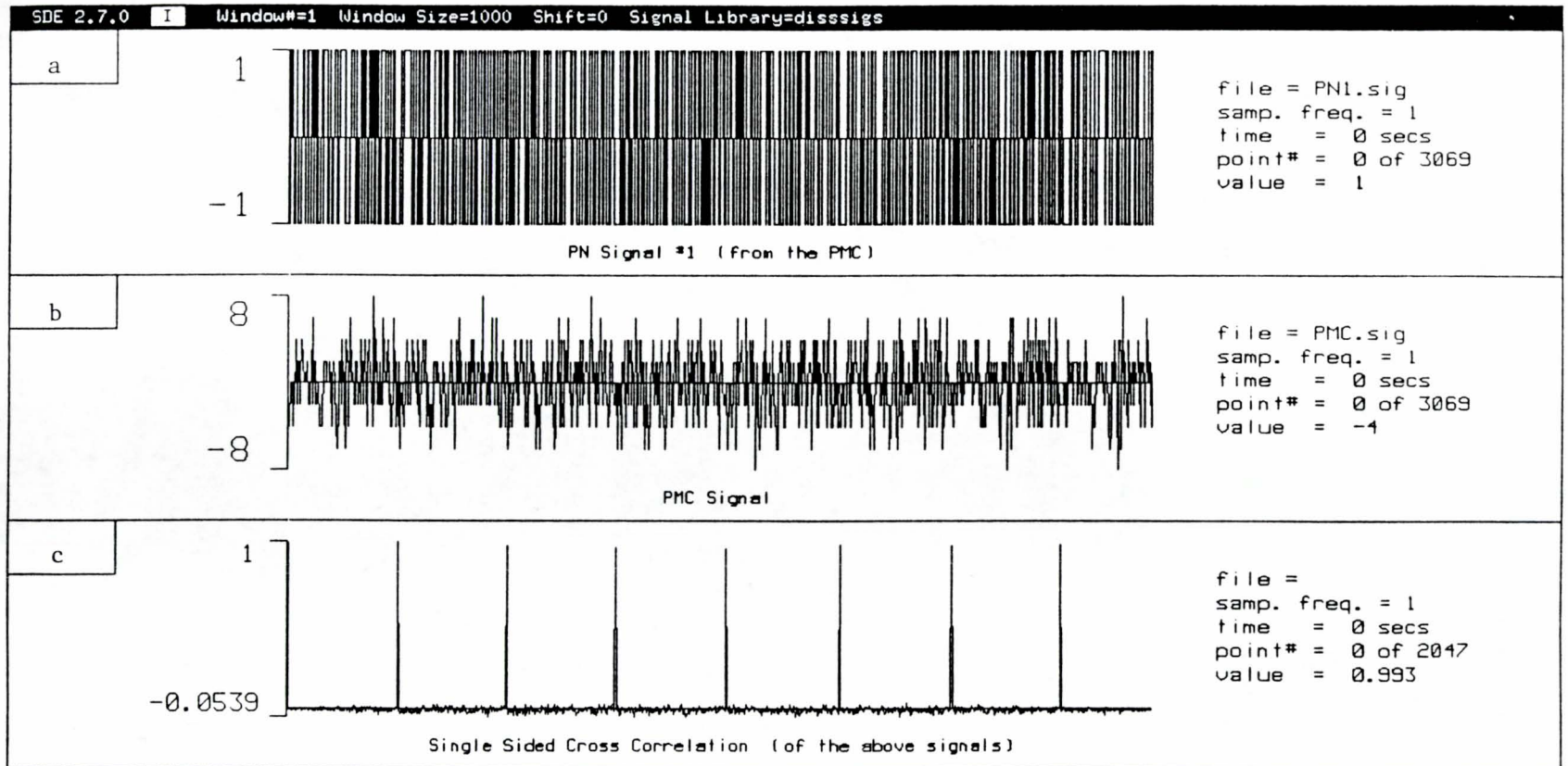


Figure 3.7 Sum of Multiple PN Sequences and their Crosscorrelation.

### 3.6 References

- [1] Comdisco Systems, Inc., Signal Processing Worksystem, Software Documentation, Product Number SPW1080, Version 2.7, August 1990.
  
- [2] R. Skaug and J. F. Hjelmsstad, SPREAD SPECTRUM IN COMMUNICATION. London, UK: Peter Peregrinus Ltd., 1985.
  
- [3] R. L. Pickholtz, D. L. Schilling, and L. B. Milstein, "Theory of Spread-Spectrum Communications - A Tutorial", IEEE Trans. Comm., vol COM-30, May 1982.
  
- [4] R. C. Dixon, SPREAD SPECTRUM SYSTEMS. New York: Wiley-Interscience, 1984.
  
- [5] G. S. Rawlins, "A RAPID ACQUISITION TECHNIQUE FOR DIRECT SEQUENCE SPREAD SPECTRUM SYSTEMS BY A PN PHASE MULTIPLEXED CORRELATOR." Master's Thesis, University of Central Florida, Orlando, Florida, 1987.

## **3.A Appendix**

### **Phase Multiplexed Correlation In Multiple Access Spread Spectrum Systems**

**Glen G. Koller & Madjid A. Belkerdid**

# PHASE MULTIPLEXED CORRELATION IN MULTIPLE ACCESS SPREAD SPECTRUM SYSTEMS

By

Glen G. Koller & Madjid A. Belkerdid

University Of Central Florida  
Electrical Engineering Department  
Orlando, Florida 32816

## Abstract

The relatively new concept of Phase Multiplexed Correlation (PMC) is applied to the Code Division Multiple Access (CDMA) Direct Sequence Spread Spectrum (DSSS) environment to determine coarse acquisition advantages. Prior to the discussion of the PMC, the Conventional Sliding Correlator (CSC) design is reviewed to establish performance guidelines. Both systems are modeled in software where simulated results are compared to predicted calculations.

## Introduction

The CSC is a coarse acquisition technique commonly used in DSSS systems. Its concept is based on an integration process that is used to exploit properties of pseudo-noise (PN) sequences. The CSC's simple design leads to an easy implementation but is rather inefficient in that it performs a serial search of the uncertainty region which usually requires a considerable amount of time. Its ability to lock onto a signal gradually deteriorates as transmitters (users) of equal power (as seen by the transmitter) are added and dramatically degrades when high powered interfering transmitters appear. Recall that the "near-far" problem is the situation where multiple transmitters are geographically located at different distances from the receiver. Even when each is transmitting at the same level (equal power), the one closest to the receiver is dominant. Attempts that are made to despread the signal of the furthest transmitter results in an overwhelming power disturbance from the closest transmitter. The disturbance appears as a high cross-correlation of the undesired codes



to the local PN sequence.

It is shown, in an upcoming section, that the CSC can be modified to form the PMC. This new design proves to be advantageous in that the number of cells to be searched to acquire synchronization is reduced to only a fraction of what is required by the CSC. However, the price paid for the improvement is an increase in both channel noise and co-user interference. Fortunately, through flexibility of design, a compromise is possible that allows for some acceleration in acquisition in exchange for moderate performance concessions. Of course, application dictates the optimal mix. As in the case of the CSC, the PMC is tested in the CDMA arena using the Signal Processing Worksystem (SPW) by Comdisco. [1]

### Conventional Sliding Correlator

Figure 3A.1 contains a model of the CSC. A DSSS transmitter and an Additive White Gaussian Noise (AWGN) channel are included to generate realistic input signals to the correlator. For simplicity, the model is baseband which eliminates the need for a carrier. The transmitter consists of a binary random number generator to create the message signal and a PN sequence generator which is used as the spreader. The AWGN channel has controllable mean and variance. At the receiver, the signal is despread by a PN generator that is identical to the transmitting generator except for a possible phase shift, which can be as small as a fraction of a chip. An integration operation is performed on the signal over the interval  $[0, T_d]$  to determine the level of correlation. The magnitude at the end of each interval is computed and sent to the comparator for threshold evaluation. A small value at the input of the comparator triggers a pulse from the pulse train which slides the local PN generator. A large value indicates a synchronized condition so no sliding occurs.

As an example, the waveforms of Figure 3A.2 are generated with the following assumptions: the order of the PN generators is  $n=6$ ; the chip rate is 63 times faster than the data rate (processing gain = 63); each chip contains two samples; the noise in the channel has zero mean and a variance of 0.5; the local generator slips by one-half chip increments; integration is performed per bit with

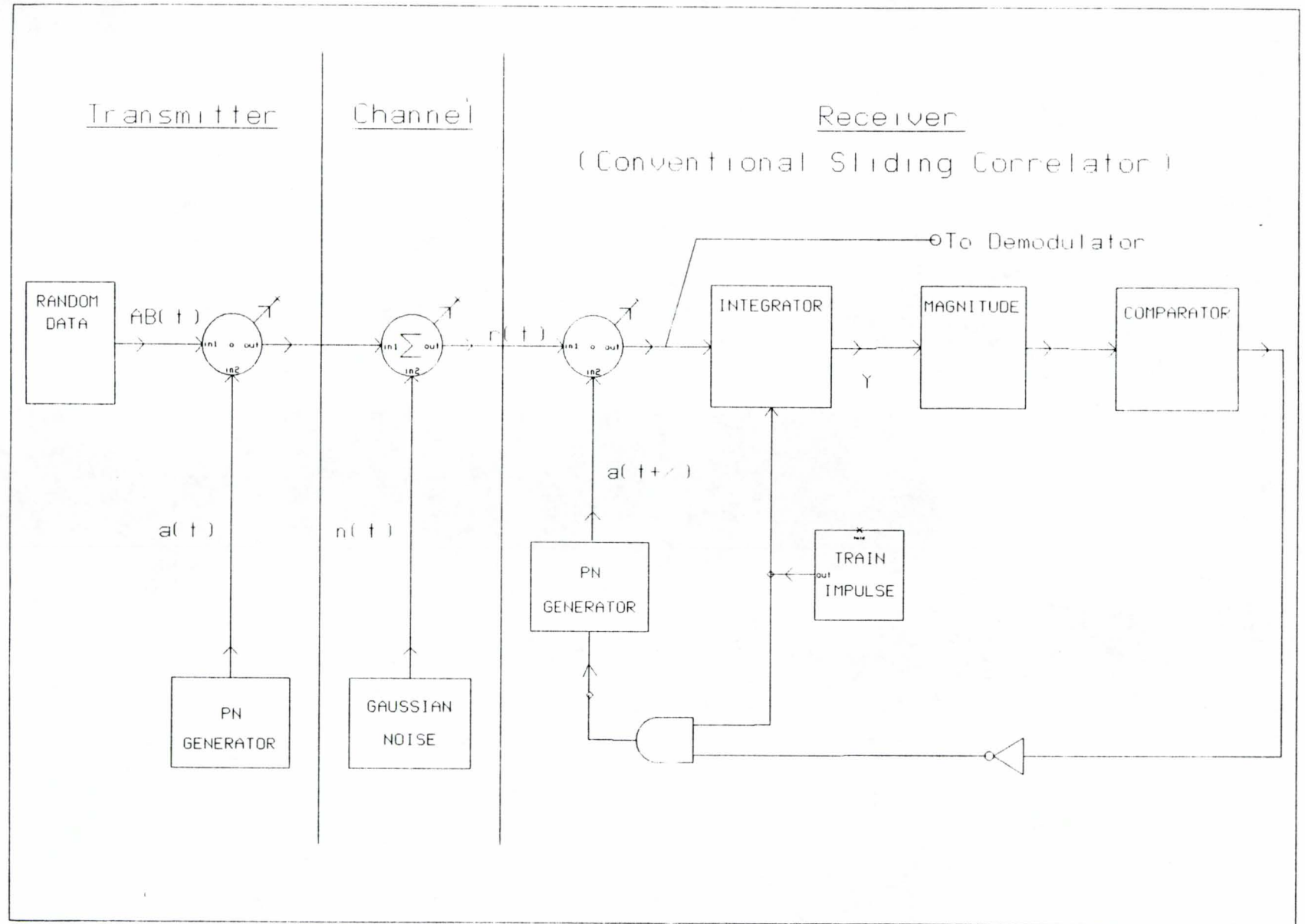


Figure 3A.1 CSC in a DSSS Setting.

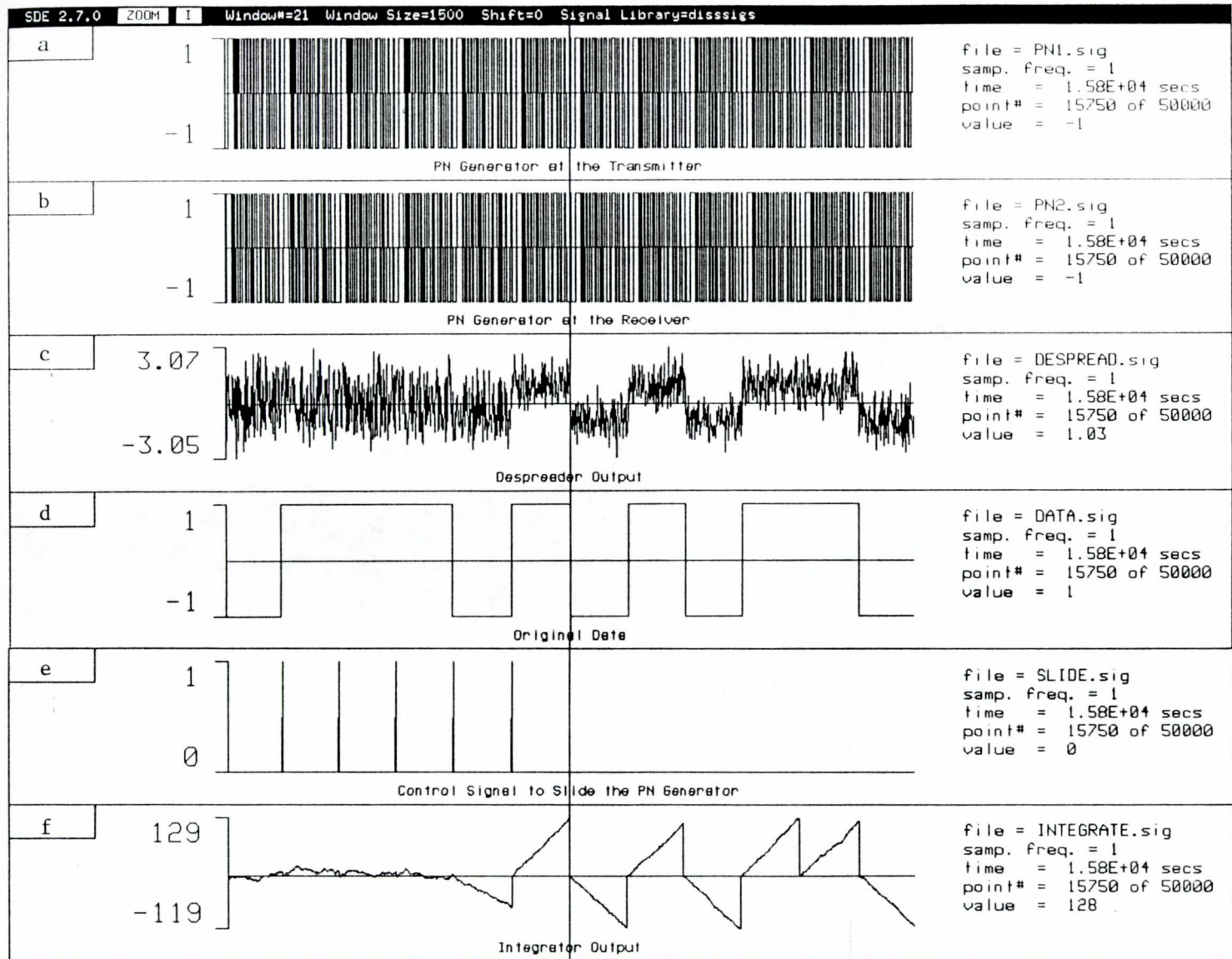


Figure 3A.2 CSC Waveforms

assumed bit and chip alignments; one chip is lost in each interval due to reset; the threshold of the comparator is set at 95. Signal 3A.2a is the sequence generated by the transmitting PN generator and 3A.2b is the output of the local generator. The receiver code is intentional delayed (misaligned) by one sample (one-half chip) to force the local code generator to slide the entire length of the uncertainty region. Note that the system is incapable of backward motion. Signal 3A.2c is the desreader output. It is a combination of pseudo random waveforms until synchronization occurs, in which it then turns into a sequence that resembles the original data stream. Signal 3A.2d is the original message and can be used to validate 3A.2c. Signal 3A.2e is the control logic that sends the command to the PN generator causing it to slide. Missing teeth in this comb-like signal indicate that either the system is in synch or false alarms have occurred. The area between adjacent peaks corresponds to an interval of integration. Signal 3A.2f is the output of the integrator. Its values are relatively small until the system reaches synchronization. The output of the integrator for the synchronized case is:

$$Y_{(synch)} = Ab_i(2p-1) + \sum_{j=0}^{2p-2} n(jt_s)a_j \quad (1)$$

The equation is similar to the one developed in [2]. For the non-synchronized case, the first term is altered:

$$Y_{(no-synch)} = Ab_i \sum_{j=0}^{2p-2} a_j a_{(j+l)} + \sum_{j=0}^{2p-2} n(jt_s)a_{(j+l)} \quad (2)$$

where A is the signal amplitude,  $b_i$  is the  $i^{\text{th}}$  data bit at the sampler (positive or negative),  $(2p-1)$  is the number of valid samples per interval,  $l$  is the phase lag of the cross-correlated codes,  $n(jt_s)$  is the sampled noise, and  $a_j$  is the local PN code. To avoid false synchronization, equation 2 should be small compared to equation 1.

The mean time to acquire a signal is derived in [3] as:

$$\bar{T}_{acq} = \left[ M \left( \lambda + \frac{1}{2} \right) T_c + \frac{(\lambda T_c P_F)}{(1 - P_F)^2} \right] + \left( \frac{(1 - P_D)}{P_D} \right) \left[ 2M \left( \lambda + \frac{1}{2} \right) T_c + \frac{(\lambda T_c P_F)}{(1 - P_F)^2} \right] \quad (3)$$

where  $\lambda$  is the area of integration,  $T_c$  is the period of one chip,  $P_D$  is the probability of detection,  $P_F$  is the probability of false alarms, and  $M$  is the additional chips examined for an incorrect decision. Equations for  $P_F$  and  $P_D$  are found in [4].

### CSC in CDMA

Figure 3A.3 contains an arrangement of multiple transmitters with data sources and spreading mechanisms comprised of individual, maximum length PN sequence generators of different code lengths. That is, no two transmitters are alike and the orders of the polynomials range from  $n=6$  to  $n=34$ , where  $N=2^n-1$  is the length of each sequence. Table 3A.1 lists specifications of the transmitters used throughout this paper. In all upcoming examples, user #1 is assumed to possess the desired message. Therefore, the local code is designed to match the spreading code of transmitter #1, except for a possible phase shift. To account for near-far conditions, on-line multipliers are mounted at each transmitting branch. The new equations describing the output of the integrator are similar to those given in [2] and are shown below:

$$Y_{(synch)}^k = A^k b_i^k (p-1) + \sum_{j=0}^{p-2} n(jt_s) a_j^k + \sum_{r=1; r \neq k}^M A^r b_{(i-1)}^r \sum_{j=0}^{p-c-1} a_j^k a_j^r + \sum_{r=1; r \neq k}^M A^r b_i^r \sum_{j=p-c}^{p-2} a_j^k a_j^r \quad (4)$$

$$Y_{(no-synch)}^k = \sum_{j=0}^{p-2} n(jt_s) a_{(j+l)}^k + \sum_{r=1}^M A^r b_{(i-1)}^r \sum_{j=0}^{p-c-1} a_{(j+l)}^k a_j^r + \sum_{r=1}^M A^r b_i^r \sum_{j=p-c}^{p-2} a_{(j+l)}^k a_j^r \quad (5)$$

The equations reflect whole chip slippage at the receiver and one lost chip due to integrator reset. The superscript  $k$  represents the "desired" user while  $r$  depicts the  $r^{\text{th}}$  interfering transmitter. The variable  $c$  is the point where neighboring bits meet.

As an example, a multiple access system using the first four transmitters of Table 3A.1 is modeled. System settings include: no channel noise; an integration period of 1023 chips; whole chip slippage; chip/bit/integrator alignment (with transmitter #1); and a threshold value of 675. Figure 3A.4b is the despreader output for the case where the transmissions are at equal power levels. For this condition, the receiver accurately obtains synchronization and maintains it. Transmitter

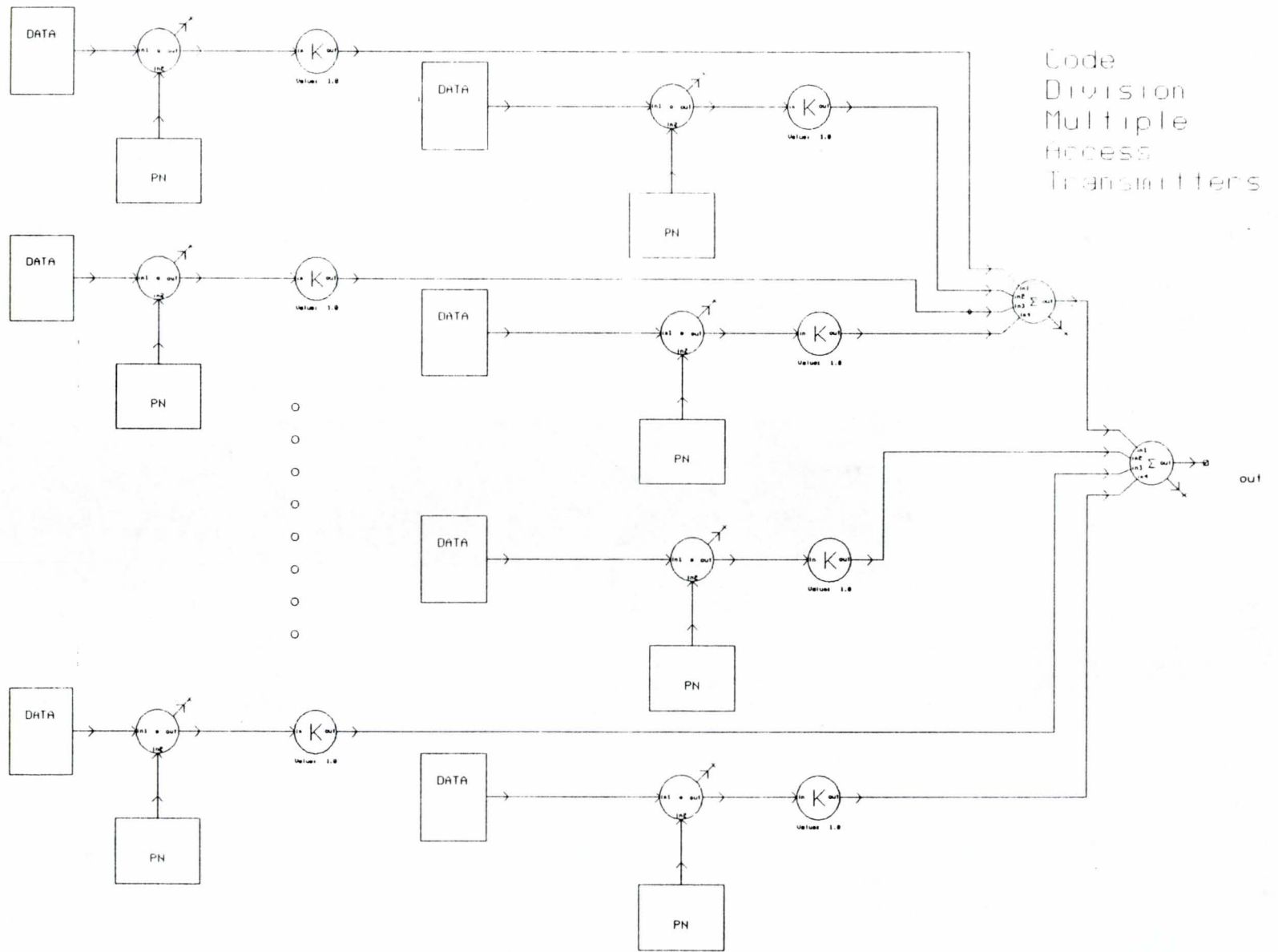


Figure 3A.3 CDMA Transmitter Configuration

Table 3A.1: CSC in CDMA (transmitters)

Transmitters	Data PN Order	Data Sampling Frequency	Spreader PN Order	Spreader Sampling Frequency	Processing Gain
1	21	1023	10	1	1023
2	22	1023	9	1	1023
3	23	1023	11	1	1023
4	6	1023	12	1	1023
5	8	1023	27	1	1023
6	15	1023	15	1	1023
7	19	1023	13	2	511.5
8	12	1023	34	16	63.94
9	11	512	20	1	512
10	7	1023	26	4	255.8
11	16	1023	18	1	1023
12	31	2047	8	1	2047
13	33	1023	16	1	1023
14	14	255	23	2	127.5
15	20	1023	29	1	1023
16	25	1023	31	1	1023
17	18	511	25	1	511
18	17	1023	6	1	1023
19	24	1023	30	1	1023
20	30	511	14	2	255.5
21	13	1023	19	2	511.5
22	32	2047	21	1	2047
23	27	1023	7	1	1023
24	34	1023	22	1	1023
25	28	1023	17	2	511.5
26	9	511	33	1	511
27	29	1023	24	1	1023
28	10	511	32	2	255.5

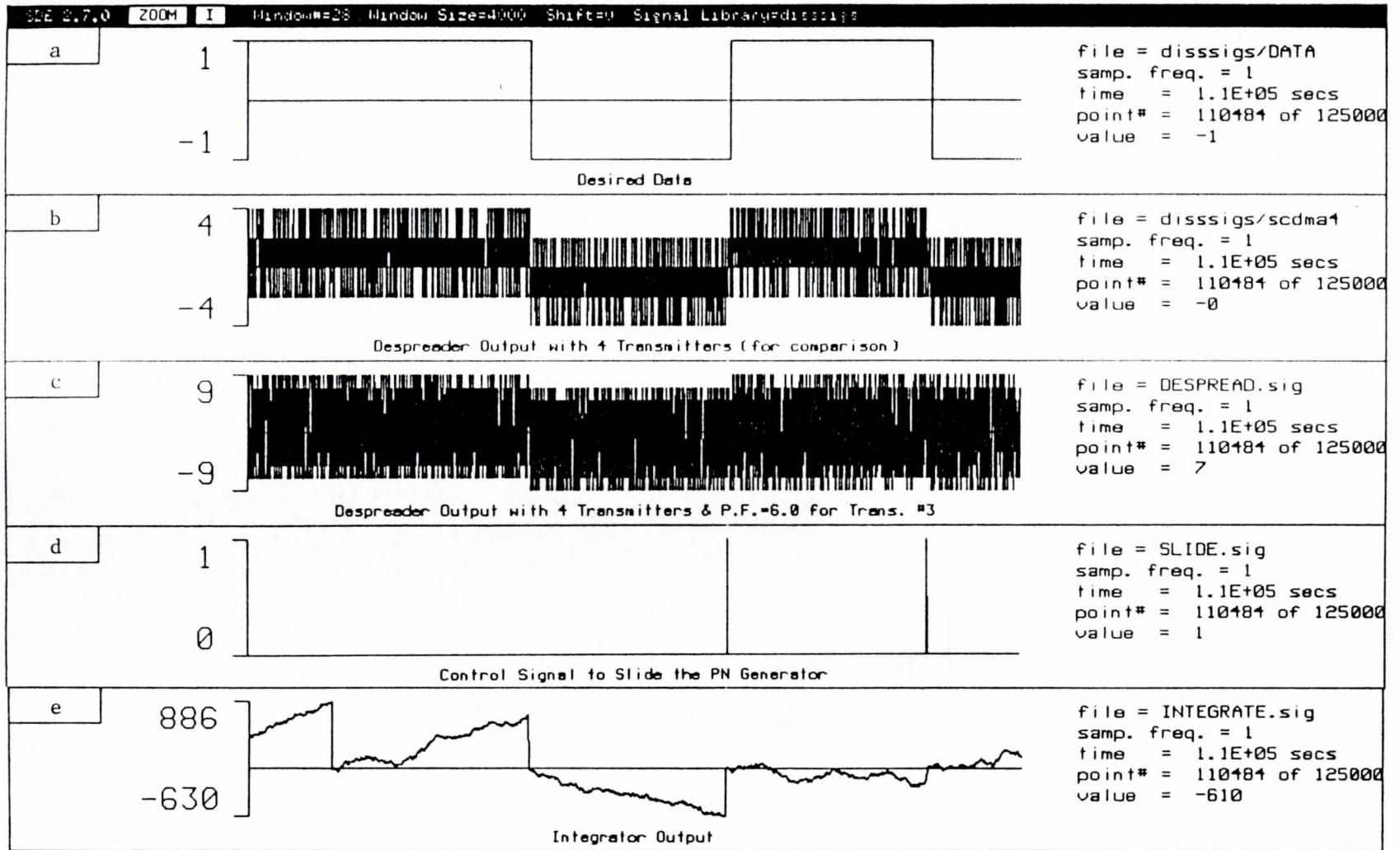


Figure 3A.4 CDMA Received Waveforms



#3 is then boosted (via the on-line multiplier) to simulate a "near" transmitter, while the other three remain at unity as the "far" transmitters. Amplification of #3 is increased, incrementally, until the system breaks down. Signals 3A.4d and 3A.4e show that with a power factor of six, the system obtains synch but eventually loses it when the magnitude of the integrator's output drops to 610 (the threshold was set to 675). Viewing transmitter #3 as six identical users with unity power, system capacity is roughly nine users.

The nonlinear characteristic of the near-far problem is best explained mathematically. Close inspection of the last two terms of equations (4) and (5) indicate a partial cancelling in the correlation process if the code sequences are dissimilar. This cancelling reduces the destructive tendencies of the interfering users. If the codes are identical, however, no cancelling occurs and the negative impact is maximized. The next section determines the number of users allowed onto the system for the ideal case of equal power. In doing so, it demonstrates (by elimination) the damaging effects of the near-far problem.

#### CSC in CDMA (Equal Power Levels)

Using the assumptions of the previous example (except here all transmitters have equal power), several simulations are performed. The first model has only two transmitters but an additional one is added for each subsequent simulation. As more transmitters are added, the system weakens until it can no longer operate effectively. The integrator output drops below threshold when the twenty-eighth transmitter is added, (see Figure 3A.5). System capacity is now approximately three times larger than it was in the previous example. Nineteen more users are permitted if the near-far problem is removed. Unfortunately, this ideal case is not very realistic. Despreader outputs for various equal powered transmitter combinations are given in Figure 3A.6. As predicted, the waveforms resemble noise filled sequences that worsen as the number of transmitters are increased. Zooming in on signal 3A.6b, we find an M-ary type format with values  $\pm 4$ ,  $\pm 2$ , and 0, (see Figure 3A.7). This is the result of summing four PN sequences. As the number of transmitters

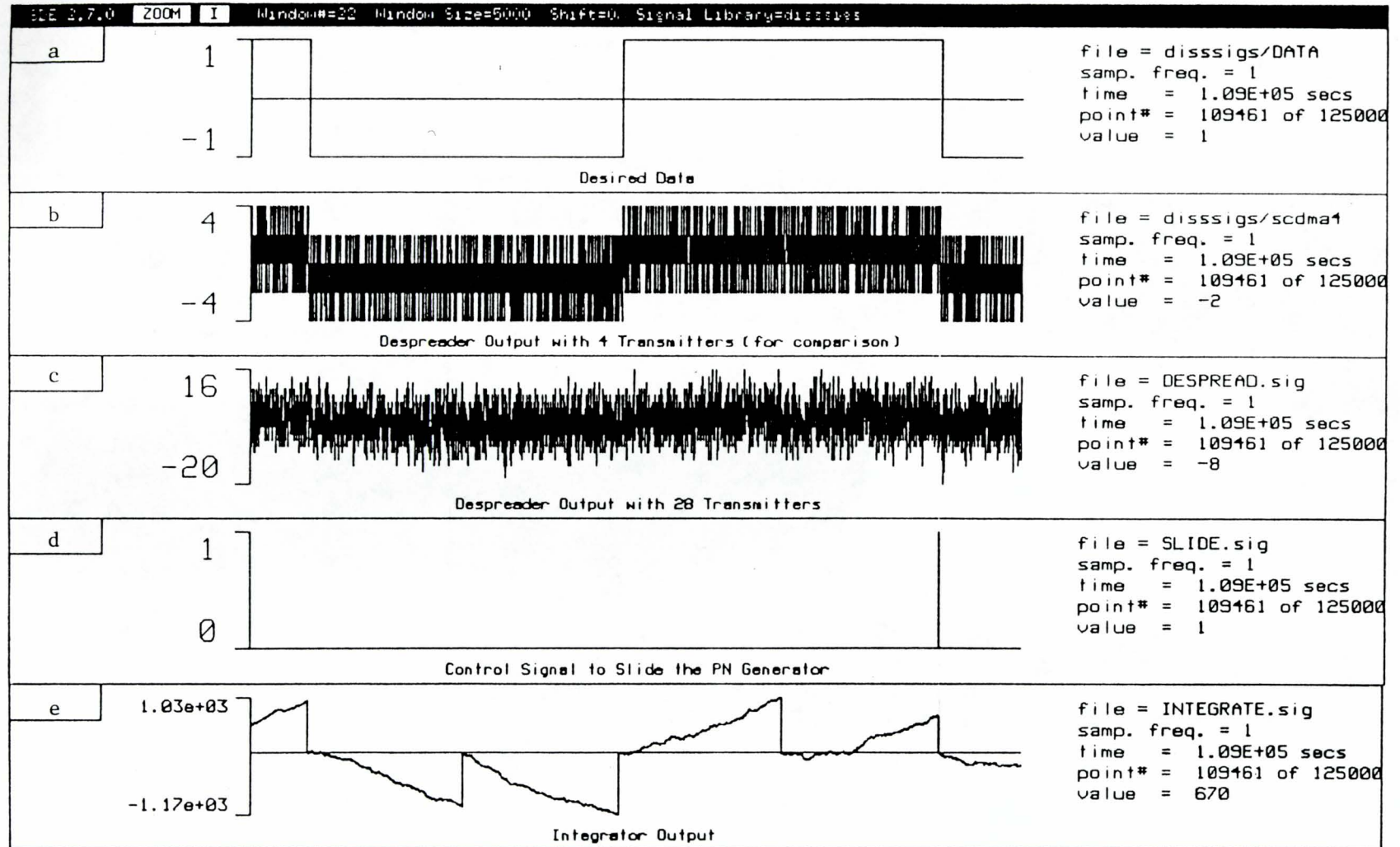


Figure 3A.5 CDMA Waveforms with 28 Transmitters

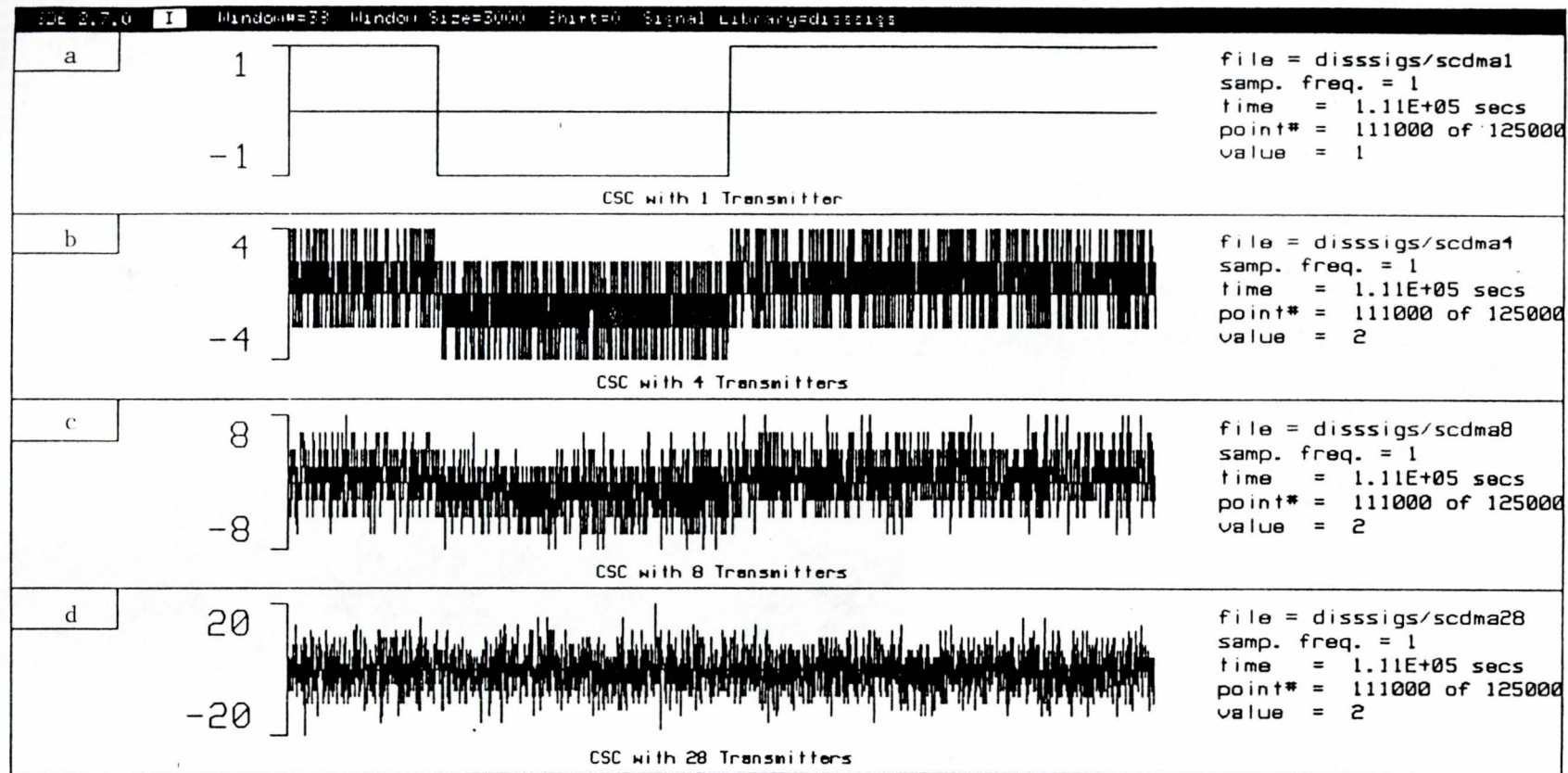


Figure 3A.6 CDMA Waveforms with Multiple Transmitters

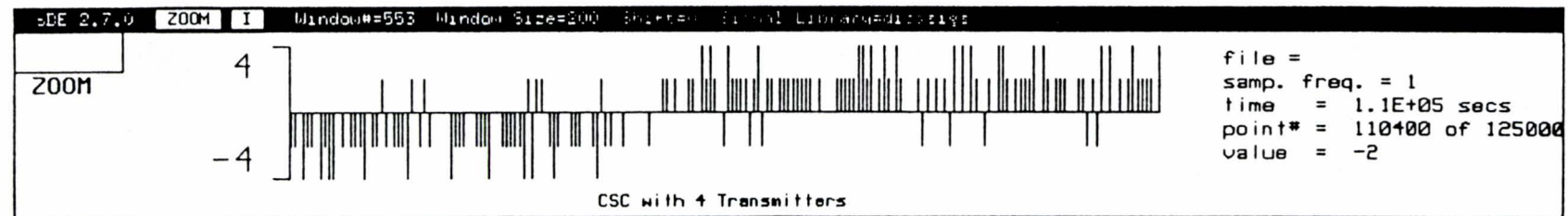


Figure 3A.7 CDMA Waveforms with Multiple Transmitters (ZOOM)

increase, so do the number of M-ary values.

### Variations of the CSC

For certain applications, the CSC may be too slow. One method of improvement is to use a parallel bank of correlators with locally generated code spaced apart by an amount equal to the slippage of the local PN generator. This eliminates the uncertainty region which reduces the mean time to acquire synch. Acquisition time is then equal to the amount of time required by the integration process. Such a system is hardware intensive and is usually replaced by a hybrid of the CSC and parallel bank. Other CSC variations can be found in reference [4].

### Phase Multiplexed Correlator

Another method of rapid acquisition is proposed in [5]. The new design is a modified CSC whose PN generator is replaced by a phase multiplexed generator (PMG). Compare the model of Figure 3A.8 to that of Figure 3A.1. The PMG produces L equally spaced, phase shifted replicas of the original maximum length PN sequence. These sequences are added together and used to despread the incoming signal. Internal redundancy of the PMG reduces the uncertainty region by a factor of L, assuming that the  $P_D$  equals one. The equation for calculating the number of phase shifts can be determined with the equation:

$$S = (N + 1)/L \quad ; \quad L < (N + 1) \quad (6)$$

One of the codes contains at least one less chip than the rest of the sequences in order to preserve the relation  $N=2^n-1$ . Of course, S cannot be increased without bound since the extra codes produce unwanted noise. Equations for the integrator output in a single transmitter system are given as:

$$Y_{(synch)}^k = A^k b_i^k (p - 1) + \sum_{j=0}^{p-2} \sum_{w=1}^L n(j t_s) a_j^w + A^k b_i^k \sum_{j=0}^{p-2} \sum_{w=1, w \neq k}^L a_j^k a_j^w \quad (7)$$

$$Y_{(no-synch)}^k = \sum_{j=0}^{p-2} \sum_{w=1}^L n(j t_s) a_{(j+l)}^w + A^k b_i^k \sum_{j=0}^{p-2} \sum_{w=1}^L a_j^k a_{(j+l)}^w \quad (8)$$

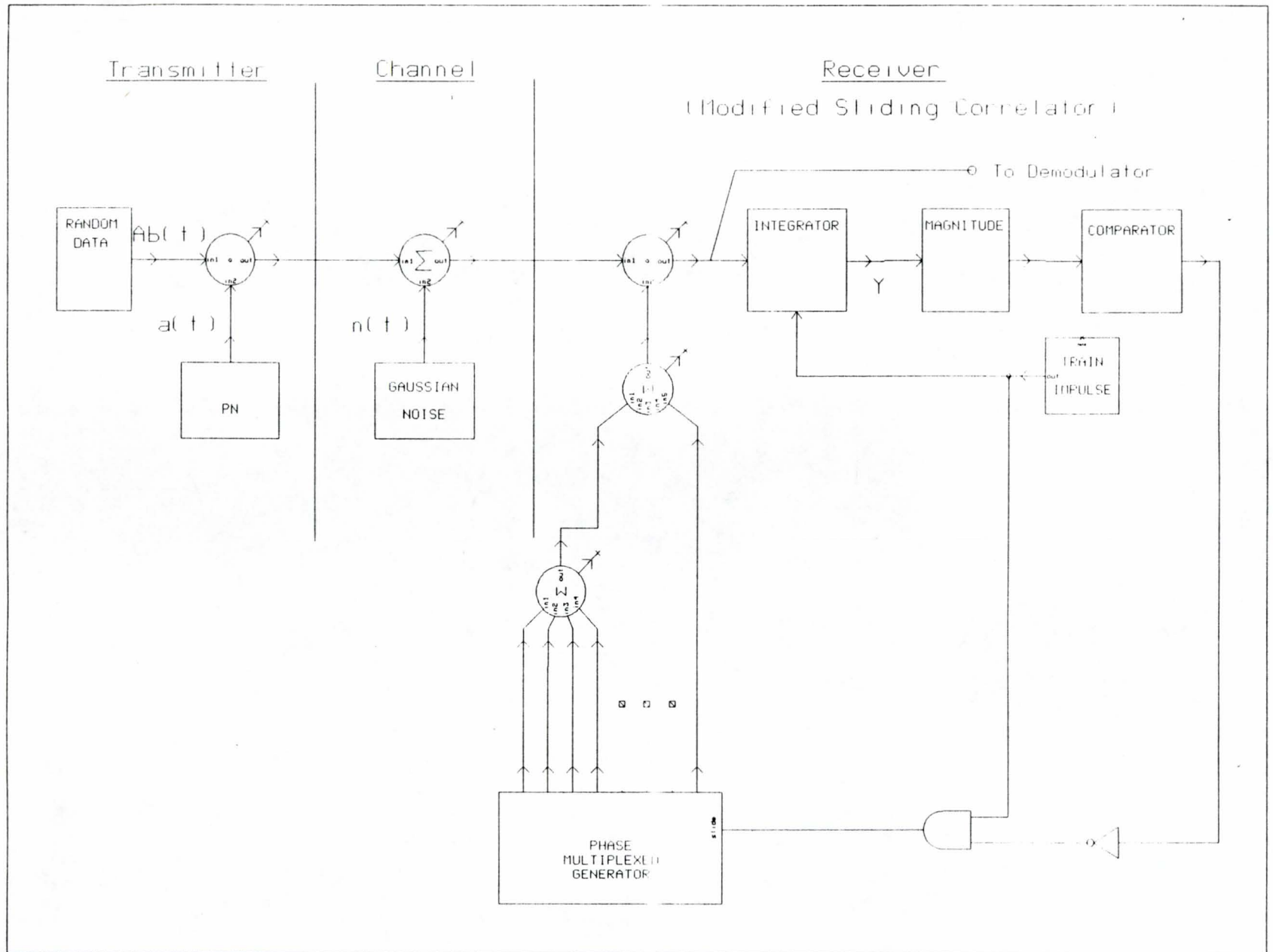


Figure 3A.8 PMC in a DSSS Setting.

As examples, a single transmitter system is modeled with 8, 32, 64, and 128 phase generators. Assumptions made include: no channel noise; whole chip slippage; and a comparator threshold level of 930. Surprisingly, the receiver acquires synchronization and maintains it in all four cases. Figures 3A.9 and 3A.10 contain despreader and integrator outputs. The seemingly unbounded characteristic of the system is explained by the last term of equation (7). It is finite and much less (in magnitude) than the first term. As a matter of fact, it can be shown that the last term is equal to the negated number of phases if  $A^k$  and  $b_i^k$  are equal to one. If noise is included, its effects are minimized when statistical constraints are applied. To verify the validity of the PMG outputs, (i.e. to prove that each PMG is designed correctly), cross-correlations of the transmitter and receiver codes are determined and appear in Figure 3A.11.

### PMC in CDMA

As more transmitters are added, system performance declines. This is seen in the following equations:

$$Y_{(synch)}^k = A^k b_i^k (p-1) + \sum_{j=0}^{p-2} \sum_{W=1}^L n(jt_s) a_j^W + \sum_{j=0}^{p-c-1} \sum_{r=1; r \neq k}^M A^r b_{(i-1)}^r \sum_{W=1}^L a_j^W a_j^r + \sum_{j=p-c}^{p-2} \sum_{r=1; r \neq k}^M A^r b_i^r \sum_{W=1}^L a_j^W a_j^r + \sum_{j=0}^{p-2} A^k b_i^k \sum_{W=1; W \neq k}^L a_j^W a_j^k \quad (9)$$

$$Y_{(no-synch)}^k = \sum_{j=0}^{p-2} \sum_{W=1}^L n(jt_s) a_{(j+l)}^W + \sum_{j=0}^{p-c-1} \sum_{r=1}^M A^r b_{(i-1)}^r \sum_{W=1}^L a_{(j+l)}^W a_j^r + \sum_{j=p-c}^{p-2} \sum_{r=1}^M A^r b_i^r \sum_{W=1}^L a_{(j+l)}^W a_j^r \quad (10)$$

The extra code phases at the receiver are correlated with the incoming signals (noise and users) which changes the outcome of the integration process. More phases results in a larger disturbance. To illustrate this, a second transmitter is added to the previous example. While synchronization still occurs, it is quickly lost (see Figure 3A.12b). Reducing the number of phases while increasing the number of users lead to a better mix. Figure 3A.12c is the integrator output for eight phases and seven transmitters. The signal looks good; however, one more user causes a breakdown (see

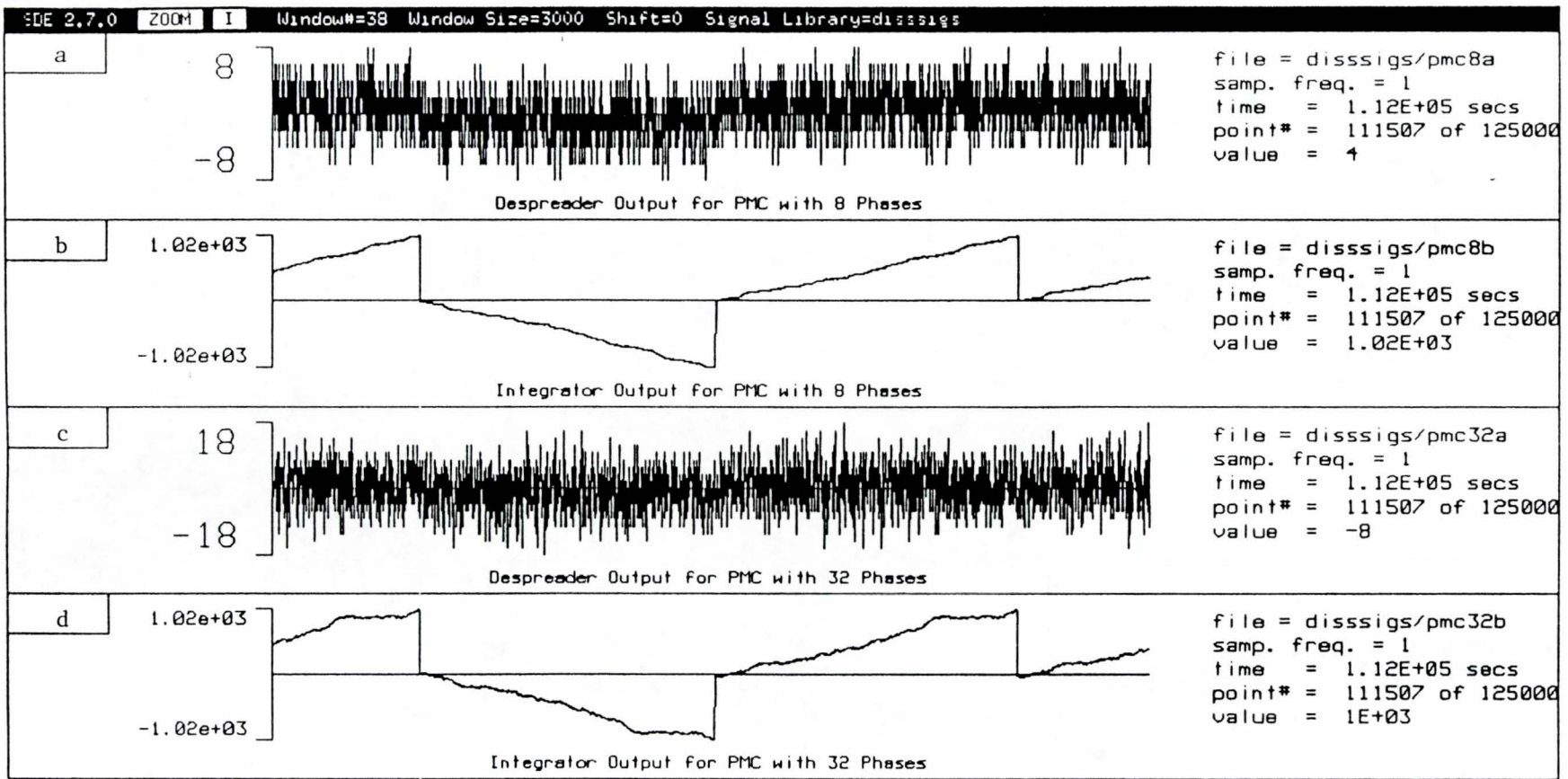


Figure 3A.9 Multiple Phase PMC (Single Transmitter)

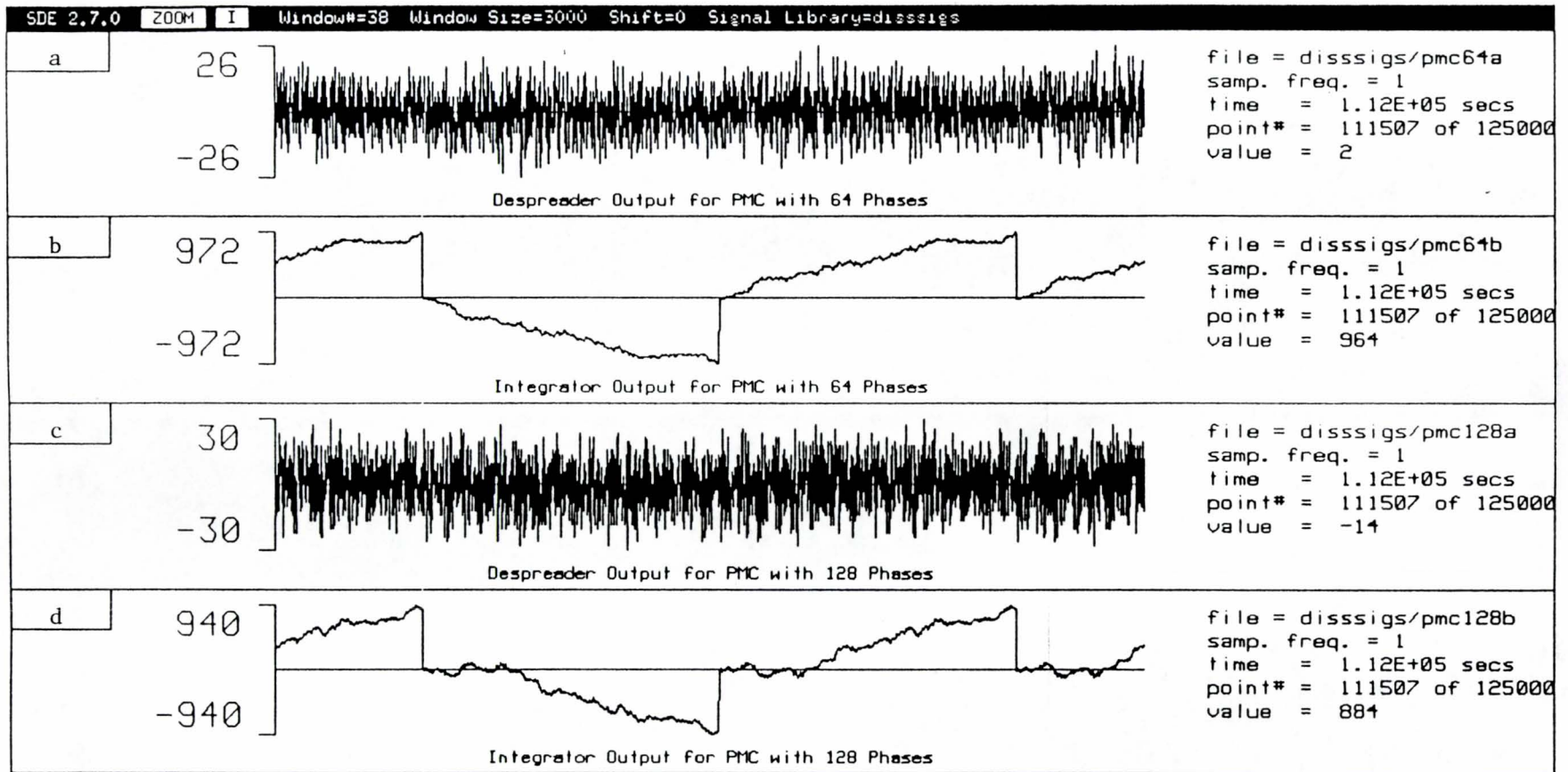


Figure 3A.10 Multiple Phase PMC (Single Transmitter)



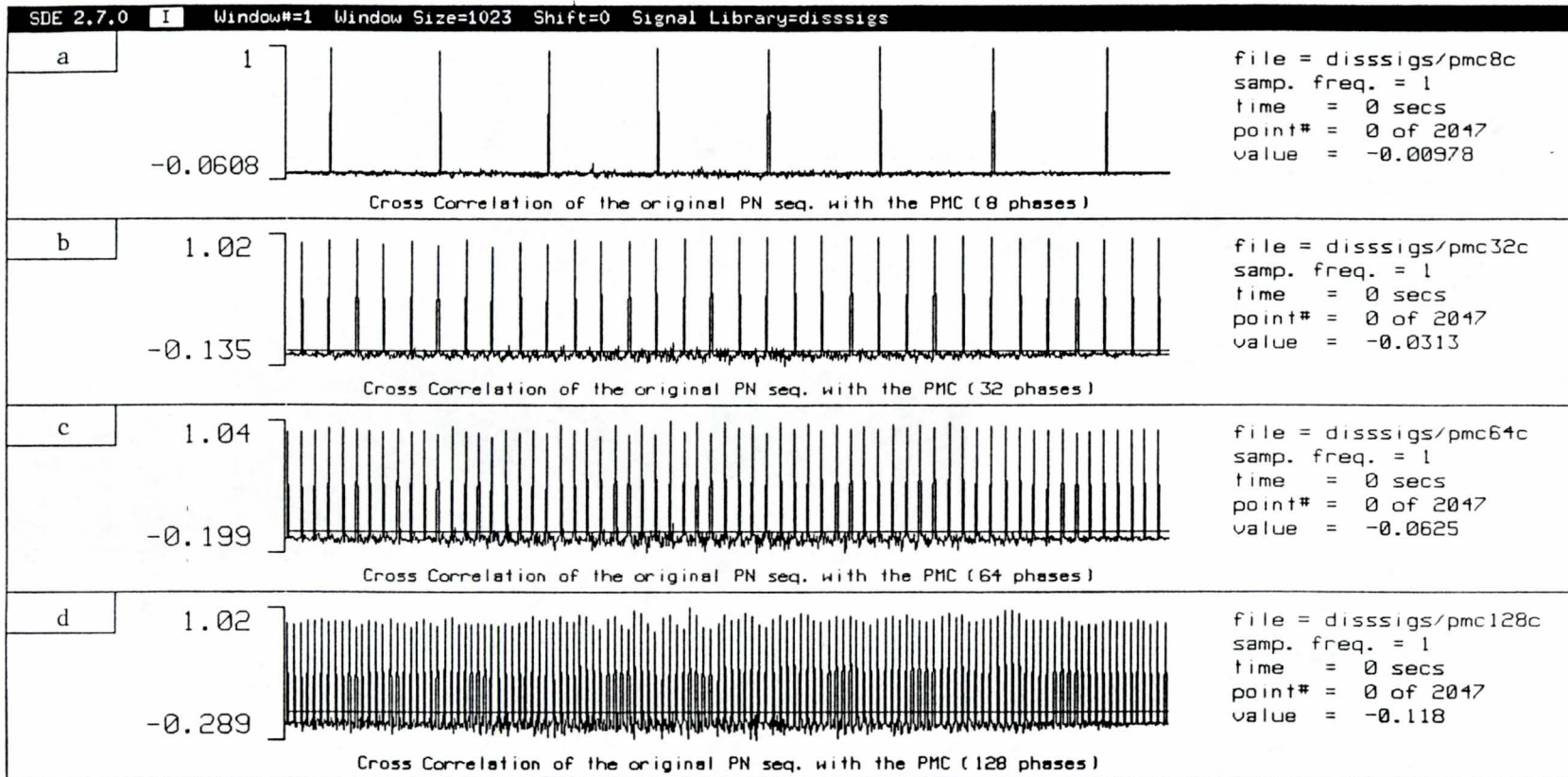


Figure 3A.11 Cross-correlation of Multiple PN Sequences

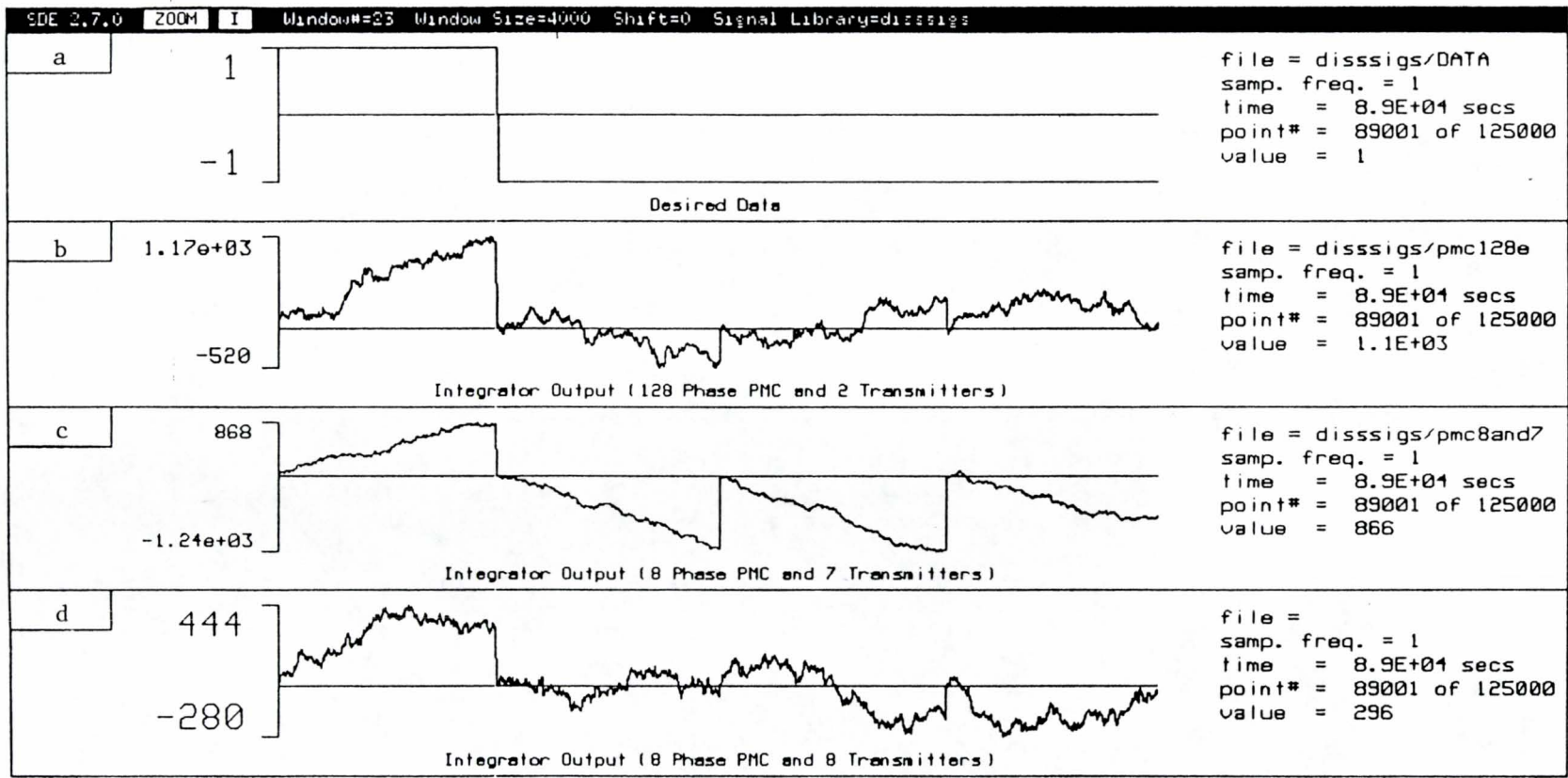


Figure 3A.12 PMC with Multiple Transmitters

140

Figure 3A.12d). For completeness, a final experiment is performed to study the near-far problem. An eight phase, four transmitter system is modeled with the on-line multiplier of transmitter #3 increased by increments from 2 to 4 in subsequent computer runs. With a multiplication factor of 2, the output was satisfactory, staying in sync for 23 integration periods. When increased to 3, the system maintained sync for 10 integration periods, and for a factor of 4, it only lasted for 2 periods. Figure 3A.13 provides sample integrator outputs for the described cases. As expected, performance dropped due to a lack of cancelling terms in the correlated codes.

### Synthesis of the PMG

In designing a PMG, a maximum length PN polynomial is selected. Phase shifted replicas are designed using a delay synthesis technique. There are many methods for creating delayed versions of a PN sequence. One method uses a parallel bank of PN generators with different initial values. Another uses strings of delay elements that are attached to the generator. An even better method (less hardware) uses polynomial theory and modulo two arithmetic to multiply the PN polynomial by the prescribed shift, and then factors it into a polynomial of degree n or less.[5] This is done for each phase shift.

An example will help to clarify the latter approach. Suppose that an eight phase PMG is desired from the following tenth order polynomial:

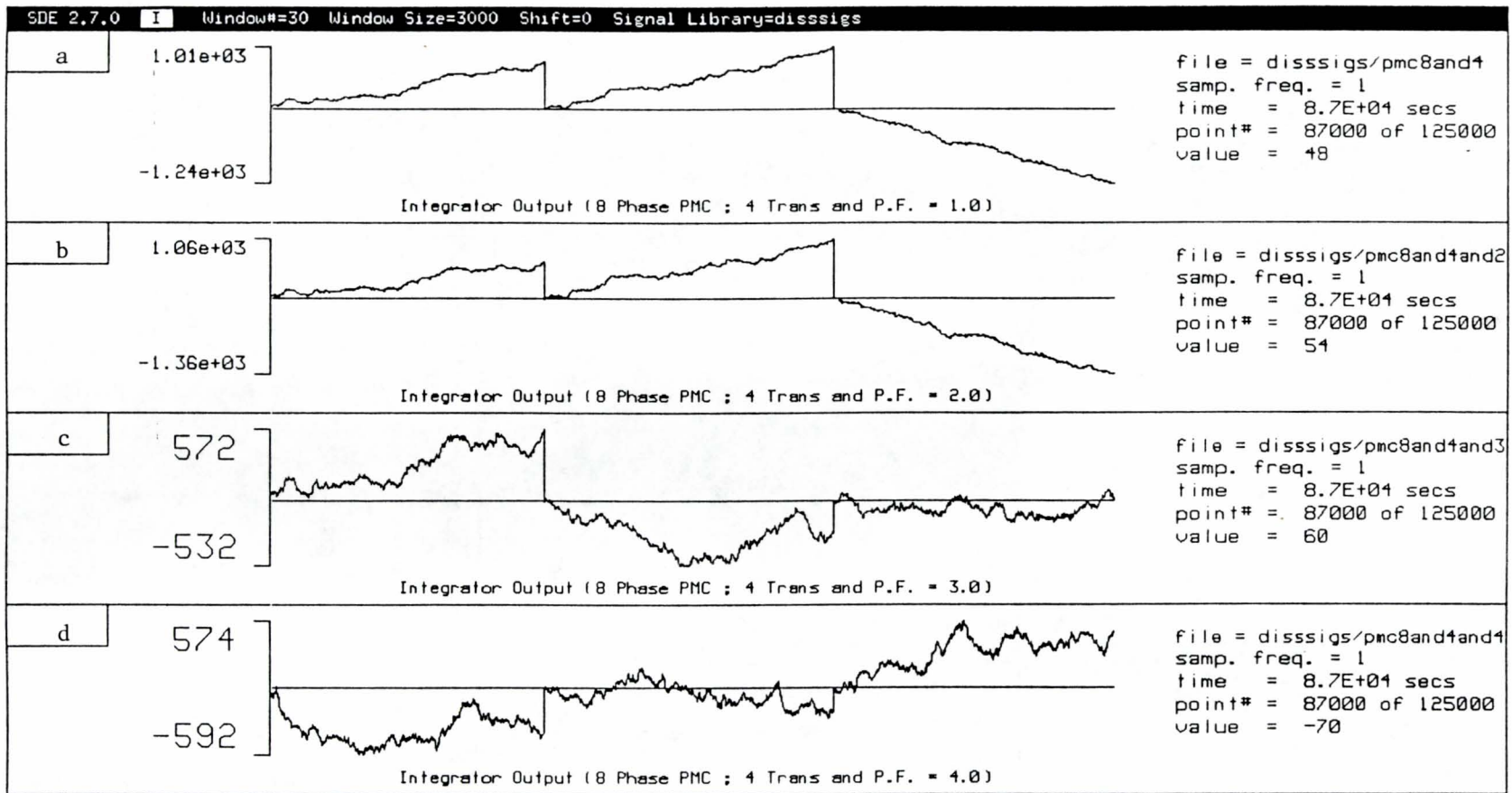
$$g(x) = 1 + X^2 + X^3 + X^6 + X^8 + X^9$$

The distance between neighboring sequences is calculated as  $(N+1)/L = 1024/8 = 128$ . However, one of the codes has a spacing of 127 in order to keep  $N=1023$ . Polynomials for phase shifted replicas are determined by individually multiplying  $g(x)$  by  $X^{128}$ ,  $X^{256}$ ,  $X^{384}$ ,  $X^{512}$ ,  $X^{640}$ ,  $X^{768}$ , and  $X^{896}$  and factoring until the orders of the replicated polynomials are less than or equal to 10:

$$g_1(x) = g(x) = 1 + X^2 + X^3 + X^6 + X^8 + X^9$$

$$g_2(x) = g(x) X^{128} = X^2 + X^4 + X^9$$

$$g_3(x) = g(x) X^{256} = X^7 + X^8$$



142

Figure 3A.13 PMC with Near-Far Effects

$$g_4(x) = g(x) X^{384} = X^2 + X^3 + X^5 + X^{10}$$

$$g_5(x) = g(x) X^{512} = X^4 + X^6$$

$$g_6(x) = g(x) X^{640} = X^3 + X^5 + X^9$$

$$g_7(x) = g(x) X^{768} = X^1 + X^2 + X^3 + X^4$$

$$g_8(x) = g(x) X^{896} = X^1 + X^7 + X^8 + X^9 + X^{10}$$

These polynomials are realized in Figure 3A.14. To verify that the sequences are indeed shifted by the prescribed amounts, the cross-correlation of signal  $g(x)$  with the output of the phase multiplexed generator is shown in Figure 3A.15. Note that the correlation peaks occur for lags of 0, 128, 256, 384, 512, 640, 768, and 896, as expected. Applying these 8 sequences to the system of Figure 3A.8 results in a despread output waveform similar to the one shown in Figure 3A.6c.

### Summary

Determining the performance of a PMC operating in a CDMA environment is no easy task, particularly when the near-far problem is considered. Equations (9) and (10) are indicative of the complexities involved. These equations could be further enhanced by incorporating the following features: individual carrier frequencies for all users; random alignments between chips, bits, and the integration process; and differing chip sizes among the spreaders. Inclusion of these items would make the results more realistic, but, would not change performance trends. For simplicity, they were omitted. To graphically illustrate system tendencies for various scenarios, many examples were given. For instance, Figures 3A.9 - 3A.11 show that a virtually unbounded number of phases is allowed at the PMG if only one transmitter is used. Once additional users appear, however, signal degradation prevails, see Figure 3A.12b. Near-far considerations drop the efficiency even further, as shown in Figure 3A.13. Of course, the PMC is not the only technique plagued by the effects of CDMA. The CSC also suffers from it. Figure 3A.5 shows that under the given conditions, 28 users are allowed and Figure 3A.4 proves that a nonlinear decline to nine users (equivalent to nine) occurs

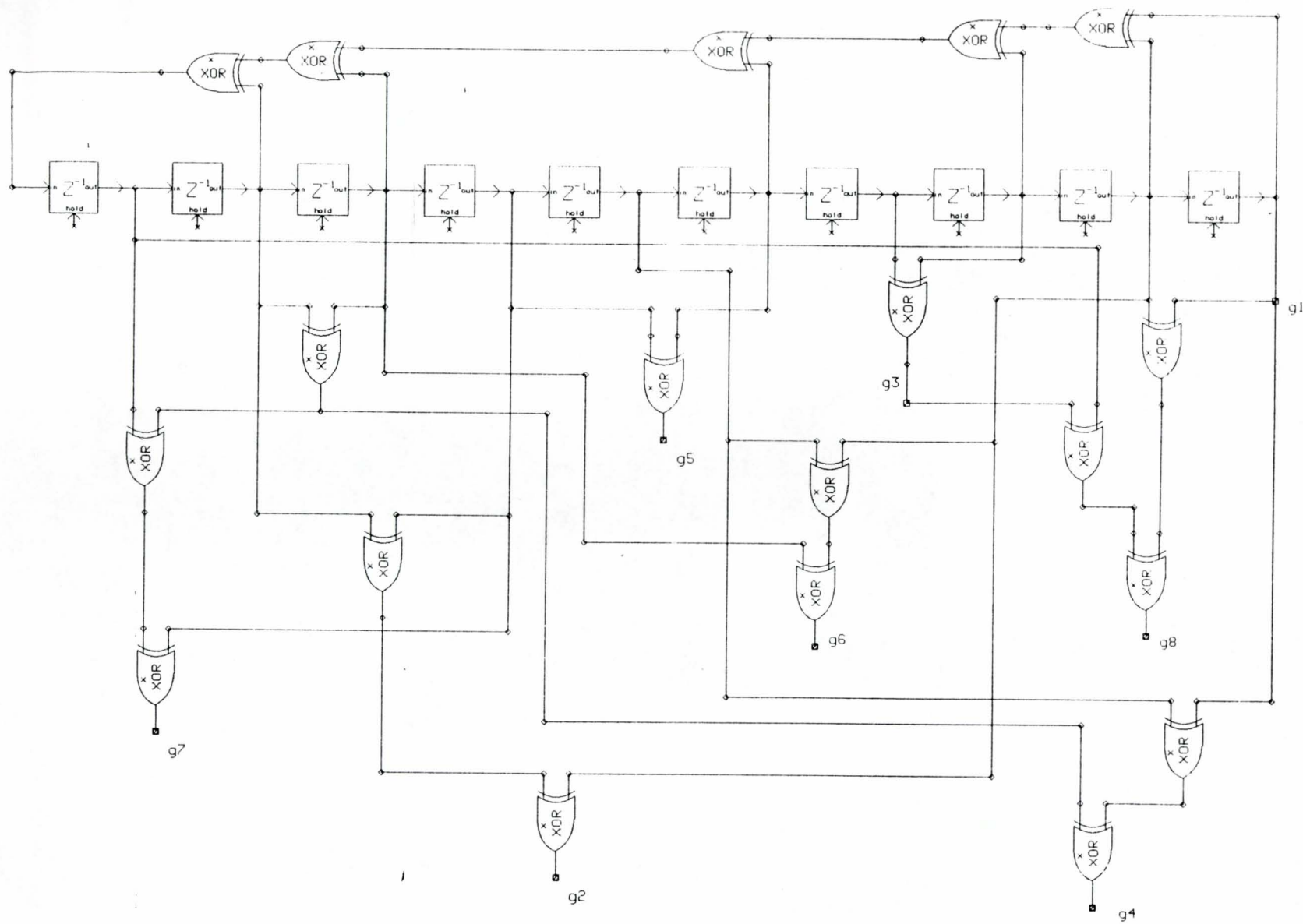


Figure 3A.14 Multiple PN Sequence Generator.

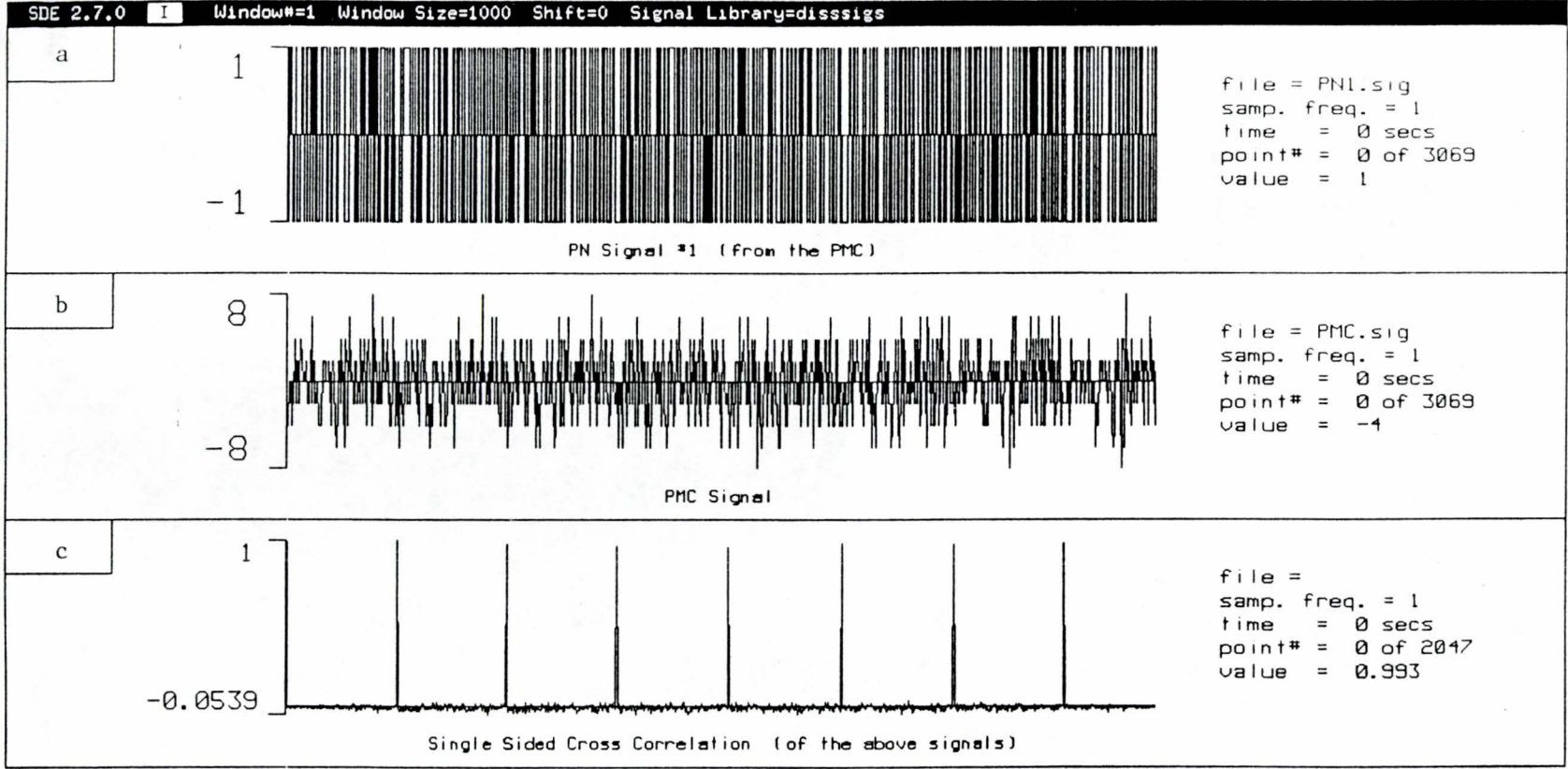


Figure 3A.15 Sum of Multiple PN Sequences and their Cross-correlation

when one of the transmitters is boosted to six times the amplitude of the others. While the CSC is shown to perform better than the PMC, it must be pointed out that the PMC concedes to sacrificing accuracy for speed. The PMC is a relatively new design that is still under development. Further improvements should make it a viable technique for rapid acquisition.

As a final comment, this paper confirms that SPW is well suited for spread spectrum simulation.

### References

[1] Comdisco Systems, Inc., Signal Processing Worksystem, Software Documentation, Product Number SPW1080, Version 2.7, August 1990.

[2] R. Skaug and J. F. Hjelmsstad, SPREAD SPECTRUM IN COMMUNICATION. London, UK: Peter Peregrinus Ltd., 1985.

[3] R. L. Pickholtz, D. L. Schilling, and L. B. Milstein, "Theory of Spread-Spectrum Communications - A Tutorial", IEEE Trans. Comm., vol COM-30, May 1982.

[4] R. C. Dixon, SPREAD SPECTRUM SYSTEMS. New York: Wiley-Interscience, 1984.

[5] G. S. Rawlins, "A RAPID ACQUISITION TECHNIQUE FOR DIRECT SEQUENCE SPREAD SPECTRUM SYSTEMS BY A PN PHASE MULTIPLEXED CORRELATOR." Master's Thesis, University of Central Florida, Orlando, Florida, 1987.





0000092